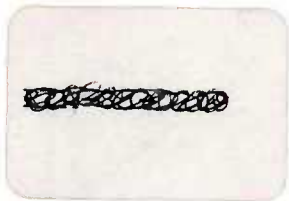


AD-A157 902



TECHNICAL REPORT ARLCD-TR-85003

TECHNICAL
LIBRARY

**INVESTIGATION OF DAMAGED LANDS OF M185 CANNON
MOUNTED ON THE 155-MM M109A1 HOWITZER**

RICHARD J. KOPMANN

JUNE 1985



U.S. ARMY ARMAMENT RESEARCH AND DEVELOPMENT CENTER

LARGE CALIBER WEAPON SYSTEMS LABORATORY

DOVER, NEW JERSEY

APPROVED FOR PUBLIC RELEASE; DISTRIBUTION UNLIMITED.

The views, opinions, and/or findings contained in this report are those of the author(s) and should not be construed as an official Department of the Army position, policy, or decision, unless so designated by other documentation.

The citation in this report of the names of commercial firms or commercially available products or services does not constitute official endorsement by or approval of the U.S. Government.

Destroy this report when no longer needed. Do not return to the originator.

UNCLASSIFIED

SECURITY CLASSIFICATION OF THIS PAGE (When Date Entered)

REPORT DOCUMENTATION PAGE		READ INSTRUCTIONS BEFORE COMPLETING FORM
1. REPORT NUMBER Technical Report ARLCD-TR-85003	2. GOVT ACCESSION NO.	3. RECIPIENT'S CATALOG NUMBER
4. TITLE (and Subtitle) INVESTIGATION OF DAMAGED LANDS OF M185 CANNON MOUNTED ON THE 155-mm M109A1 HOWITZER		5. TYPE OF REPORT & PERIOD COVERED Final 1980-1984
7. AUTHOR(s) Richard J. Kopmann		6. PERFORMING ORG. REPORT NUMBER
9. PERFORMING ORGANIZATION NAME AND ADDRESS ARDC, LCWSL Weapons Div (SMCAR-LCW-S) Dover, NJ 07801-5001		8. CONTRACT OR GRANT NUMBER(s)
11. CONTROLLING OFFICE NAME AND ADDRESS ARDC, TSD STINFO Div (SMCAR-TSS) Dover, NJ 07801-5001		10. PROGRAM ELEMENT, PROJECT, TASK AREA & WORK UNIT NUMBERS
14. MONITORING AGENCY NAME & ADDRESS (if different from Controlling Office)		12. REPORT DATE June 1985
		13. NUMBER OF PAGES 135
		15. SECURITY CLASS. (of this report) Unclassified
		15a. DECLASSIFICATION/DOWNGRADING SCHEDULE
16. DISTRIBUTION STATEMENT (of this Report) Approved for public release; distribution unlimited.		
17. DISTRIBUTION STATEMENT (of the abstract entered in Block 20, if different from Report)		
18. SUPPLEMENTARY NOTES		
19. KEY WORDS (Continue on reverse side if necessary and identify by block number) M109A1 self-propelled howitzer Projectile rammer 155-mm M185 cannon Interior ballistics data Rifling land damage Tube damage		
20. ABSTRACT (Continue on reverse side if necessary and identify by block number) This is a final report on the investigation into the prime cause of damaged lands in the M185 cannon and into the safety of firing fielded ammunition in an M185 cannon with land damage. It was determined that firing projectiles from an unseated position in the chamber can result in flattened and stripped lands representative of that reported near the commencement of rifling. When compared to an undamaged tube with similar wear, the damaged tube showed an (cont)		

20. ABSTRACT (cont)

insignificant difference in the probable error of range and deflection. No inbore forces could be identified which would compromise the safe firing of a projectile/fuze system. Consequently, a change to the criteria for tube condemnation was initiated to exclude the type of land damage reported.

CONTENTS

	Page
Introduction	1
System Mission and Description	1
Background	1
Reported Incidence of Land Damage and Program Initiation	1
Statement of the Problem	2
Fault Analysis and Conclusions on Land Damage Problem	2
Purpose and Problem Definition	2
Considerations	3
Mechanism of Land Flattening and Land Stripping	3
Land Damage Fault Tree	4
Conclusions of the Root Cause Failure Analysis	4
Fallback Test, Yuma Proving Ground	5
Background and Purpose	5
Test Procedure	6
Results	6
Conclusions	9
Ramming Test, Picatinny Arsenal, ARDC	9
Purpose and Assumptions	9
Test Procedure	9
Results	10
Follow-Up Data Reduction	11
Ramming Test Addendum, Picatinny Arsenal, ARDC	11
Purpose	11
Background and Procedure	12
Results	12
Degradation Test, Aberdeen Proving Ground	12
Background, Purpose and Procedures	12
Evaluation of Results	17
Results and Conclusions	20
Tube Investigation	20
Discussion	20
Change Recommended in Condemnation Criteria	21

Results and Conclusions	21
Recommendations	23
References	25
Appendix	117
Distribution List	127

TABLES

	Page
1 155-mm M185 cannon damaged lands reports	27
2 Recorded location of land damage	29
3 Fallback test, round-by-round data	30
4 Fallback distances and reference velocity and pressure values--M107 projectile	32
5 Camera data	33
6 Projectile damage	33
7 Selected values from breech pressure and chamber pressure plots	34
8 Contact loads, M107 projectile in M185 cannon	36
9 Summary of contact loads, M107 projectile in M185 cannon	37
10 Comparison of selected ramming test data	37
11 Lo-Z accelerometer output	38
12 Results from Lo-Z accelerometer output	39
13 Comparison of extraction forces with seating loads and velocities	39
14 M107B2 projectile ram--extract test (2 August 1982)	40
15 Summary of range firings from M185 cannon tubes, M107 projectiles, M557 fuze, M4A2 charge	41
16 Summary of range firings from 155-mm damaged tube S/N 25460 using charge M119, zone 8, conditioned to +130°F	42
17 Results of modeling the modified M107 projectile used in phase D of the degradation test	43
18 Range data from phase D firings	43
19 Comparison of test results (ranges) with firing table values	44
20 Comparison of test results (deflections) with firing table values	45
21 Summary of fuze functioning and spin rate data	46
22 Location of break with accelerometer wires	47

23	Table of accelerations in 1000's of g's	48
24	Comparison of actual and theoretical acceleration values	49
25	Material properties of damaged and undamaged tubes	50
26	Mechanical properties of damaged and undamaged tubes	51

FIGURES

1	155-mm M109A1 SP howitzer	53
2	M185 cannon tube forcing cone modification	54
3	M185 cannon tube grooved forcing cone modification	55
4	Damage to tube S/N 25460	56
5	Nomenclature for worn or deformed rifling. Transverse sections normal to axis of gun tube	58
6	Mechanism of land stripping--fragments sheared down	59
7	Mechanism of land stripping--fragments lifted	60
8	Land damage fault tree	61
9	Rifling damage to tube S/N 24715 after tube round 9--12 o'clock position	62
10	Recovered projectile--fallback test	63
11	Smear camera photographs of projectile's muzzle exit	65
12	Tube S/N 28317 at end of fallback test--3 o'clock position	66
13	Smear camera photographs of flight instability and fuze damage	67
14	Tube round no. 23 fired from tube S/N 28317. Note the engraving on the ogive, front bourrelet and the body from contact with the rifling.	68
15	Breech and chamber pressure curves--tube S/N 24715	69
16	Pictorial schematic of Deram tool	80
17	M185 cannon tube S/N 26066 after ramming test--shows debris but no damage	81
18	Extraction force--700 mil QE case	82

19	Ramming test 4--velocity and pressure and acceleration curves	83
20	Ramming test 8	87
21	Ramming test 12	91
22	Rotating band configurations--all dimensions nominal	95
23	M185 cannon tube S/N 25460 at start of degradation test	96
24	Artillery interface drawing--tube chamber and projectile	97
25	Collector cup with accelerometers--top view	98
26	Range and deflection PE versus range	99
27	Range firings with damaged tube S/N 25460--6000 meters	100
28	Comparison of range firings--undamaged tube S/N 25460 versus damaged tube S/N 25460--9000 meters	103
29	Range firings with damaged tube S/N 25460--10,000 meters	106
30	Range firings with damaged tube S/N 25460--12,000 meters	107
31	Range firings with damaged tube S/N 25460--M577 fuze and M483A1 projectile	109
32	Range firings with damaged tube S/N 25460--M549 projectile, rocket off	110
33	155-mm M185 howitzer tube S/N 25460 at start of degradation test after firing 458 rounds	111
34	155-mm M185 howitzer tube S/N 25460	113
35	Type of rifling damage not warranting condemnation of the tube	115

INTRODUCTION

System Mission and Description

M109 is the designation for a series of 155-mm self-propelled howitzers (SPH) used by the U.S. Army (including the National Guard), U.S. Marines, and by several armies abroad. The weapon uses all standard and nuclear 155-mm ammunition. It has undergone two retrofits, including a long tube conversion and a mid-life product improvement program (PIP), and is currently planned for modification under the Howitzer Extended Life Program (HELP). Since 1970 when the weapon was classified an M109A1, it has carried the M185 cannon (fig. 1). The application of the M185 cannon increased the maximum range of the weapon 25 percent to 18 kilometers. This cannon is essentially a modification of the original M126 short-tube cannon design. Consequently, though it has an expanded chamber volume and a length of 39 calibers, it retains both the M126 muzzle brake and the breech mechanism. Two changes to the original cannon design are noteworthy. The first, a change to a steep forcing cone (fig. 2) was implemented in response to a low zone sticker problem which surfaced during service test of the cannon. (The weapon is still not compatible with the M3A1 zone 1 charge.) The second modification to the cannon (fig. 3) consisted of annular grooving of the forcing cone to improve the cannon's projectile retention characteristic. This was the approach selected over the alternative of transitioning back to a shallow taper for the region extending from the origin to the commencement of rifling

The rammer on board the M109A1 is a weapon mounted, two-stage telescoping device powered hydraulically and controlled by a solenoid-operated spool valve in series with an adjustable timer. This rammer replaced a cab mounted, fixed quadrant elevation (QE) loader which was part of the original M109 design. In the current production M109A2 and retrofitted M109A3 vehicles, the U.S. has eliminated the timer and solenoid from the rammer circuit and has opted for manual control of the ramming operation. The adjustable feature of the timer permitted shortening the total time available to complete ramming but that precipitated short rams and a series of fallback incidents.

Background

Reported Incidence of Land Damage and Program Initiation

In June 1979, the Army of the Netherlands reported that five of their M185 cannons had sustained damage, one after only 101 rounds or 25 effective full charges. Retrofit of their M109 fleet to the M109A1 configuration had been completed only four months earlier. This report, together with the United Kingdom experience in late 1978 with flattened or stripped rifling lands in three of their M185 cannons and the U.S. experience with two damaged tubes (one from Fort Hood and one from the Wyoming National Guard), prompted a request in September 1979 to formally investigate the problem. In February 1980, a program was approved by the configuration control board (CCB). The program outline consisted

of five phases: data collection, fault analysis, component testing, tube investigation, and a final report.

Statement of the Problem

A list of the tubes reported as damaged as of October 1981 is provided in table 1. Photos depicting damage representative of the kind reported by the Netherlands are contained in figure 4. (Tube S/N 25460 was condemned.) In general, criteria for tube condemnation are based on accuracy loss of the weapon. Sudden erratic deviations from the probable error of velocity, range, and deflection can be associated with a considerable loss of propellant energy (as would be found from firing an unseated projectile) or a stripped or sheared rotating band (i.e., the removal of the entire rotating band, or of the engraved portion of the band so that the band surface is smooth). Loss of propellant energy is termed blowby and, when it occurs with a seated projectile, it is the result of poor obturation of the rotating band. When damage occurs at or near the commencement of rifling, other deleterious effects of blowby in terms of gas wash and gas wear are enhanced. Gas wash is the smooth enlargement of the bore due to the surface metal's being gradually washed away by hot, high velocity propellant gases. Surface erosion is prevalent at the origin of rifling due to the greater gas temperatures and rotating band pressures that are found there. Gas wear, otherwise known as scoring, is attributed to the nozzle or venting action of gases escaping past the rotating band. As the nozzle area grows, so do scoring effects. These effects are more prominent at the 12 o'clock position because of the clearance found due to the weight of the projectile. The effects are usually discernible as longitudinal streaks in the bore which develop into irregular gutters and holes extending gradually over the grooves and into the non-driving side of the land (see fig. 5). Most tubes will fail ballistically, however, before deep scoring poses a serious problem in terms of gun tube strength.

FAULT ANALYSIS AND CONCLUSIONS ON LAND DAMAGE PROBLEM

Purpose and Problem Definition

The methodology of failure analysis seminars, techniques, and teams (FASTT) was used by a diagnostic team charged with studying the cause of rifling damage in the 155-mm M185 cannon.¹ Specifically, the team was to identify the probable

¹ Taken from an unpublished report entitled "Diagnostic Case Study, Rifling Land Damage Problem, M185 Cannon, 155-mm M109A1 Self-Propelled Howitzer," prepared by Joseph F. Throop and Jeffrey J. McFadyen, ARRADCOM, Dover, NJ, August 1980. Several illustrations from this report are reproduced herein as figures 7, 8, and 9.

failure modes which could result in the damage as reported; to define the associated causes for these failure modes; and to qualify the likelihood of these failure modes' contributing to or being responsible for the land damage.

The statement of the problem was as follows: flattening of the lands at random circumferential locations occurs at about 6 mm (1/4 in.) from the beginning of rifling, followed by stripping of the flattened lands by a shearing action. Both flattening and stripping occur downbore in some cases at approximately 8 cm (3 in.), 14 cm (6 in.), and 23 cm (9 in.). The downbore damage is usually on the opposite side; that is, 180 degrees opposed to the origin of rifling damage.

Considerations

Some of the facts taken into consideration by the team were that:

1. In general, there was nothing unusual reported about the firing behavior of the weapon on which land damage occurred.
2. The Yuma Proving Grounds Firing Report No. 12827, TECOM Project No. 2-WE-200-109-024, indicated that M107 rounds fired from the fallback position resulted in significantly shorter-than-normal range (ref 2). Moreover, at the last bore inspection in February 1979, the tube used in the test (S/N 22538) displayed no rifling damage.
3. At least three instances of fallback were observed and reported: one, by a U.S. Army unit in West Germany; the other two, by Canada.
4. A safety and interchangeability accord exists with Germany, the United Kingdom, Canada, the Netherlands, Belgium, and France as an assurance that any ammunition produced and inspected abroad is certified as being in accordance with the U.S. technical data package and specifications (ref 3).
5. An earlier investigation of similar damage in the 8-in. M201 cannon indicated that accuracy was not affected by the land damage and that the land damage could be attributed to firing from the fallback position.
6. Fifty M185 cannons were processed by Letterkenny Army Depot in the first seven months of 1980; none exhibited land damage.

Mechanism of Land Flattening and Land Stripping

The mechanism by which land flattening can occur was then formulated:

1. Large-scale drawings of the tube and projectile show that during ramming or during firings from a fallback position in the chamber, the bourrelet of the projectile can impact the rifling, hitting the lands at the 1/4-inch location from the beginning of rifling where the land flattening is observed.

2. The flattening downbore appears to be the result of radial balloting of the projectile as it accelerates forward, causing damage on opposite sides, 180 deg opposed, at spacings of about 3 in.

3. Downbore flattening may be more severe in some cases than the flattening at the origin of rifling because of the increasing velocity of the projectile as it is accelerated forward.

4. The recorded location of land damage at the 1/4-in. position, as listed in table 2, shows that the 12 o'clock to 4 o'clock locations are those having the highest incidence of damage. Damage at the 4 o'clock to 10 o'clock locations had a much lower damage incidence. This seems to indicate that the projectile may be moving upward and to the right in relation to the axis of the tube at the time it arrives at the origin of rifling.

The mechanism by which land stripping can follow flattening is then:

1. As illustrated in figure 6, land stripping may result from the movement of metal along shear zones created by the compression force of the bourrelet's striking the land and flattening it. Stripping may be the result of a single impact, or of repeated impacts from successive firings. It could produce fragments of lands sheared down into the grooves and could leave marks in the bottom of the grooves adjacent to the portion of the land that was stripped. Also, since the land material is harder than the rotating band or the projectile body, the fragments could embed in either of these and produce additional markings downbore.

2. Land stripping may be the result of the lifting action exerted by the near-fluid pressure from the rotating band material as it is being squeezed through the channel formed by the flattening of the land. Shearing action would then occur along the inclined planes illustrated in figure 7. The rotating band can then sweep away the sheared pieces as the projectile moves forward. This action would not require a very large lateral force and may occur progressively as the result of successive firings, one the lands have been flattened. This could produce land fragments and make markings downbore. The fragments would not mark the bottom of the grooves.

Land Damage Fault Tree

Consonant with these observations, a land damage fault tree was constructed (fig. 8).

Conclusions of the Root Cause Failure Analysis

1. Damage of lands at the beginning of rifling is the result of flattening of the lands by impact of the projectile bourrelet against them.

2. The most likely cause of flattening of the rifling lands is firing of projectiles from the fallback position.

3. Flattening of lands is also likely to occur during improper ramming.

4. Stripping of flattened lands can occur either by their being compressed and sheared by the projectile body or by being lifted and sheared by the copper of the rotating band. Stripping generally occurs on the driving side of the land, but also occurs on both sides of the land.

5. Downbore damage is most likely caused by balloting of rounds fired from the fallback position. It is unlikely that this damage would be caused during the ramming action.

6. Individual reasons for land damage are: (1) rotating band/forcing cone mismatch (most likely), (2) rammer-projectile misalignment (very likely), (3) improper rammer operation by user (very likely), and (4) inadequate rammer characteristics (likely).

7. The incidence of land stripping can be reduced or eliminated by ensuring that the projectiles do not flatten the lands during ramming, and by ensuring that the projectiles are not fired from the fallback position.

FALLBACK TEST, YUMA PROVING GROUND

Background and Purpose

First reports of projectiles' falling back into the chamber of the tube after ramming roughly coincide with the initiation of the long-tube howitzer conversion program in the 1972-1973 timeframe. These reports noted instances of short rounds while the M4 propelling charge was used and instances of inbore separation of metal ammunition parts. As a consequence, several investigations were conducted to determine the cause for fallback in the M109A1 SPH. These investigations centered either on the adequacy of the power rammer design used in the system, or on the projectile retention capability of the M185 cannon. This test at Yuma Proving Ground (ref 4), as part of the Damaged Lands Study, was intended to establish: 1. if a correlation existed between rifling damage, as reported, and projectile firings from a fallback position; 2. whether the rifling damage was the result of an interaction with loose projectile or fuze parts; 3. the severity of any damage sustained by the fallback projectile as gaged by metal parts integrity and the size, location, and number of cracks; and 4. the frequency at which failure occurred with fallback and the identifiable characteristics of the failure mechanism.

Test Procedure

Fallback was achieved by slowly pushing the round (inert M107 projectile) through the chamber into the forcing cone for a depth from the rear face of the tube of 39 in., loading the propellant and the two copper crusher gages, and then elevating the cannon until the sound of the shell's impacting the bag was detected. Provisions were made to record the sound of the shell as it fell back into the chamber. If, after bumping the cannon against the maximum QE stop, fallback had still not occurred, the cannon was depressed and the round was manually pushed into the chamber with a ramming staff.

All rounds were fired at 400 mils QE. After each round the forcing cone was scrubbed clean of residue and a 155-mm full-form go/no-go gage was applied to the rifling to detect land flattening. Then the tube from the origin of rifling to about 30 in. forward was inspected with a borescope. Borescope photographs of the rifling were taken before firing and after every four rounds. This schedule corresponded to a change either in the charge or in the zone used for firing. If damage was detected, photos and castings were taken as necessary to adequately document the initial damage and any subsequent damage as it progressed. Standard sound motion picture coverage was obtained of a selected number of firings to record the effects of propellant associated with fallback (blowby, muzzle flash, etc.). Smear and Fastex cameras monitored the area forward of the muzzle to check the metal parts integrity of the projectile and fuze, and the flight characteristics of the round. The projectiles, after firing and recovery, underwent visual and magnetic particle inspection for surface cracks.

A modified M1 towed artillery carriage served as a mount for the two tubes used in the tests (S/N 24715 and S/N 28317). Firings were remotely controlled from an instrumentation van. Test instrumentation included radar to measure muzzle velocity and five piezoelectric pressure transducers to monitor gas pressure variations over time. One transducer was mounted in the spindle and one each was mounted at 12, 19, 27, and 34.1 in. from the rear of the tube.

Results

The round-by-round test data are presented in table 3. The first eight rounds of the test were characterized by significant amounts of smoke and flame preceding out of the tube. After borescoping, no damage was observed and the rifling gage entered the tube without resistance. On the number nine round--the last in the scheduled series of firings with the M4A2 zone 4 charge--eight lands were partially stripped between the eleven o'clock and two o'clock positions, another eight were chipped, and all but three were flattened. Borescope photos of the damage can be seen in figure 9 and can be compared with the Government-of-the-Netherlands case (fig. 4). The comparisons reveal similar patterns of rifling land distortion and stripping. The nine shells fired were later recovered, inspected, and photographed (fig. 10). All except the number nine round appeared normal. The anomalous round had engraving marks on the ogive, body, and bourrelet. However, magnetic particle inspections failed to identify any surface

cracks in this or in any of the other projectiles. On the ninth round, photographic evidence of fuze damage was provided by smear cameras located just forward of the muzzle (fig. 11). In addition, this round was earmarked by a distinct foreshortening of the "Roman candle" effect so pronounced in the earlier fallback rounds. This suggests that the obturation in this case was both rapid and abrupt. Testing on tube S/N 24715 ended since the damage sustained was sufficient to warrant condemnation.

Testing continued on tube S/N 28317. The objective was to explore whether damage could be induced with charges and zones other than the M4A2 zone 4. No significant variations were made in the test plan outlined earlier. What was discovered was that a progressive-type failure can occur when either M4 or M3 mid-zone charges are used--mid-zone charge being defined as a zone 4, a zone 5, or a zone 6. This failure produced damage identical to that observed in the single shot case (fig. 12). Its progressive nature also served to provide insights into the characteristics and effects of a fallback event. Effects are a function of the charge and the zone used. Effects are charge-related in that M4 series charges generate more brilliant and catastrophic weapon effects. One can only speculate from the available data, but in examining a tabulation of weapon and charge parameters (table 4), it can be gleaned that the M4 charge has a squatter, more compact configuration which allows the projectile to fall back a greater distance into the chamber. In addition, in a zone-to-zone comparison with the M3, the M4 delivers higher velocities and greater ranges to the extent that there exists no zone-to-zone interchangeability. Extrapolating to firings in a fallback condition leads to the conclusion that projectile velocities at rifling land impact would be correspondingly greater with the M4 charge. Physically, the only material difference between the two charges is that the M3 has a single-perforated web of 0.016 in. nominal thickness, whereas the M4 has a multiple-perforated web of 0.032 in. nominal thickness. Both charges are composed of M1-type propellant.

The effects of projectile fallback are zone-related because of the combined influence of available volume and available energy. Low zone increments (zones 1 through 3) allow the maximum space for fallback travel in the chamber, but generate the least gas (table 4). This condition results in considerable blowby, in loss of energy, and in a round that either gets stuck in the rifling (a sticker), or is left in the chamber (a black round). Damage to weapon or ammunition components was not observed. Also, all high zone charges (zones 7 and above) offer the least chamber volume for fallback travel, but are the most energetic. The effects of firing from fallback under these conditions seem confined to decreases of 10 percent or less in the expected range to impact. These decreases are proportional to the energy lost in blowby.

Firings using mid-zone charges (zones 4 through 6) under fallback conditions have revealed the development of two courses of events. The first is that a significant portion of the propellant's energy is lost in blowby. Consequently, shortfalls of as much as 50 percent of range have been observed. There is, however, no concomitant observation of weapon or ammunition damage. The other course of events results in shortfalls of similar magnitude but, at the same time, severe weapon and ammunition damage occurs. Qualitatively, blowby is not so conspicuous, and obturation seems sudden. The projectile apparently enters the rifling at a high velocity and its momentum at impact converts into sufficient

energy to distort and strip the lands of the cannon. Moreover, the high axial acceleration of the projectile, resulting from its free run in the chamber, translates at full rifling engagement into a torsional twist's being abruptly imparted to the projectile. This impulsive twist can initiate relative motion between component parts of the projectile and fuze assemblies. Cargo and rocket assisted rounds and mechanical time fuzes are particularly susceptible to the adverse effects of this type of motion.

Results of stargage and borescope examinations of tube S/N 28317 revealed the following:

1. Very light carbon, stains, scratches, and other deposits throughout chamber.

2. Origin of rifling: (1) 12 o'clock, one land chipped, (2) 1 o'clock through 4 o'clock, 13 lands were sheared on driving edge of lands, (3) 4 o'clock through 5:30, lands were moderately flattened, (4) 6:30 o'clock through 11:30 o'clock, lands were moderately rounded with light-to-moderate gas erosion, (5) one land chipped or sheared at 9 o'clock, (6) two lands chipped or sheared at 11 o'clock.

3. Light to very light 360° coppering from origin of rifling to approximately 86 in. from rear face of tube.

4. Light carbon, stains, and scratches with very light machine marks at various times and distances throughout bore.

5. Condition of tube: Clean.

Examinations were scheduled prior to and following the test which consisted of 29 rounds. After 29 rounds, tube S/N 28317 was in a damaged but serviceable condition. A summary of smear camera observations is given in table 5 and sample photos comprise figure 13. Instability in projectile flight patterns was observed in 11 cases; fuze damage, in 4 cases. The instability was not predictive, that is, not associated with any charge/zone parameter. And, even though fuze damage occurred only with the M4A2 zone 4 charge, the sample size is too small to draw a definitive conclusion as to whether this correlation is unique and exclusive. A summary of the inspection conducted on the recovered projectiles is given in table 6. The type of projectile damage produced in firings from tube S/N 28317 is shown in figure 14. This should be compared with photos of round 9 from tube S/N 24715 (fig 10a). It is interesting to note that rounds 1, 2, 4, and 5 had distinctive engraving marks on the bourrelet whereas S/N 24715 exhibited no associative damage whatsoever.

Sample breech and chamber pressure curves are provided in figures 15a through 15k. A comparison of peak pressure values for rounds 7 and 8 (figs. 15a and 15b) revealed a 1/3 drop in magnitude for equivalent ammunition in an identical weapon. This demonstrates the wide unpredictable variations in the ballistics of "fallback" firings (in this case, with an M4A2 zone 4 charge, the instantaneous projectile velocity for round 7 was 266.1 m/s whereas for round 8, it was 194.0 m/s). This dramatic pressure reduction is caused by gas blowby which, in turn, fuels the spectacular visual signature characteristic of fallback, that

which was earlier termed the "Roman candle effect." The signature of a fallback round's producing damage is a choppy, erratic pressure curve as exemplified by figure 15g. This erratic behavior is coupled to a relatively short rise time, when compared to rise times of other fallback rounds; e.g., compare 26.3 msec, the average rise time for the breech pressure curve of round 9, all rounds being M107 projectiles with M4A2 zone 4 charges. Selected values from the instrumented rounds were tabulated (table 7) and pressure profiles distinguished by an abrupt, erratic signature were annotated.

Conclusions

To summarize, firing a projectile from an unseated position in the chamber is the prime cause of rifling land damage in the M185 cannon. In conjunction with weapon damage, adverse ammunition effects have been demonstrated. However, only limited observations of one type of projectile-fuze combination were documented. Further observations of all types should be made. Although not all fallback rounds are damage producing, those using M4A2 zones 4 through 6 are the most suspect. Damage-producing rounds are not predictable nor discernible from other fallback rounds except under test conditions. Fallback firings, in general, have a distinctive signature identifiable under most circumstances by an aware observer. Shortfalls of 5 to 50 percent of range can be expected, depending on the charge/zone used.

RAMMING TEST, PICATINNY ARSENAL, ARDC

Purpose and Assumptions

The purpose of the ramming test was to determine if the rifling damage in the M185 cannon could be directly associated with the mechanism used for power ramming a 155-mm M107 projectile in the M109A1 weapon configuration. The assumption was that projectile balloting in a new M185 cannon would result in accelerations of such magnitude as to damage the rifling lands when the round enters the bore. The damage would take the form of a distortion or flattening of the lands at the origin of rifling, would appear in cross section as a mushroom overhang, and would lead to stripping of the sidewalls or to chipping of the lands during firing(s).

Test Procedure

The power rammer of the M109A1E1 test vehicle was returned to an M109A1 configuration with parts obtained from Letterkenny Army Depot. The rollover switch was removed from its normal position in the rammer tray and manually activated during the test to allow time for preparing the round. Rammer reliability and zero pressure checks were performed in accordance with the instructions in

the M109A1 operators manual to confirm the rammer's operational readiness (ref 5). A tube with 98.7 percent remaining life--based on a service life of 5000 effective full charges--was mounted on the vehicle. A go/no-go rifling gage furnished by Watervliet Arsenal provided the means by which any distortion of the lands that occurred during the test would be detected. In the event that the tube was damaged, a borescope was on hand for visual inspection and for taking photographs to document the initial damage and any damage progression. The d.c. power to the hydraulic pump was supplied by the vehicle and maintained by idling the engine at 1000 rpm. Hydraulic temperature was monitored at the reservoir and hydraulic pressure at the outlet port of the power pack/accumulator. Accelerometers were mounted on both the rammer head and the inert M107 test projectiles to record motion. On the rammer head, a single axis, low-g range accelerometer was oriented so that its sensitive axis paralleled the center line of the tube (i.e., the z-axis). On the projectile, 3-axis sensitivity was employed with the z-axis having both a high-g and a low-g range (1000 g and 10 g, respectively). A modified lifting plug with eye removed, served as a foundation for the accelerometer housing. Supplementary data collected during the test included the depth to ram from the breech ring, the extraction force, and the length of band engraving. Figure 16 describes the deram equipment consisting of a push rod with a bell-shaped head, a load cell and a hydraulic cylinder and pump similar to that used in an earlier M109A1 Fallback study (ref 6). The triaxial accelerometer wires were threaded through the bell shaped rammer head and through the centering guides to the recording equipment. The modified plug with accelerometer housing was screwed on/off each test round prior to/following the ram. Rounds were rammed only once.

Results

Projectile motion in an XY plane of the tube (i.e., the z-axis on tube centerline) has been termed balloting. Such balloting of the projectile from the powder chamber to the bore is enhanced in a cannon with a chamber that does not have a constant diametral taper throughout. The steep diametral taper forming the forcing cone region of the M185 cannon is an example of this phenomenon (fig. 3). Gawreluk (ref 7) differentiated this region of the cannon by its binding effect on the projectile and by the significant and abrupt loss of loading energy that is incurred during ramming. In Gawreluk's investigation, however, the concern was what effect this had on power rammer performance. This test is concerned with whether the energy that is transferred during impact will cause plastic deformation of the rifling lands.

To determine the angular displacement of the tube at which projectile balloting was most severe--as gaged by accelerations in the XY plane--a series of rounds were rammed at 0, 100, 300 400, 500, and 700 mils. The results for two points in the forcing cone where the projectiles made contact are presented in tables 8 and 9. From this data and from a qualitative examination of the curves, a 700-mil elevation was deemed to produce the overall worst-case balloting situation in the tube. Out of a total of 216 rounds, 190 were rammed at this elevation, after which tube S/N 26066 revealed copper deposits and debris but no damage (fig. 17).

The round-by-round results for the data collected on-site during the test included depth of ram, length of band engraving, and extraction force. Comparison of data from the 700-mil case with that collected for all cases did not reveal any significant differences (table 10). The value of 38 1/2 in. for the depth of ram in round 8, together with a 1/16-in.-length of band engraving, indicates that during this event the round fell out from a seated position. This was attributed to human error and specifically to the inadvertent and premature termination of the ramming cycle. Consequently, no extraction load was recorded for this event. A bar graph of extraction loads for the 190 rounds which make up the 700-mil case is provided in figure 18. The results appear to follow a normal distribution.

Follow-Up Data Reduction

Accelerometer data for the first 25 rounds were reduced following the test. Representative curves are provided for rounds 4, 8, and 12 as figures 19 through 21. For clarity, the rammer head velocities are depicted 180 degrees out of phase from the projectile velocities. Due to a computer idiosyncrasy in the integration of the acceleration data, the velocities do not return to a zero baseline after projectile seating; in reality, they should. The output from the low-g range accelerometer, whose sensitive axis was oriented along the centerline of the tube, displays a maximum positive peak at second stage, rammer cylinder extension. Rammer motion for each of 25 events has been quantified in terms of velocities and low range accelerations, presented in table 11 and recapitulated in table 12. At the high range, projectile contact with the forcing cone, projectile bourrelet contact with the forcing cone, and projectile seating can be discerned (fig. 19). The region of the plot where seating occurred has been isolated and magnified. Seating loads and seating velocities were reviewed to determine if a correlation to the extraction force existed. Round 8 had a seating load of -411 g, a seating velocity of 8.8 ft/s, and a zero extraction force (table 13). If a correlation existed, it was not consistent.

RAMMING TEST ADDENDUM, PICATINNY ARSENAL, ARDC

Purpose

As an addendum to the ramming test, a brief investigation was conducted into a report that the M107B2 projectile is inadequately retained by the M185 cannon. The report by the Army of the Netherlands stated that the M107B2 was involved in a projectile fallback incident.

of the rifling damage was thought to be quantifiable as an irregularity in the axial acceleration of the projectile, an increase in the initial loading of the projectile in torsion, or an increase in inbore balloting. The first of these could be the result of perturbations in the breech pressure due to propellant gas blowby, or the result of variations in the resisting force (the frictional force) along the surface of contact with the tube. The increase in inbore balloting, in the pitch, and in the yaw motion of the projectile can result from the nonuniform acceleration of the projectile. Lastly, increased torsional loading could result from an increase in projectile free run. Free run can be defined as the distance a projectile has traveled in an artillery tube after primer ignition before it experiences the torsional impulse, or the abrupt increase in angular acceleration, which is linked to the full engagement of the rotating band with the rifling. Torsional impulse will increase with an increase in free run because of the direct relationship between the axial and angular acceleration of a projectile; that is:

$$\alpha = \frac{At}{R} = \frac{(\pi/20)Ax}{R}$$

Where

α = the angular acceleration

At = the tangential acceleration

R = the maximum radius of contact between the shell and tube

Ax = the axial acceleration

$\pi/20$ = the rifling twist; that is, one revolution in 20 calibers

All projectiles experience some degree of free run because, after ramming, they seat at some finite distance from full depth rifling. The free run of a 155-mm projectile in the tube is roughly 1/2 in. This value has been approximated by using figure 24 (taken from ref 9) and calculating $(X + Y) - (R + L)$. If the rotating band were fully engraved at seating (i.e., if the projectile's free run were zero), axial and angular accelerations would occur simultaneously.

The repercussions of inbore axial, lateral, and angular perturbations in a projectile's motion can be ordnance damage, gyroscopic instability of the projectile in flight, and deviations from expected deflection and range to impact. The damage reported on the tube may, in itself, be the direct or indirect results of these anomalies in projectile accelerations and, more specifically, the result of shell balloting. A torsional load will foment damage if the load exceeds the ability of the projectile to transmit it across component interfaces in the assembly. This ability is determined by the friction factor whose value in a tube with a one-in-twenty twist is ideally $\pi/20$. The inability to transmit the load will result in slip, and this slip may stress an explosive joint in the projectile. The torsional impulse problem is more commonly associated with the land erosion resulting from tube wear. But, because the reported damage to the M185 cannon has typically been localized at or near the origin of rifling, the existence of a similar type problem, stemming from a different cause, was suspect

From reference 10, the maximum torsional load for the M107 projectile can be computed from the maximum setback load:

$$\alpha_{M107} = \pi/20 \times 1/R \times A_x$$

where for the M185 cannon tube

$$R = 3.05 \text{ in.}$$

$$A_x = g \times 9350 \text{ g}$$

so that

$$M107 = 186 \times 10^3 \text{ rads/s}$$

Likewise the maximum torsional loads for M483A1 and M549A1 projectiles are 168×10^3 rads/s and 199×10^3 rads/s, respectively.

An array of five accelerometers--four tangential, positioned 90 degrees apart, and one axial--was housed in a collector cup (fig. 25) mounted on a modified M107 projectile. The projectile was an inert type cut to a length of 21 in. (excluding the base plate) and drilled and tapped to 3.25-12UN-2B to accept the accelerometer housing. The projectile was then weighted to 86.25 pounds using an inert filler. The housing was designed such that its resonant frequency, about 30 kHz, exceeded the frequencies inherent in the projectile's motion. The mass of the housing, however, necessitated the modification of the test projectiles to achieve a ballistic match with the nominal case in weight, height to center of gravity, and transverse and polar movements of inertia. A computer algorithm was used to model the nominal case and to generate a ballistic match between the model and a projectile with a collector cup housing by a manipulation of model parameters. The results of this effort, which were considered acceptable, are shown in table 17.

For the axial mounting, Kulite GS-500-10-10000 accelerometers were used; for the tangential mounting, Kulite GS-500-10-2500's were used. The Kulite 2500 series accelerometers--the 2500 indicating rated g capacity--have a maximum specified cross-axis sensitivity of 3 percent. Cross-axis sensitivity is the unwanted response to forces directed perpendicular to the axis being measured. The output from the tangential accelerometers will include reactions to both the centripetal and axial accelerations of the projectile as well as those balloting accelerations whose sense is parallel to the sensitive axis of the accelerometer. In terms of magnitude, the effect on the output from these transverse responses can be ascribed primarily to the axial term during early projectile motion. The centripetal term will rotate the sense of the cross axis vector that sums these transverse responses. Therefore, assuming a constant cross axis sensitivity (i.e., independent of the orientation) and neglecting all but the axial term in the cross axis effect on the output, the magnitude of the output from a tangential accelerometer can be quantified as:

$$a_T = \frac{\pi}{20} \times \frac{r}{R} A_x \pm 0.03 A_x$$

where

a_T = the output from the tangential accelerometer with no projectile balloting

r = the mounting radius which is 2.5 in.

R = the maximum radius which is 3.05 in.

A_x = the axial acceleration

so that

$$a_T = (0.129 \pm 0.03) A_x$$

This direct relationship between the tangential accelerometer output and the axial acceleration will be sensitive to balloting forces and the anomalous effects on acceleration caused by the rifling damage. By adding and subtracting outputs from accelerometers 180 degrees out of phase, the forces due to balloting can be isolated from the tangential or torsional forces and identified. That is, assuming the balloting force can be resolved into components which are perpendicular to the axial or x-direction and assigning quarter clock positions to the four tangential accelerometers, we have at any single moment in time:

$$a_{12} = a_T + A_{Bz}$$

$$a_3 = a_T + A_{By}$$

$$a_6 = a_T - A_{Bz}$$

$$a_9 = a_T - A_{By}$$

where

A_{Bz}, A_{By} = the components of the balloting acceleration in the z, y plane

The axial term in this expression will be measured directly with the axial accelerometer and compared to the ideal value computed from the breech pressure. The rise of breech pressure over time will be monitored with a transducer mounted in the spindle. In this way, any irregularity in the axial motion of the projectile due to rifling damage can be isolated.

The accelerometers housed in the collector cup were wired directly to the requisite electronics and recorders. This method is good only for early motion (about 6 in. of projectile travel) but it saves the cost of telemetry. Ten rounds were fired with an M119A1 propelling charge at ambient temperature (70° F). Five rounds were fired from a damaged tube and, for comparison, five were

fired from an undamaged tube with similar overall wear. Each round was slowly hand-rammed into a seated position to avoid any balloting of the collector cup in the chamber. Ignition time was established by means of a micro-miniature semiconductor strain gage mounted in the firing lock. The range data from the firings are provided in table 18.

Evaluation of Results

The range and deflection data collected during phases A and B were compared to the values published in firing table FT-155-AM-1. These comparisons are provided in tables 19 and 20. They show that the actual values from both the damaged and the undamaged tube firings proved in some cases better, and in some cases worse, than the predicted range and deflection values. There were, however, two cases in which acceptable norms were exceeded and both appeared in the damaged tube group. Specifically, the 6000-m series, with the M4A2 zone 7 charge, exceeded the probable error of 0.50% of range; and the 10,000 meter series, with the M4A2 zone 5 charge, exceeded the probable error of 1 mil in deflection. Figure 26 graphically depicts the probable error values received in both groups of firings (from damaged and undamaged groups) and their relationship to frequently applied criteria. The outliers are indicated with arrows. Plots of the aim point, impact coordinates, and the statistically generated center of impact for the 6000-, 9000-, 10,000-, and 12,000-m groups are given in figures 27 through 30. Special attention should be given to plots of the 9,000-m groups which provide a visual reference for comparing firings from a damaged tube with those from an undamaged tube.

The results of the M483 firings, presented in table 21, were compared with the published values in firing table FT-155-AN-1, "Table G: Supplementary Data for Projectile, HE, M483A1 and Fuze, MTSQ, M577." There is a variation from the firing table (FT) values of about 5 m in range probable error and 4 m in deflection probable error. The 6 August 1981 and 7 August 1981 firing groups are plotted (fig. 31). The unusual number of duds observed during testing prompted a follow-up investigation to learn the probable cause. The acceptance test record on M577 fuze lot no. BWV79L008-029 (ref 11, JPG Firing Record No. 79-1082) was requested from the Nuclear and Fuze Division of the Large Caliber Weapon Systems Laboratory (LCWSL). This record documented the firing of 20 rounds from a 155-mm howitzer. Of these, there were no outliers, offtimes, or duds. A review of peak chamber pressures, muzzle velocities, and spin rates by APG confirmed that the fuzes had been subjected to the required setback forces and spin rates for fuze arming. From this it was concluded that the most likely cause for the modifications was the type of spotting charge used and not the M577 fuze or the rifling damage in the M185 cannon.

The M549A1 range and deflection data were compared to those reported by a BRL publication in March 1979.² This comparison was necessary because of the

² Test data, "Provisional Aiming Data for Cannon, 155-mm Howitzer, M199 on Howitzer, Medium, Towed, 155-mm, M198 Firing Projectile, HE, M549A1, Rocket Off."

unavailability of a firing table for an M549 projectile with rocket off, fired from an M185 cannon, mounted on an M109 SPH. The range and deflection probable errors from the test were greater than the 45 m and 9 m, respectively, predicted by the BRL data at 15,000 m (table 21). However, the validity of the correlation between sets of data is uncertain so the difference in values is not quantitative. A plot of the M549A1 range and deflection data is given in figure 32.

A summary of the fuze functioning, muzzle velocity, and spin rate data collected during phases A through C of the test is given in table 21. APG considered the 3 percent difference between the calculated and observed spin velocities of the M107, M483, and M549 projectiles to be within the reading error of the smear film. In the check on projectile obturation, a small amount of gas preceded the projectile out of the gun tube. The amount was not considered excessive. Stargage measurements that were taken periodically during the test revealed a pattern of normal wear. No significant changes developed between initial and subsequent inspections. Photographs of two damaged regions in tube S/N 25460 comprise figure 33. After 153 rounds, photographs of the same clock position at the origin of rifling show the smoothing of areas of land shear and the rounding of sharp edges (fig. 34). Although new damage was not observed, land damage sustained prior to test did progress and was manifested in the removal of metal along well developed crack lines. Compare figure 39c with figure 40c.

The Applied Science Division of LCWSL performed the analysis of phase D of the degradation test.³ Samples of the data from phase D are provided as the appendix. The measured data, after digitizing at 50 kHz and filtering at 10 kHz consists of the breech pressure curve and the curves of tangential accelerations and of actual axial acceleration. From the breech pressure curve, the ideal linear displacement, velocity, and acceleration were obtained. Actual linear displacements and velocities were determined by integrating the actual axial acceleration. The remaining data sets describe:

- average tangential acceleration versus time
- axial acceleration versus pressure
- tangential acceleration versus axial acceleration
- half the difference between opposite tangential responses versus time
- half the sum of opposite tangential responses versus axial acceleration

Since the hard wire approach was chosen, data received following a short or break will be questionable. The location where the first data break occurred--as identified by the time, the distance traveled, and the spindle pressure--is provided

³ Kenneth Klingeman and Richard W. Collett, "Accelerometer Tests in Damaged Land Gun Tube," unpublished report.

for each round in table 22. Rifling damage in tube S/N 25460 occurred at the origin (12 lands), at 5 in. (14 lands), and at 9 in. (10 lands) forward of the origin. Consequently, passage over a major segment of the damage region (less than or equal to 5 in.) was consistently monitored by all channels. Point data taken at the 5-in. mark were tabulated (table 23). Since the ideal motion, derived from the breech pressure curve, seems to typically start prior to the recorded actual motion, a baseline time coinciding with 1,000 psi on the pressure curve was a best-fit solution for comparing motions. The percent differences between the ideal and actual axial acceleration data in both damaged and undamaged sets are large and nonuniform. This apparently is due to the random perturbations in the curves themselves, making correlations between like points or like segments unreliable. This is also true of the tangential acceleration data.

Since there were no observed instances of rotating band separation (all spin velocity values were of an acceptable order), it may be assumed that the data on the angular twist associated with full rifling engagement were collected. If it is also assumed that the instrumentation was operating properly, then when the output from the tangential accelerometer is compared to that from the axial accelerometer, the result should be a straight line whose slope is 0.129. Choppy lines could be due to a torsional impulse or balloting, and, with errors and uncertainties, the actual slope of the curve could deviate as much as 25 percent from the absolute value. In a review of the curves, it was evident that although some curves approximated a straight line, others did not. Removing balloting effects by averaging the outputs from opposing pairs of tangential accelerometers does not alter this effect. It can also be seen, from table 24, that the observed slope of the curve in many cases exceeds the upper or lower bounds set by routine uncertainty and predicted errors. Whether these general results are due to the use of the wrong sensitivity or a change in the sensitivity from the calibration during test setup is not clear. The conditions of the test itself--wires that could be run over, crimped, or stretched during the ramming of the projectile--could lead to a failure or to erratic behavior of the test equipment.

The observations made of the various curves were as follows:

- There are two kinds of pressure curves: those that seem smooth and those that are not. Both types appear in each firing group.
- The shapes of the axial acceleration-versus-pressure curves are similar for those cases where the pressure curves are similar.
- Where there are changes in the slope of the axial acceleration-versus-pressure plots, peaks or valleys occur in the tangential-versus-axial acceleration plots.
- For those cases where the output from opposing pairs of tangential accelerometers appeared consistent, there is evidence of:

Balloting forces having frequencies of the order of 500 Hz

Slight torsional impulses at early motion. These impulses seem to have approximately the same magnitude in both groups.

Since these effects were observed in both firing groups, any deviations from expected behavior seem unrelated to whether or not rifling damage was present. The torsional and balloting effects discernible in some rounds may have been the result of minute differences in seating or some other aspects which were peculiar to the configuration of these rounds prior to firing.

Results and Conclusions

In summary, for projectiles fired in test phases B and C, the deviations from the referenced values for the probable error of range and deflection can be measured in a proving ground environment, but the magnitude of the deviations would be negligible in a battlefield environment. The inbore forces on phase D projectiles instrumented with an array of axial and tangential accelerometers and fired in a damaged gun tube (tube S/N 25460) were not observed to be significantly different from those fired in a normal gun tube with the same overall wear (tube S/N 23418). Moreover, no forces were observed that would produce any additional hazard to the safe operation of the projectile/fuze system.

TUBE INVESTIGATION

Discussion

An investigation into the manufacture, processing, and physical and metallurgical characteristics of the M185 cannon tube was conducted by Watervliet Arsenal and Benet Weapons Laboratory in an attempt to identify any shortcoming which would lead to land damage in the tube or which would help categorize the tubes which were damaged. The results follow:

1. The quality assurance records of 14 of the damaged tubes were compared to a random sample of 28 tubes produced during the same timeframe at Watervliet Arsenal. The material and mechanical properties of these tubes were statistically evaluated and results are shown in tables 25 and 26, respectively. No significant differences between the damaged tubes and the sample were noted at confidence levels below 95%.

2. A review of the available historical data on the production of the tubes which showed damage revealed no singularities.

3. Gun records of damaged tubes were compared to those of tubes with similar overall wear, as gaged by effective remaining service life. A strong correlation exists between the age of the tube and the presence of damage. Relatively new tubes seem most likely to sustain damage. This suggests that the progressive effects of heat checking the metal may alleviate or minimize this phenomenon. The kind of service rounds fired does not appear to be directly associated with the damage. Excluded, of course, are deviations from normal accepted use and any defects in manufacture.

4. All M185 cannon tubes are mechanically swaged for autofrettage by pushing an oversized mandrel through the lubricated bore of the tube. The autofrettage process induces residual compressive stresses in the tube which improve its ability to overcome firing stress. There exists some evidence that as over-strain from autofrettage increases, there is a corresponding decrease in impact energy, the change being slightly greater with a decrease in the local temperature (ref 12). It should be noted that the same evidence indicates that material yield strength increases with autofrettage.

5. A metallurgical examination of tube S/N 25396 was conducted by the Advanced Engineering Section of Benet Weapons Laboratory. The conclusion arrived at by macro and micro examination and photography was that damage was due to a heavy, high velocity blow which flattened and distorted the lands. The distortion, with microcracking and clear-cut adiabatic shear zones, provides a desirable path for land stripping on successive rounds. Adiabatic shear zones are typified by a fine-grained, untempered martensitic structure with an apparent absence of retained austenite which together suggests an extremely rapid heating and quenching process within a localized region (ref 13). Adiabatic heating normally occurs during a deformation of the metal at high strain rates and can result in a decrease in the local flow stress. Cracks progressing along adiabatic shear zones can consequently be arrested by a relaxation or redistribution of the stress in the metal matrix. Without stress relief, failure generally ensues.

Change Recommended in Condemnation Criteria

Based on a review of the data collected in this investigation and particularly on a report of the performance of damaged tubes in ballistic tests conducted at APG (ref 6), BWL initiated a change to TM9-1000-202-14, "Evaluation of Cannon Tubes," which acknowledged the frequent presence of damage to the lands in the area up to 10 in. forward of the origin of the rifling. Damage of this type would not be cause for condemnation and if succeeding rounds are properly seated, there would be no effect on ballistics (fig. 41).

The recommendation is consistent with the observation made in the now superseded publication, "Evaluation of Erosion and Damage in Cannon Bores (TB-9-1860-2)," which is:

"In medium and high velocity guns, a flattening of the lands has the same effect as an equal amount of erosion. In low velocity weapons, a large number of lands missing at the origin, flattened lands, chipped edges, or sheared sidewalls have a negligible effect."

RESULTS AND CONCLUSIONS

1. Damage to the rifling lands of the M185 cannon is due to a heavy, high velocity blow as would occur from firing projectiles from an unseated position in the chamber of the tube. Such firings have been termed fallback.

2. A single fallback incident is sufficient to cause land damage, but not every fallback round is damage producing. Fallback firings with mid-zone charges (zones 4 through 6) have the greatest likelihood of effecting damage to the tube. Stickers, or projectiles which fail to exit the tube, will normally result when a zone-3 charge is used due to the magnitude of the fallback-associated propellant gas blowby.

3. Shortfalls of as much as 50 percent of expected range will occur with fallback. In general, the lower the charge zone used, the greater the probable error in muzzle velocity and the greater the shortfall.

4. Projectile and fuze damage may occur during fallback firings. However, though the damage noted did not appear to be severe, insufficient information was collected to determine what repercussions the observed damage had on safety. Since inert M107 projectiles and inert fuzes were used in the fallback test, the consequences of fallback firings with high explosive rounds and live fuzes, or alternative projectile/fuze combinations, would be speculative.

5. Fallback firings have a definitive signature characterized by smoke and flame which precede the projectile out of the cannon.

6. Fallback will not occur if the projectile is within production specifications and is seated properly. Factors which inhibit the consistent occurrence of a proper seat are the variability of the available time for ram completion, which may result in a short ram, and the steep forcing cone of the M185 cannon, which allows the projectile to bind in the tube short of a seated position. The first factor may be obviated by design of a rammer to respond to flow conditions within the hydraulic circuit rather than to a timer. The second factor may be surmounted, without changing the profile of the tube, by modifying the rammer head to assist the projectile through the bind position.

7. The kinetic energy of a projectile during the ramming operation is insufficient to be responsible for flattening or distorting the lands.

8. An examination of the physical and mechanical properties of a damaged tube failed to reveal a metallurgical problem which could be held culpable for the damage. Moreover, there were no significant differences noted in a comparison between the properties of damaged tubes and a random sample of tubes produced during the same timeframe.

9. A slight difference exists for the probable error in range and deflection of the damaged tube when compared to an undamaged tube of similar overall wear. The spin rates of projectiles exiting the damaged tube were equal to the referenced values within the measurement uncertainty.

10. Land damage at or near the commencement of rifling will not significantly affect the interior ballistics of the M185 cannon. Specifically, no inbore forces were observed which would produce a hazard to the safe operation of the projectile/fuze system. Consequently, such damage will not be cause for tube condemnation.

RECOMMENDATIONS

1. A limited data base is available on whether a fallback problem is pertinent to the M549 and M483 families of projectiles. If such a problem exists, the effects of firing these projectiles from a fallback position should be investigated.

2. Firing from a fallback position should be simulated by computer to identify what deleterious effects, if any, are sustained by the fuze. In particular, it should be ascertained if a malfunction of mechanical time fuzes will occur. This is suspect because of the torsional twist imparted to the fuze at full rifling engagement following the free run of the projectile in the chamber.

3. A modification to the rammer head is being explored by the United Kingdom to resolve the problem of projectile binding in the M185 cannon tube (ref 14). The design of this modification should be examined by the U.S. Army for application to its family of M109 SPH.

4. A determination should be made as to whether the wear of the M185 cannon tube is affected by the presence of land damage at or near the commencement of rifling.

5. It is desirable that, when and where possible, the rough surfaces of lands with chipped or sheared sidewalls at or near the commencement of rifling be stoned or filed to prevent problems with projectile loading and to prevent fragments from embedding in the projectile and causing damage downbore.

6. If a study of inbore forces is repeated, it is recommended that either a torsional accelerometer be developed for virtual insensitivity to cross axis effects or that provisions be made that these effects are accurately accounted for during the calibration of the applied sensors. Also, longer lasting, more meaningful data could be gathered if the sensors were coupled to a wireless telemetry system.

REFERENCES

1. "Evaluation of Erosion and Damage in Cannon Bores," TB 9-1860-2, Department of the Army, Washington, D.C, 29 November 1945.
2. Firing Report No. 12827, Yuma Proving Ground, Yuma, Arizona, 6 June 1974.
3. William J. Pryor, "Safety and Interoperability Agreements on Bilateral Use of Artillery, Tank, and Mortar Ammunition During Training--Germany, the United Kingdom, Canada, the Netherlands, Belgium, France, and the United States," Special Publication ARLCD-SP-79003, ARRADCOM, Dover, New Jersey, October 1979.
4. Firing Report No. 81-55-0183-L5, Yuma Proving Ground, Yuma, Arizona, 21 September 1981.
5. "Operation and Maintenance Manual (Crew) for Howitzer, Medium, Self-Propelled 155-mm M109 and 155-mm M109A1," TM-9-2350-217-10N, Department of the Army, September 1979.
6. Thomas L. Brooks, "M109A1 Self-Propelled Howitzer Fallback Investigation," Technical Note R-TN-74-011, Rock Island Arsenal, General Thomas J. Rodman Laboratory, Rock Island, Illinois, April 1974.
7. D. Gawreluk, "Projectile Fallback Investigation in the M185 Cannon (M109A SP Howitzer)," Final Report R-TR-75-041, Rock Island Arsenal, Rock Island, Illinois, July 1975.
8. Firing Record No. P-82914, Aberdeen Proving Ground, Maryland, 11 May 1982.
9. J. Kammerer, "155-mm Artillery Weapon Systems," Reference Data Book, U.S. Army ARRADCOM, LCWSL, May 1980.
10. Science Application, Inc., "Torsional Impulse in Artillery Tubes, vol I," ARRADCOM Product Assurance Directorate Report DRDAR-QAN-59-82, Dover, New Jersey, November 1982.
11. Firing Record No. 79-1082, Jefferson Proving Ground, Madison, Indiana, 14 January 1980.
12. H. Goodheim, L. Alix and V. Calangelo, "Effect of Overstrain in Autofrettage Upon Mechanical Properties of Gun Tubes," Memorandum Report ARLCB-MR-80041, ARRADCOM, LCWSL, Benet Weapons Laboratory, Watervliet, NY, October 1980.
13. Peter A. Thornton and Francis A. Heiser, "Observations on Adiabatic Shear Zones in Explosively Loaded Thick-Wall Cylinders," Metallurgical Transactions, vol 2, May 1971, pp 1496-1499.
14. A. T. Leonard, "Supplementary Report to Development Branch Report No. 26 on the Investigation into the 'Fallback' of Projectiles in Howitzer 155-mm SP M109A2," Report No. 27, Quality Assurance Directorate (Ordnance), August 1983.

Table 1. 155-mm M185 cannon damaged lands reports

Tube S/N	Date	No. of rounds as of 9 Oct 1981	EFC as of 9 Oct 1981	Source	No. of lands damaged	Position of damage (o'clock)	Remarks
22683	Later than Mar 1974	96		B-Btry 2d BN 39FA WAM 580			Damaged at origin.
22825	May 1975	36	9.0	B-Btry 1st BN 22FA WA FS80	17	10-2:30 stripped 2-10:10 flattened	Damaged at origin. Mainz Army Depot reported.
25363	Oct 1979	88	26.5	Netherlands	12	10-5	Damaged at origin.
25396	Oct 1979	40	10.0	Netherlands	7 5 3 17	6-8 3 11 13 cm from start rifling 10-2	Condemned. Shipped to WVA.
25418	Jan 1980	173	47.25	Netherlands	5 24	12-4 light damage	Damaged at origin.
25421	Oct 1979	279	89.5	Netherlands	5 23	12-4 light damage	Damaged at origin.
25403	Oct 1979	735	183.75	Netherlands	13	12-3	Damaged at origin. Shipped to WVA.
25385	Jan 1980	148	37.75	Netherlands	14	9-12	Damaged at origin.
25460	Oct 1979	268	83.00	Netherlands	12 14	2-4 13 cm from start rifling 2-4	Condemned. Shipped to WVA.
25434	Jan 1980	261	83.75	Netherlands	9	1-4	Damaged at origin.
25369	Oct 1979	230	67.50	Netherlands	16 5	12-3 8 cm from start rifling 7-8	Condemned.

EFC--Effective full charge
WA--Watervliet Arsenal

Table 1. (cont)

Tube S/N	Date	No. of rounds as of 9 Oct 1981	EFC as of 9 Oct 1981	Source	No. of lands damaged	Position of damage (o'clock)	Remarks
24604	Oct 1978	120		United Kingdom			Damaged at origin.
26722	Jun 1979	202		Fort Hood	15	2-5:30	Damaged at origin. Pieces missing.
22561	Aug 1979	1341	411.0	Nebraska National Guard (Camp Gearney)			Partial damaged lands at origin. Rejected at WVA after borescope inspection for reported crack.
24202	Mar 1980		201.75	Canada	5	1	Damaged at origin.
24390	Feb 1980		442.5	Canada	8	12	Damaged at origin.
24094	Feb 1980		144.0	Canada	7	12	Damaged at origin.
22921	Aug 1980	814	210.5	Ft. Polk, LA 2nd BN 21FA	20 4 flattened	11-4 9-10	Condemned.
22894	Aug 1980	827	214.75	Ft. Polk, LA 2nd BN 21FA	10 32 flattened	2-4:30 5-1	
24042	Sep 1980	571	242.25	Nat. Guard found at LEAD	12 36 flattened	12-3 3-12	On hold at LEAD in special purpose code.
24351	Aug 1980	80	20.00	Netherlands	23	10-2	Damage at origin.
25371	Aug 1980	161	42.25	Netherlands	18	10-2	Damage at origin.
25386	Oct 1980	142	41.50	Netherlands	18	12-3	

LEAD = Letterkenny Army Depot

Table 2. Recorded location of land damage

<u>Units</u>	<u>Tube S/N</u>	<u>Position from origin of rifling</u>			
		<u>0.6 cm</u>	<u>8 cm</u>	<u>13 cm</u>	<u>23 cm</u>
		<u>(o'clock positions)</u>			
Canadian	24094	12			
Canadian	24202	1			
Canadian	24390	12			
Netherlands	25363	10-5			
Netherlands	25369	7-8	12-3		
Netherlands	25385	9-12			
Netherlands	25396	6-8			
Netherlands	25396	3		10-2	
Netherlands	25396	11			
Netherlands	25403	12-3	7-8		
Netherlands	25418	12-4			
Netherlands	25421	12-4			
Netherlands	25434	1-4			
Netherlands	25460	2-4		2-4	7-10
United States	26722	2-5:30			

Table 3. Fallback test, round-by-round data

Chg./Zone	Time fired (MST)	Tube round no.	Test round no.	Copper gage pressure (psi)	Breach pressure (psi)	Inst vel (m/sec)	Projectile weight (lb)	Fall-back at Q ^a (mil)	Range (mil)	Defl (R) ^b (mil)	TOFC (sec)	Remarks			
Date fired: 31 March 1981				Tube S/N 24715											
M3A1/4	1154	1	1	16.4	114.5	1,0307	71.0	377.1	95.1	43.14	920	7462	59	26.7	Stuck round. Data are for an M3A1, Z/5 used to clear the stuck round.
	1240	2	2	-	-	5,748	39.6	209.0	95.1	43.14	-	1,334	-472	19.6	Slight marking of two lands at 12:00 after this round.
M3A1/4	1321	3	3	-	-	7,470	51.5	250.1	95.0	43.09	-	4,158	18	20.1	
	1341	4	4	-	-	7,555	52.0	257.3	95.0	43.09	-	4,352	36	20.6	
Date fired: 1 April 1981				Tube S/N 28317											
M3A1/4	0936	5	5	6.3	43.4	5,001	34.5	202.0	92.25	43.20	-	2,672	-23	19.3	
M4A2/4	0953	6	6	7.8	53.8	6,321	43.6	259.9	95.25	43.20	400	5,401	295	21.5	
	1018	7	7	7.6	52.4	6,083	42.0	266.1	95.0	43.09	-	4,566	-103	21.4	
	1036	8	8	5.2	35.9	3,957	27.3	194.0	95.15	43.16	-	2,573	3	19.3	
M4A2/4	1057	9	9	6.2	42.7	4,917	33.9	247.8	95.10	43.14	1,100	4,105	15	20.6	Severe tube damage.
Date fired: 8 May 1981				Tube S/N 28317											
M4A2/7	1026	1	10	28.4	195.8	27,334	188.4	550.9	95.25	43.20	607	11,353	154	-	
	1054	2	11	26.1	180.0	25,039	172.7	535.9	95.20	43.18	522	10,908	58	33.7	
	1117	3	12	26.9	185.5	26,569	183.2	550.5	95.6	43.36	^d	11,412	158	34.0	
M4A2/7	1156	4	13	26.2	180.6	25,482	175.6	525.8	95.20	43.18	^d	10,706	234	33.6	
M4A2/6	1251	5	14	11.5	79.3	10,820	74.6	415.8	95.25	43.20	1,127	8,528	59	29.7	155-mm pull-over gage would not enter rifling.
M4A2/6	1339	6	15	18.8	129.6	17,795	122.7	447.3	95.25	43.20	^d	9,347	220	29.2	Additional damage at 8:00 to 12:00. Lands flattened at 8:30 to 10:00 position.

^a Quadrant elevation.^b (R) - range, right.^c Time of flight.^d Round would not fall back. Tube was depressed and the round was pushed back against the charge.

Firing QE was 400 mls.

Table 3. (cont)

Chg./Zone	Time fired (MST)	Tube round no.	Test round no.	Copper gage pressure (psi)	Breach pressure (psi)	Inst vel (m/sec)	Projectile weight (lb)	Fall-back at Q ₀ ^a (mil)	Range (mil)	Defl (R) ^b (mil)	TOF ^c (sec)	Remarks
Date fired: 9 May 1981												
M4A2/6	0930	7	16	17.8	122.7	17,594	121.3	463.0	95.20	43.18	d	
M4A2/6	0951	8	17	17.2	118.6	16,366	112.9	456.3	95.10	43.14	1,132	Additional damage at 7:00 to 12:00.
M4A2/5	1033	9	18	-	-	10,917	75.3	365.4	95.25	43.20	1,019	
	1054	10	19	-	-	9,939	68.6	362.5	95.25	43.20	793	
	1112	11	20	-	-	10,209	70.3	327.8	95.30	43.23	438	Some damage at 2:00 position.
M4A2/5	1134	12	21	11.8	81.4	11,167	76.0	373.6	95.20	43.18	971	
M3A1/5	1308	13	22	15.3	105.5	14,567	100.5	348.3	95.25	43.20	d	
	1323	14	23	13.2	91.0	12,637	87.2	316.2	95.20	43.18	372	App. 1-in. long crease on 3 lands at 12:30 position.
	1344	15	24	13.3	91.7	12,687	87.5	329.2	95.25	43.20	802	App. 1-in. long crease on 8 lands at 12:30 and on 3 lands at 6:00.
M3A1/5	1358	16	25	13.3	91.7	12,778	88.1	328.2	95.00	43.09	d	
Date fired: 11 May 1981												
M3A1/3	1135	17	26	-	-	9,698	66.9	351.6	95.0	43.09	d	
M4A2/3	1206	18	27	-	-	9,653	66.6	351.1			d	Stuck round. Fired out w/M3A1, Z/4.
M4A2/4	1248	19	28	11.5	79.3	10,414	71.8	352.9		364	27.2	Stuck round. Fired out w/M3A1, Z/4.
M4A2/4	1309	20	29	-	-	7,160	49.4	299.1			30	
M4A2/4	1338	21	31	-	-	6,198	42.7	227.0	95.0	43.09	d	
Date fired: 12 May 1981												
M4A2/4	0926	22	32	10.7	73.8	10,069	69.4	351.8	95.0	43.09	d	
	0957	23	33	3.6	24.8	4,232	29.2	250.2	95.10	43.14	1,133	
	1155	24	34	6.8	46.9	6,188	41.6	253.6	95.2	43.18	1,132	
	1227	25	35	5.4	37.2	4,705	32.4	251.1	95.0	43.09	1,131	
	1250	26	36	4.0	27.6	3381	23.3	243.6	95.25	43.20	991	
M4A2/4	1321	27	37	4.7	32.4	3949	27.2	273.7	95.25	43.20	e	
M3A1/4	1331	28	38	12.6	86.9	11,844	81.7	319.5	95.0	43.09	e	
M3A1.4	1344	29	39	12.3	84.8	11,673	80.5	321.0	95.25	43.20	e	

a Quadrant elevation.

b (R) - range, right.

c Time of flight.

d Round would not fall back. Tube was depressed and the round was pushed back against the charge.

e No attempt made to get fall-back. Round pushed in between 33.75 and 35.75 in. from rear of breech.

Table 4. Fallback distances and reference velocity and pressure values--M107 projectile

Dimension	Description	Distance from Swiss Notch (in.)	Velocity (ft/s)	Pressure (psi)	Magnitude (in.)
A	M3A1 ^{a,b} Zone 2	7.2	780	5,900	
B	Zone 3	9.0	910	7,900	
C	Zone 4	11.4	1,045	10,600	
D	Zone 5	15.6	1,230	15,400	
E	M4A2 ^c Zone 3	6.8	960	6,200	
F	Zone 4	8.6	1,105	7,800	
G	Zone 5	11.3	1,290	10,600	
H	Zone 6	15.7	1,560	15,100	
I	Zone 7	21.0	1,855	25,100	
J	M107 max length				27.553
K	to bourrelet ^d				14.85
L	to rotating band				4.563
M	rotating band				1.02
N	boattail				2.760
O	M3/M107 fallback				15.65
P	M4/M107 fallback				10.25
Q	Bourrelet to rifling				8.273
R	To origin of rifling ^e				35.68
S	To rear face of breech ring				7.85

^a Zone 1 of the M3A1 is not type-classified for use with the M185 cannon.

^b Max diameter of bag is 5.0 in.

^c Max diameter of bag is 5.8 in.

^d Max bourrelet diameter is 6.0984 in.

^e For full depth rifling, add 0.51 in.

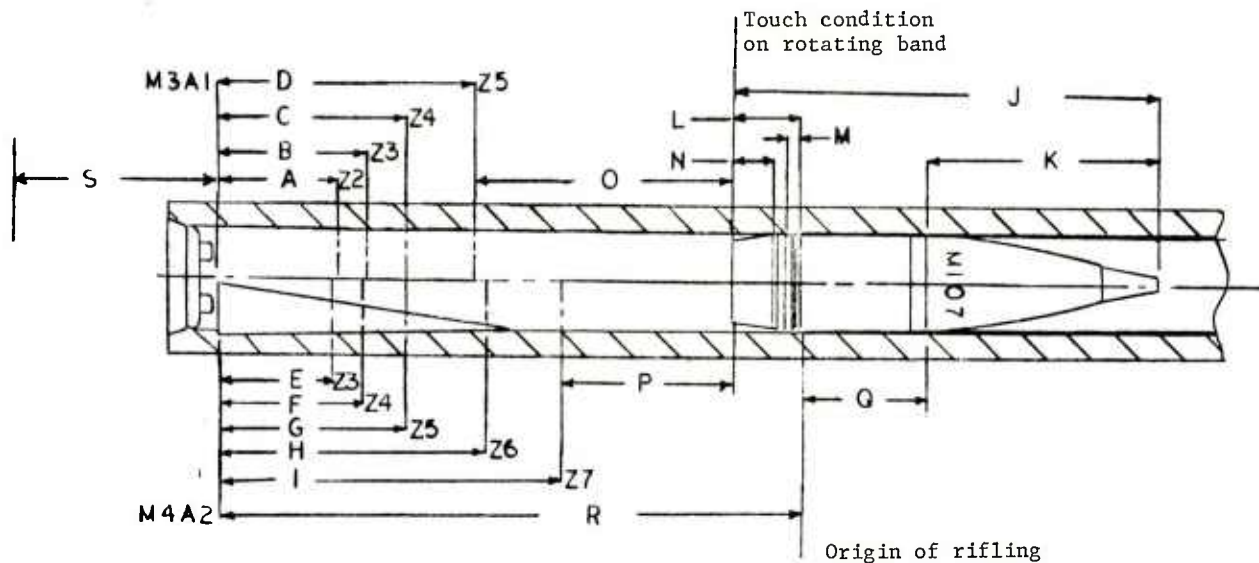


Table 5. Camera data

<u>Tube S/N</u>	<u>Date fired (1981)</u>	<u>Tube round no.</u>	<u>Observations</u>
24715	1 April	9	Fuze windshield missing
28317	8 May	1	Projectile unstable near muzzle
		2	Projectile unstable near muzzle
		3	Projectile unstable near muzzle
		4	Projectile unstable near muzzle
		5	Projectile unstable near muzzle
		6	Projectile unstable near muzzle
	9 May	15	Projectile unstable near muzzle
	11 May	17	Projectile unstable near muzzle
	12 May	23	Fuze windshield missing
		24	Fuze windshield missing, projectile unstable near muzzle
		25	Fuze windshield missing
		26	Fuze windshield missing
		27	Projectile unstable near muzzle
		29	Projectile unstable near muzzle

Table 6. Projectile damage

<u>Tube S/N</u>	<u>Tube round no.</u>	<u>Sample no.</u>	<u>Date fired (1981)</u>	<u>Charge/ zone fired</u>	<u>Area engraved by rifling</u>		
					<u>Ogive</u>	<u>Front bourrelet</u>	<u>Body</u>
24715	1	1	31 Mar	M3A1/4		X	
	2	2	31 Mar			X	
	4	4	31 Mar			X	
	5	5	1 Apr	M3A1/4		X	
	23	33	12 May	M4A2/4	X	X	X
28317	24	34			X	X	X
	25	35			X	X	X
	26	36	12 May	M4A2/4	X	X	X

Table 7. Selected values from breech pressure and chamber pressure plots

Round no.	Ignition delay (msec)	Breech gage				Chamber gage										
		Positive		Rise time (msec)	No. 1		No. 2		No. 3		No. 4					
		Positive peak (psi)	Positive peak time (msec)		Positive peak (psi)	Positive peak time (msec)	Positive peak (psi)	Positive peak time (msec)	Positive peak (psi)	Positive peak time (msec)						
Tube S/N 24715																
1	93.41	10,307	98.55	5.15	10,935	98.52	5.22	10,643	98.54	4.89	10,887	98.67	5.22	9,125	98.69	5.22
2	81.48	5,748	97.65	16.17				6,245	98.76	15.99	6,321	97.32	16.22	6,140	97.32	16.74
3	86.54	7,470	97.83	11.30	8,139	98.10	11.63	7,989	97.47	11.06	8,075	98.49	12.51	7,852	97.89	11.86
4	87.39	7,555	98.67	11.28	8,208	99.29	11.63	8,168	99.54	11.81	8,130	98.64	11.66	7,971	98.63	11.76
5	87.57	5,001	104.97	17.40				5,926	105.02	17.24	5,990	104.97	17.52	5,819	105.02	16.07
6	82.29	6,321	108.95	26.66	7,523	109.52	27.56	7,438	109.55	27.24	7,510	108.18	26.75	7,300	108.66	27.12
7	83.52	6,083	107.39	23.87	7,338	108.27	24.60	7,148	108.15	24.71	7,264	107.61	25.19	7,074	107.19	24.50
8	80.01	3,957	108.41	28.40				4,689	109.49	29.48	4,790	108.39	26.38			
9*	112.05	4,917	116.03	3.98	5,879	115.88	3.77	5,199	117.50	4.34	3,837	120.80	6.66	4,364	120.90	2.87
Tube S/N 28317																
1	95.09	27,334	101.24	6.15	26,645	101.06	6.29	27,551	101.25	6.47	26,991	101.21	6.54	26,255	101.37	6.69
2	93.51	25,039	100.19	6.68	24,510	100.07	6.92	25,102	100.20	6.96	24,545	100.23	7.08	23,839	100.29	7.02
3	93.75	26,569	100.14	6.39	25,847	100.07	6.56	26,449	100.08	6.62	25,937	100.13	6.81	25,245	100.20	6.77
4	93.60	25,482	100.49	6.89	25,097	100.31	7.19	25,289	100.53	7.25	25,083	100.32	7.17	24,466	100.53	7.16
5*	90.20	10,820	99.45	9.26	10,596	99.12	9.15	10,566	99.62	9.37	10,637	98.69	7.25	10,245	98.70	6.09
6	93.93	17,795	103.07	9.14	17,500	102.93	9.57	17,395	103.07	9.66	17,501	102.83	9.56	17,023	103.05	9.71
7	93.08	17,594	101.57	8.49	17,160	101.63	9.21	17,577	102.09	9.69	17,459	101.52	9.15	16,848	101.94	9.45
8	93.50	16,366	101.87	8.37	16,030	101.93	9.14	16,346	102.35	9.39	16,143	101.93	9.26	15,647	102.32	9.50
9	90.21	10,917	103.32	13.11	10,452	103.17	13.88	10,643	103.83	14.48	10,499	103.37	13.64	10,204	103.91	14.49
10	89.94	9,939	102.65	12.71	9,814	102.93	14.51	9,906	102.89	14.07	9,776	102.75	13.80	9,464	102.62	13.79

* Choppy, erratic pressure curves.

Table 7. (cont)

Round no.	Breach gage			No. 1			No. 2			Chamber gage			No. 3			No. 4		
	Ignition delay (msec)	Positive peak (psi)	Positive peak time (msec)	Rise time (msec)	Positive peak (psi)	Positive peak time (msec)	Rise time (msec)	Positive peak (psi)	Positive peak time (msec)	Rise time (msec)	Positive peak (psi)	Positive peak time (msec)	Rise time (msec)	Positive peak (psi)	Positive peak time (msec)	Rise time (msec)	Positive peak (psi)	Positive peak time (msec)
11	86.99	10,208	103.86	16.68	10,080	103.94	16.36	10,085	104.09	16.82	10,124	103.94	18.15	9,809	104.00	18.57	9,809	104.00
12	91.35	11,167	103.23	11.88	10,916	102.98	12.48	10,991	103.37	13.01	10,908	103.32	12.93	10,657	103.34	13.23	10,657	103.34
13	94.95	14,567	100.26	5.31	14,208	100.11	5.49	14,958	100.17	5.46	14,061	100.17	5.66	13,710	100.43	5.96	13,710	100.43
14	94.34	12,637	100.97	6.63	12,370	101.01	7.17	12,143	101.00	7.14	12,288	101.03	7.18	12,057	101.10	7.29	12,057	101.10
15	93.89	12,687	100.31	6.42	12,485	100.10	6.78	12,262	100.26	6.75	12,411	100.29	6.93	12,165	100.31	6.89	12,165	100.31
16	94.56	12,778	100.80	6.24	12,592	100.74	6.65	12,302	100.83	6.60	12,550	100.80	6.71	12,331	100.88	6.86	12,331	100.88
17	90.81	9,698	102.59	11.78	9,633	102.62	12.66	9,481	102.84	12.39	9,620	102.60	12.59	9,364	102.56	12.60	9,364	102.56
18	91.41	9,653	103.46	12.05	9,578	103.35	12.95	9,427	103.59	12.87	9,476	103.23	12.69	9,256	103.59	13.11	9,256	103.59
19	92.94	10,414	105.24	12.30	10,295	105.29	13.13	10,013	105.23	12.90	10,234	105.20	12.89	9,912	105.33	13.11	9,912	105.33
20	84.45	7,160	107.04	22.59	7,155	106.56	24.24	6,867	106.97	24.09	7,020	106.56	23.34	6,874	106.77	24.26	6,874	106.77
21	80.01	6,198	108.95	28.94	6,301	108.86	28.85	5,987	108.95	28.94	6,204	108.72	28.71	6,048	108.81	28.80	6,048	108.81
22	92.34	10,069	105.50	13.16	9,913	105.63	14.37	10,166	106.04	14.70	10,024	105.72	14.46	9,568	105.87	14.66	9,568	105.87
23*	87.54	4,232	92.79	5.25	4,430	92.90	5.43	4,451	92.78	4.17	3,578	97.04	6.84	4,321	96.92	1.61	4,321	96.92
24*	89.19	6,188	92.66	3.47	6,233	92.48	3.32	7,089	93.84	3.59	4,003	97.25	6.36	5,146	97.29	2.84	5,146	97.29
25*	88.13	4,705	93.11	4.98	4,880	92.79	4.74	4,836	93.74	4.40	3,793	97.29	6.68	4,664	97.07	1.82	4,664	97.07
26*	85.64	3,381	92.75	7.11	3,622	92.79	7.31	3,574	93.03	5.66	3,380	100.43	11.12	3,662	96.53	3.62	3,662	96.53
27	86.85	3,949	103.61	16.76	4,213	103.77	17.94	4,129	100.86	18.00	4,116	103.91	16.08	4,047	104.51	15.29	4,047	104.51
28	94.46	11,844	100.89	6.44	11,780	100.85	6.92	11,644	100.89	6.77	11,803	100.88	6.63	11,450	100.98	6.78	11,450	100.98
29	94.35	11,673	100.68	6.33	11,596	100.50	8.75	11,477	100.64	6.50	11,652	100.58	6.47	11,343	100.67	6.56	11,343	100.67

* Choppy, erratic pressure curves.

Table 8. Contact loads, M107 projectile in M185 cannon

Round no.	Ele- vation (mils)	Projectile ogive/forcing cone			Projectile bourrelet/forcing cone		
		X plane (g)	Y plane (g)	Resultant (g)	X plane (g)	Y plane (g)	Resultant (g)
1	100	0	-120	120	-225	220	315
2	100	-75	-150	168	-165	220	275
3	100	315	-280	421	-170	210	270
4	300	465	-45	467	-170	250	302
5	300	-50	-70	86	-190	235	302
6	300	-55	-75	93	-210	230	311
7	500	-65	-75	99	-205	245	319
8	500	0	-40	40	-190	185	265
9	500	-45	-100	110	-210	210	297
10	700	-40	-105	112	-205	185	276
11	700	-55	-145	155	-175	210	273
12	700	270	-65	278	-160	190	248
13	0	120	-140	184	-210	260	334
14	400	-45	-95	105	-200	210	290
15	700	-	-	-	-100	135	168
16	0	95	-175	199	-220	200	297
17	400	-55	-75	93	-210	230	311
18	700	115	-240	266	-190	150	242
19	0	85	-241	256	-200	245	316
20	400	-95	-90	131	-160	220	272
21	700	295	-250	387	-70	160	175
22	100	0	-120	120	-220	220	311
23	100	435	-300	528	-145	105	179
24	700	175	-200	266	-85	125	151
25	100	200	-155	253	-220	210	304
26	700	115	-125	170	-100	140	172
27	100	45	-215	220	-215	235	319
28	700	285	-185	340	-125	140	188
29	100	90	-150	175	-210	230	311
30	700	150	-210	258	-140	110	178
31	100	40	-100	108	-120	255	282
32	700	190	-415	456	-100	185	210
33	100	55	-120	132	-	-	-
34	100	45	-130	138	-170	270	319

Table 9. Summary of contact loads, M107 projectile in M185 cannon

Elevation (mils)	Projectile ogive/forcing cone Resultant force		Projectile bourrelet/forcing cone Resultant force	
	Mean (g)	Standard deviation (g)	Mean (g)	Standard deviation (g)
0	213	38.0	316	18.5
100	217	137.1	289	42.7
100 ^a	159	49.6		
300	215	218.0	305	5.2
300 ^b	90	5.0		
400	110	19.4	291	19.5
500	83	37.6	294	27.2
500 ^c	105	7.8		
700	269	106.2	207	44.9
700 ^d	265	77.3		

^a Less round nos 3 and 23 which were considered outliers.

^b Less round no. 4.

^c Less round no. 8.

^d Less round nos 10 and 32.

Table 10. Comparison of selected ramming test data

	700-mil case				All cases			
	Mean	Standard deviation	Max	Min	Mean	Standard deviation	Max	Min
Extraction force (lb)	5,589	989	8,130	3,020	5,622	1,047	10,750	3,020
Depth of ram (in.)	39.18	0.03	39.19	39.13	39.18	0.03	39.38	38.5
Length of engraving (in.)	0.182	0.057	0.438	0.125	0.183	0.056	0.438	0.063

Table 11. Lo-Z accelerometer output

Round	Acceleration		Velocity			
	+ Peak (g)	Time (sec)	Peak ^a (f/sec)	Time (sec)	Transition ^b (f/sec)	Time (sec)
1	4.241	1.225	9.636	1.278	3.818	1.191
2	4.479	1.186	8.818	1.222	3.364	1.149
3	4.449	1.210	8.454	1.250	2.545	1.163
4	4.791	1.201	8.273	1.240	2.727	1.165
5	4.795	1.160	8.727	1.201	3.000	1.125
6	4.982	1.164	9.182	1.201	3.454	1.127
7	4.959	1.175	8.000	1.219	2.364	1.139
8	4.908	1.157	8.818	1.201	3.182	1.122
9	4.943	1.115	8.864	1.159	3.182	1.078
10	4.828	1.104	7.913	1.145	2.348	1.072
11	4.898	1.137	8.652	1.179	3.130	1.122
12	4.731	1.082	7.565	1.127	2.174	1.048
13	3.307	1.179	7.545	1.224	2.727	1.092
14	4.830	1.157	8.727	1.203	3.000	1.074
15	4.717	1.107	7.727	1.147	2.364	1.086
16	4.129	1.166	8.364	1.208	2.636	1.139
17	4.889	1.098	8.273	1.139	2.454	1.076
18	4.914	1.109	8.000	1.149	2.545	1.086
19	4.557	1.108	9.909	1.149	3.636	1.078
20	5.053	1.085	8.273	1.123	2.454	1.059
21	4.855	1.118	7.364	1.165	1.818	1.097
22	4.086	1.181	8.682	1.218	3.000	1.150
23	4.702	1.181	8.545	1.220	2.909	1.160
24	4.533	1.273	7.727	1.312	2.500	1.255
25	4.846	1.091	8.364	1.133	2.454	1.070

^a Peak values correspond to the maximum second-stage rammer velocities.

^b Transition values correspond to the maximum first-stage rammer velocities.

Table 12. Results from Lo-Z accelerometer output

	<u>Maximum value</u>	<u>Minimum value</u>	<u>Average value</u>	<u>Standard deviation</u>
Acceleration (g)	5.053	3.307	4.657	0.385
First stage, rammer maximum velocity (ft/s)	3.818	1.818	2.791	0.482
Second stage, rammer maximum velocity (ft/s)	9.909	7.364	8.416	0.625

Table 13. Comparison of extraction forces with seating loads and velocities

<u>Round no.</u>	<u>Maximum load at seating (g)</u>	<u>Maximum seating velocity (ft/s)</u>	<u>Extraction load (lb)</u>
1	-339.6	9.636	10,750
2	-564.0	8.818	7,750
3	-562.3	8.454	6,500
4	-514.5	8.273	5,250
5	-510.7	8.727	6,625
6	-481.2	9.182	5,875
7	-480.5	8.000	5,625
8	-411.0	8.818	0 ^a
9	-508.2	8.864	6,500 ^b
10	-511.3	7.913	
11	-474.7	8.652	5,250
12	-469.1	7.565	5,250

^a Round fall-out from a seated position.

^b Instrumentation failure.

Table 14. M107B2 projectile ram--extract test (2 August 1982)

Average force = 5,464 lb
 Standard deviation = 512 lb
 Maximum force = 6,540 lb
 Minimum force = 4,440 lb

Round	Depth to ram (in.)	Extraction force (lb)	Length of engraving (in.)
1	39 1/8	5,570	3/16
2	39	5,200	3/16
3	39	5,100	3/16
4	39	5,263	3/16
5	39	4,860	3/16
6	39	5,330	3/16
7	39	5,710	3/16
8	39	5,480	3/16
9	39	5,940	3/16
10	39	6,540	3/16
11	39 1/16	4,890	3/16
12	39	5,110	3/16
13	39 1/16	5,714	3/16
14	39	5,700	3/16
15	39	5,040	3/16
16	39 1/16	5,560	3/16
17	39	4,440	5/32
18	39	5,490	3/16
19	39	6,470	3/16
20	39	5,260	5/32
21	39	6,160	3/16
22	39	5,260	3/16
23	39	4,890	5/32
24	39	6,160	3/16

Note: 1. Temperature ranged between 70°F and 75°F.

2. M109A3 SPH no. 12D 34568.

Table 15. Summary of range firings from M185 cannon tubes, M107 projectile, M557 fuze, M4A2 charge

Date of firing	Chg zone	QE ^a (mil)	Muzzle velocity (ft/s)			Pressure (ksi)			Range (m)			Deflection (m)			
			N ^b	Avg	SD	N ^b	Avg	SD	Obs Avg	Corr Avg	N ^b	Obs Avg	Corr Avg		
Phase A															
Undamaged tube S/N 23418															
22 Dec 1980	5	513	e			10	11.8	0.34	10	8,668	9,014	10	135	119	6.1
	6	372	e			10	16.6	0.43	10	8,634	8,927	10	127	102	4.8
	7	267	e			10	26.7	0.45	10	8,695	8,925	10	223	89	2.1
Phase B															
Damaged tube S/N 25460															
23 Jan 1981 ^f 24 Jan 1981	5	513	3	1,319	(6)	3	11.4	(0)	3	8,897		3	-17		(177)
	5	513	7	1,314	3.5	7	11.1	0.21	7	8,854	8,917	7	50	124	7.3
	6	372	10	1,583	3.7	10	16.0	0.32	10	8,764	8,891	10	21	78	5.2
	7	267	10	1,883	4.9	10	25.8	0.73	10	8,843	8,847	10	-3	68	8.8
12 Feb 1981	5	654	10	1,312	6.2	10	11.0	0.32	10	9,665	9,948	10	62	171	13.2
	6	650	10	1,579	3.5	10	16.2	0.31	10	11,556	11,928	10	59	226	8.8
	7	438	10	1,876	3.3	10	25.8	0.49	10	11,536	11,863	10	21	174	8.4
3 Mar 1981 4 Mar 1981	5	280.9	10	1,315	8.7	10	10.8	0.18	10	5,913	5,931	10	-12	30	5.0
	6	205.4	10	1,585	5.7	10	16.1	0.29	10	5,887	5,915	10	41	28	3.4
	7	141.0	10	1,878	6.5	10	25.7	0.44	10	5,908	5,902	10	37	26	3.4

^a QE - quadrant elevation.

^b Sample size considered.

^c Ranges corrected to service velocity, to standard projectile weight of 95.00 lb, and to standard International Civil Aviation Organization (ICAO) metro. Deflections corrected to standard ICAO metro.

^d PE - probable error.

^e Velocities not measured. For the purposes of range corrections, the average velocities for each zone of phase B were used to correct phase A.

^f Three rounds fired on 23 Jan 1981 not considered valid uniformity groups although their results appeared to be normal. Numbers in parentheses are maximum dispersions.

Table 16. Summary of range firings from 155-mm damaged tube S/N 25460 using charge M119, zone 8, conditioned to +130°F

Date of firing	QEA (mil)	Range and functioning data														No. duds					
		Muzzle velocity (ft/s)				Pressure (ksi)		Range (m)		Deflection (m)		Burst height (m)		Fuzed function time (sec)							
		N ^b	Avg	SD	N ^b	Avg	N ^a	Avg	N ^b	Avg	N ^b	Avg	N ^b	Avg	N ^b		Avg				
		M483A1 projectile, M577 fuze, setting 38.7 sec																			
6 Aug 1981	400	6	2,201	14.8	6	32.4	1.28	5 ^e	14,067	33.4	5 ^e	107	13.2	5	107.0	31.9	48	38.44	0.80	1	
7 Aug 1981	400	17	2,186	6.1	17	31.1	0.51	12 ^{e,f}	14,157	37.1	12 ^e	156	11.8	13	84.8	18.1	8 ^h	39.01	0.38	4	
Pooled: ⁱ		23	2,190	9.0	23	31.4	0.77	17 ^e	14,131	36.2	17 ^e	142	12.8	18	91.0	22.4	12	38.82	0.54	5	
M549 projectile, rocket off, M557 fuze																					
10 Aug 1981	400	17 ^j	2,284	11.4	24	32.6	9.7	24	15,410	76.6	24	153	14.6							1	

a QE - quadrant elevation.

b Sample size considered.

c PE - probable error.

d Fuze functioning time measured with four infrared (IR) chronographs.

e Range and deflection data shown for airburst rounds only.

f One round, range estimated to airburst (14,153 meters) omitted from calculations.

g IR times lost for one round.

h IR times lost for five rounds.

i Results for 6 and 7 August statistically pooled.

j Velocities lost for seven rounds.

Table 17. Results of modeling the modified M107 projectile used in phase D of the degradation test

	Nominal	Model difference from nominal	Modified difference from nominal
Weight	95 lb	95.64 lb (0.67%)	95.99 lb (1.04%)
Height to center of gravity	9.45 in.	9.53 in. (0.85%)	9.59 in. (1.48%)
Polar moment of inertia	499 lb-in. ²	491.49 lb-in. ² (-1.51%)	517.17 lb-in. ² (3.64%)
Transverse moment of inertia	4,322 lb-in. ²	4,310.82 lb-in. ² (-0.004%)	4,407.98 lb-in. ² (2.11%)

Table 18. Range data from phase D firings

Projectile: Modified M107 inert Fuze: Collector cap Charge: M119A1 zone 8 Elevation: 400 mils					
Date of firing	Test round	Seating distance (in.)	Copper gage pressure no. 1 (ksi)	Copper gage pressure no. 2 (ksi)	Average gage pressure (ksi)
<u>Undamaged tube S/N 23418</u>					
22 April 1981	1	39 1/16	28.4	28.5	28.5
	2	39 1/8	28.6	29.3	29.0
	3	39 3/16	29.4	29.6	29.5
	4	39 3/16	29.4	29.4	29.4
23 April 1981	5	39 5/16	29.2	29.3	29.3
<u>Damaged tube S/N 25460</u>					
24 April 1981	6	39 3/8	28.8	28.6	28.7
	7	39 1/8	28.4	30.2	29.3
	8	39 1/8	29.8	29.9	29.9
	9	39 1/8	30.3	29.7	30.0
	10	39 1/8	29.2	29.7	29.5
Grand average		39.175			29.3

Table 19. Comparison of test results (ranges) with firing table values

Date of firing	Chg zone	QE ^b (mil)	N ^c	Test data			FT data ^a			Range difference from corrected average CI ^e (m)
				Corrected avg (m)	PE ^d (m)	PE ^d % range	CI ^e (m)	PE ^d (m)	PE ^d % range	
<u>Phase A Undamaged tube S/N 23418</u>										
22 Dec 1980	5	513	10	9,014	40.4	0.45	9,000	30	0.33	14
	6	372	10	8,927	27.4	0.31	9,000	24	0.27	-73
	7	267	10	8,925	20.0	0.22	9,000	25	0.28	-75
Average PE %						0.33			0.29	
<u>Phase B Damaged tube S/N 25460</u>										
24 Jan 1981	5	513	7	8,917	22.7	0.25	9,000	30	0.33	-83
	6	372	10	8,891	26.4	0.30	9,000	24	0.27	-109
	7	267	10	8,847	30.0	0.34	9,000	25	0.28	-153
Average PE %						0.30			0.29	
12 Feb 1981	5	654	10	9,948	41.2	0.41	10,000	34	0.34	-52
	6	650	10	11,928	21.4	0.18	12,000	31	0.26	-72
	7	438	10	11,863	27.0	0.23	12,000	30	0.25	-137
Average PE %						0.27			0.28	
3 Mar 1981	5	280.9	10	5,931	17.9	0.30	6,000	22	0.37	-69
	6	205.4	10	5,915	22.1	0.37	6,000	20	0.33	-85
	7	141.0	10	5,902	31.6	0.54	6,000	19	0.32	-98
Average PE %						0.40			0.34	
<u>Grand average</u>										
Phase A			3 groups			0.33			0.29	
Phase B			9 groups			0.32			0.31	

^a Data extracted from firing table 155-AM-1.

^b QE - quadrant elevation.

^c Sample size considered.

^d PE - probable error.

^e CI - center of impact.

Table 20. Comparison of test results (deflections) with firing table values

Date of firing	Chg zone	Q _E ^b (mil)	Test data				Nominal range (m)	FT data ^a			Deflection difference from corrected average		
			Corrected avg (m)	N ^c	PE ^d (m)	PE ^d (mil)		CI ^e (m)	PE ^d (m)	PE ^d (mil)	CI ^e (m)	(mil)	
Phase A Undamaged tube S/N 23418													
22 Dec 1980	5	513	119	10	6.1	0.68	9,000	125	9	1.00	-6	-0.67	
	6	372	102	10	4.8	0.53	9,000	104	5	0.56	-2	-0.22	
	7	267	89	10	2.1	0.23	9,000	86	5	0.56	3	0.33	
Average PE mils													
0.48													
Phase B Damaged tube S/N 25460													
24 Jan 1981	5	513	124	7	7.3	0.81	9,000	125	9	1.00	-1	-0.11	
	6	372	78	10	5.2	0.58	9,000	104	5	0.56	-26	-2.89	
	7	267	68	10	8.8	0.98	9,000	86	5	0.56	-18	-2.00	
Average PE mils													
0.79													
12 Feb 1981	5	654	171	10	13.2	1.32	10,000	192	10	1.00	-21	-2.10	
	6	650	226	10	8.8	0.73	12,000	262	7	0.58	-36	-3.00	
	7	438	174	10	8.4	0.70	12,000	188	7	0.58	-14	-1.17	
Average PE mils													
0.92													
3 Mar 1981	5	280.9	30	10	5.0	0.83	6,000	43	5	0.83	-13	-2.17	
	6	205.4	28	10	3.4	0.57	6,000	38	3	0.50	-10	-1.67	
	7	141.0	16	10	3.4	0.57	6,000	30	3	0.50	-4	-0.67	
Average PE mils													
0.66													
Grand average													
Phase A 3 groups 0.71													
Phase B 9 groups 0.68													

^a Data extracted from firing table 155-AM-1.^b QE - quadrant elevation.^c Sample size considered.^d PE - probable error.^e CI - center of impact.

Table 21. Summary of fuze functioning and spin rate data

Date of firing	Tube ^a no.	Projec- tile model	Fuze functioning data					Muzzle velocity			Projectile spin rate				
			Time (sec)					(f/sec)			(rps)				
			No. fired	No. duds	No. cons	Avg	SD	No. cons	Avg	SD	No. cons	Avg	SD		
Fuze: M577, setting 38.7 sec															
6 Aug 1981	25460	M483	M119	8 ^d	6	1	4 ^e	38.44	0.80	6	2,201	14.8	6	226	2.0
7 Aug 1981					17	4	8 ^f	39.01	0.38	17	2,186	6.1	17	221	1.4
Fuze: M557, setting SQ															
22 Dec 1980	23418	M107	M4A2	5	10	0				3	1,319	(6) ^h	1	122	-
				6	10	0				7	1,314	3.5	2	128	(3) ^h
				7	10	0				10	1,583	3.7	10	150	5.5
23 Jan 1981	25460	M107	M4A2	5	3	0				10	1,883	4.9	10	189	2.2
24 Jan 1981				5	7	0				10	1,312	6.2	10	124	3.5
				6	10	0				10	1,579	3.5	10	146	4.6
12 Feb 1981	25460	M107	M4A2	7	10	0				10	1,876	3.3	8	177	4.6
				5	10	0				10	1,315	8.7	5	129	4.3
3 Mar 1981	25460	M107	M4A2	6	10	0				10	1,585	5.7	10	149	2.2
4 Mar 1981				6	10	0				10	1,878	6.5	10	182	3.1
				7	10	0				17 ^g	2,284	11.4	23	231	2.2
10 Aug 1981	25460	M549	M119	8 ^d	24	1									

^a Tube S/N 25460, damaged; S/N 23418, undamaged.

^b PE - probable error.

^c Missing rounds, spin lost, due in most cases to inability to see spiral helix painted on projectile ogive. For a few rounds, the timing marks were missing.

^d Charge conditioned at 130°F.

^e Time lost for one round.

^f Times lost for five rounds.

^g Velocities lost for seven rounds.

^h Numbers in parentheses are maximum dispersions.

Table 22. Location of break with accelerometer wires

<u>Round no.</u>	<u>Pressure (kpsi)</u>	<u>Time (msec)</u>	<u>% of Peak pressure</u>	<u>Distance[*] (in.)</u>
<u>Tube S/N 23418</u>				
1	24	7.82	87	8.4
2	28	8.15	98	16.0
3	26	9.13	89	15.5
4	26	8.88	89	8.9
5	28	9.14	97	21.4
<u>Tube S/N 25460</u>				
6	27	8.44	96	11.6
7	28	8.30	95	13.5
8	24	7.19	82	5.0
9	29	10.67	99	6.5
10	27	9.72	96	13.1

* The distances were computed from the actual axial acceleration.

Table 23. Table of accelerations in 1000's of g's

Round no.	Axial acceleration at $t_1 t_2^*$		Tangential acceleration at $t_1 t_2^*$						
	Ideal	Actual	T12	T3	T6	T9	Average	T12+6 2	T3+9 2
<u>Tube S/N 23418</u>									
1	0.302/6.30	0/5.94	0/0.667	0/1.087	0/1.079	0/0.694	0/0.890	0/0.868	0/0.890
2	0.331/6.667	0/5.660	0/0.304	0/0.534	0/1.125	0/1.000	0/0.748	0/0.716	0/0.750
3	0.281/5.281	0/7.779	0/0.569	0/0.669	0/2.047	0/0.718	0/1.000	0/1.322	0/0.730
4	0.357/6.531	0/5.953	0/-0.034	0/0.342	0/1.598	0/1.318	0/0.816	0/1.021	0/0.842
5	0.347/6.719	0/5.178	0/0.821	0/0.750	0/1.109	0/1.387	0/1.021	0/0.962	0/1.086
<u>Tube S/N 25460</u>									
6	0.361/6.528	0/5.148	0/1.012	0/0.895	0/1.080	0/1.435	0/1.058	0/1.029	0/1.183
7	0.381/6.349	0/6.874	0/0.489	0/0.750	0/0.539	0/1.50	0/0.809	0/0.457	0/0.976
8	0.303/7.407	0/5.056	0/0.838	0/-0.020	0/1.101	0/0.586	0/0.616	0/0.949	0/0.263
9	0.372/8.455	0/2.793	0/0.672	0/-0.178	0/0.286	0/0.845	0/0.400	0/0.583	0/0.222
10	0.248/6.446	0/5.928	0/-0.306	0/-0.078	0/1.113	0	0/0.254	0/0.413	0/-0.039

* t_1 is the time at which the pressure curve has a value of 1,000 psi.

t_2 is the time at which the displacement, computed from the actual axial acceleration, is five inches (see table 24 for values of t_1 and t_2).

Table 24. Comparison of actual and theoretical acceleration values

Round no.	Time ^a		Ratio of averaged tangential 6+12 to actual axial acceleration ^b	Percent difference from theoretical ^c	Ratio of averaged tangential 3+9 to actual axial acceleration ^d	Percent difference from theoretical ^c
	t ₁ (msec)	t ₂ (msec)				
<u>Tube S/N 23418</u>						
1	2.66	7.12	0.140	8.5	0.147	14.0
2	1.88	6.33	0.127	1.6	0.135	4.7
3	3.10	7.53	0.161	24.8	0.096	25.6
4	3.20	8.09	0.135	4.7	0.146	13.2
5	3.28	7.25	0.156	20.9	0.177	37.2
<u>Tube S/N 25460</u>						
6	2.49	7.02	0.210	62.8	0.254	96.9
7	2.78	6.82	0.086	33.3	0.125	3.1
8	2.59	7.20	0.172	33.3	0.055	57.4
9	4.08	10.12	0.220	70.5	0.094	27.1
10	3.31	8.28	0.067	48.1	--	--

^a t₁ is the time in msec at which the pressure curve has a value of 1000 psi.
t₂ is the time in msec at which the displacement, computed from the actual axial acceleration, is five inches.

^b This ratio was determined from the slope of the curve displaying the averaged tangential 6+12 velocity versus the actual axial velocity.

^c The theoretical value for the tangential acceleration to axial acceleration expression is 0.129.

^d This ratio was determined from the slope of the curve displaying the averaged tangential 3+9 velocity versus the actual axial velocity.

Table 25. Material properties of damaged and undamaged tubes

	Content (%)								
	Carbon	Manganese	Phosphorus	Sulfur	Silicon	Nickel	Cromium	Molybdenum	Vanadium
Damaged tubes sample size: 14									
Average	0.3264	0.5836	0.0086	0.0083	0.1814	2.518	1.009	0.5271	0.1100
Std deviation	0.0108	0.0401	0.0012	0.0011	0.0376	0.2461	0.0296	0.0463	0.0162
Minimum value	0.3100	0.4900	0.0060	0.0070	0.0800	2.360	0.9700	0.4400	0.0800
Maximum value	0.3500	0.6200	0.0110	0.0110	0.2200	2.990	1.080	0.5800	0.1300
Undamaged tubes sample size: 28									
Average	0.3196	0.6018	0.0085	0.0082	0.2021	2.377	0.9964	0.5450	0.1154
Std deviation	0.0129	0.0147	0.0007	0.0012	0.0193	0.0698	0.0170	0.0215	0.0064
Minimum value	0.3000	0.5800	0.0070	0.0060	0.1600	2.070	0.9700	0.4600	0.1000
Maximum value	0.3700	0.6300	0.0100	0.0100	0.2400	2.550	1.040	0.5800	0.1300
Comparison of samples									
Significant difference	No	Yes at 97.5% confidence level	No	No	Yes at 97.5% confidence level	Yes at 99.5% confidence level	No	No	No

Table 26. Mechanical properties of damaged and undamaged tubes

	Yield strength (ksi)		Reduction in area (%)		Charpy impact (ft-lb)	
	Breech end	Muzzle end	Breech end	Muzzle end	Breech end	Muzzle end
Damaged tubes sample size: 14						
Average	169.50	169.27	39.69	43.61	22.49	21.70
Std deviation	3.85	3.27	5.64	7.22	3.44	3.15
Minimum value	163.05	162.80	28.25	27.60	15.40	16.40
Maximum value	174.75	173.90	49.00	51.55	28.25	28.75
Undamaged tubes sample size: 28						
Average	170.61	170.67	41.97	47.77	23.19	23.39
Std deviation	2.43	2.68	3.76	3.37	2.28	2.71
Minimum value	165.75	162.25	34.00	38.45	19.25	18.50
Maximum value	175.90	173.80	47.75	52.70	27.50	28.00
Comparison of samples	No	No	No	Yes at 99.0% confidence level	No	Yes at 95.0% confidence level
Significant difference						

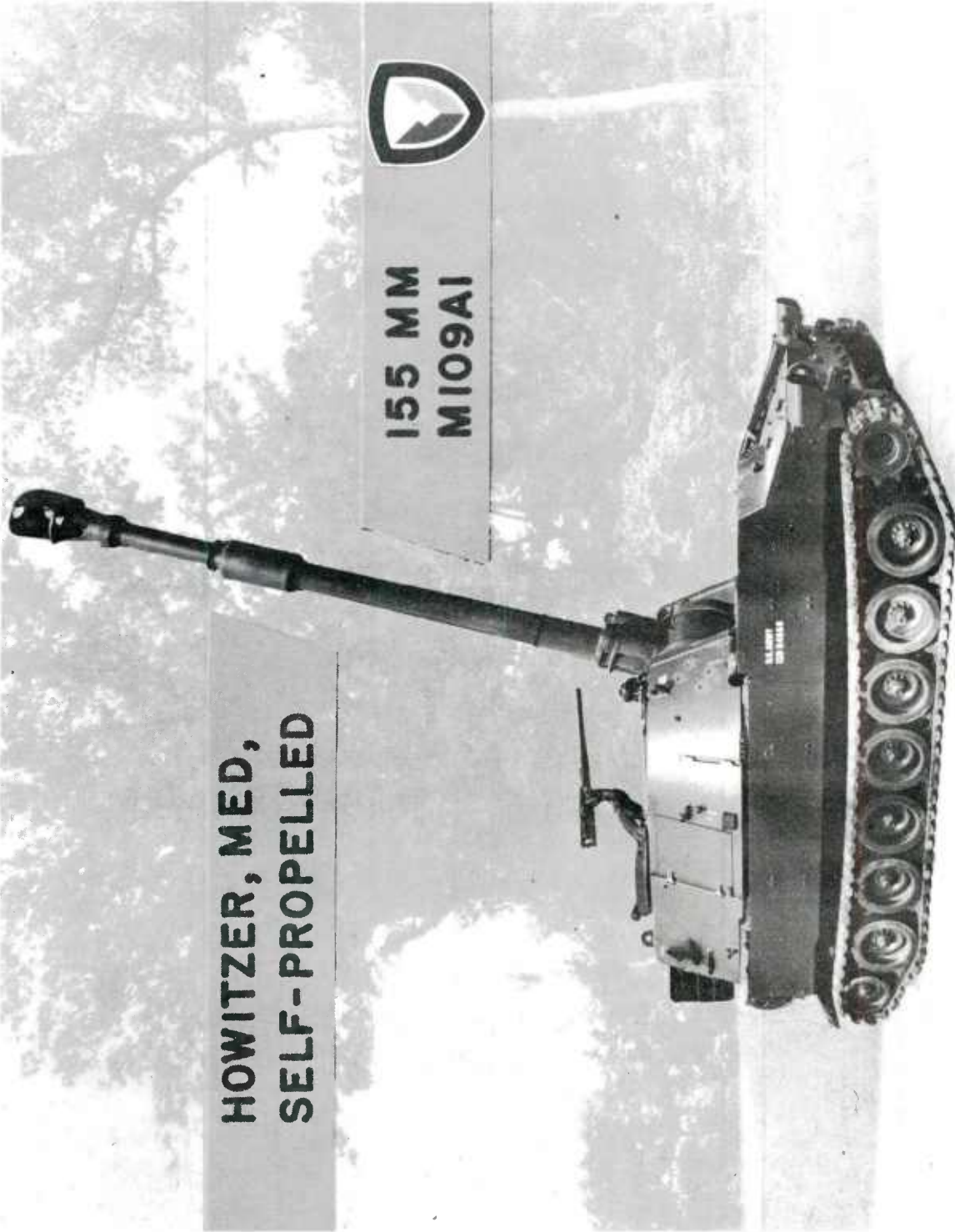
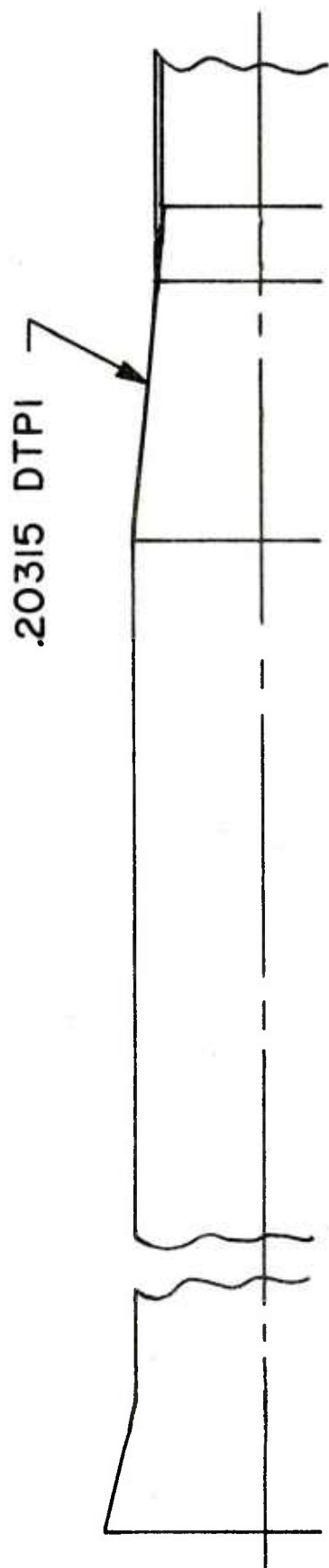
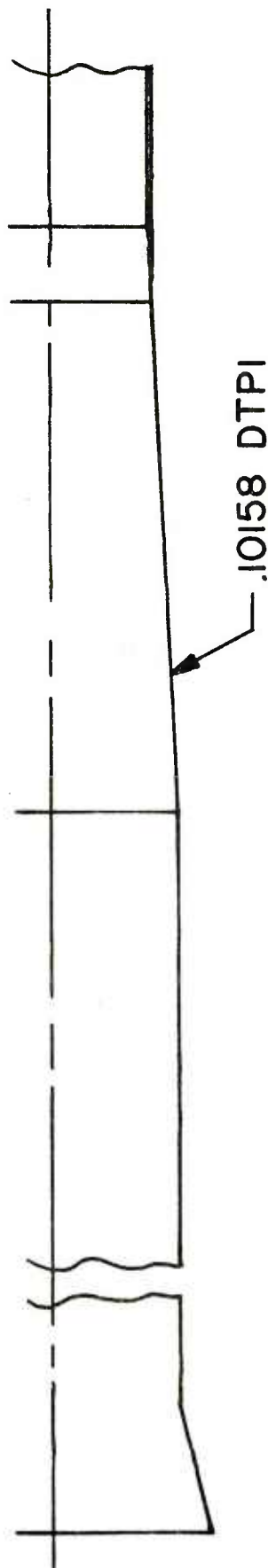


Figure 1. 155-mm M109A1 SP howitzer

M185 STEEP CONE

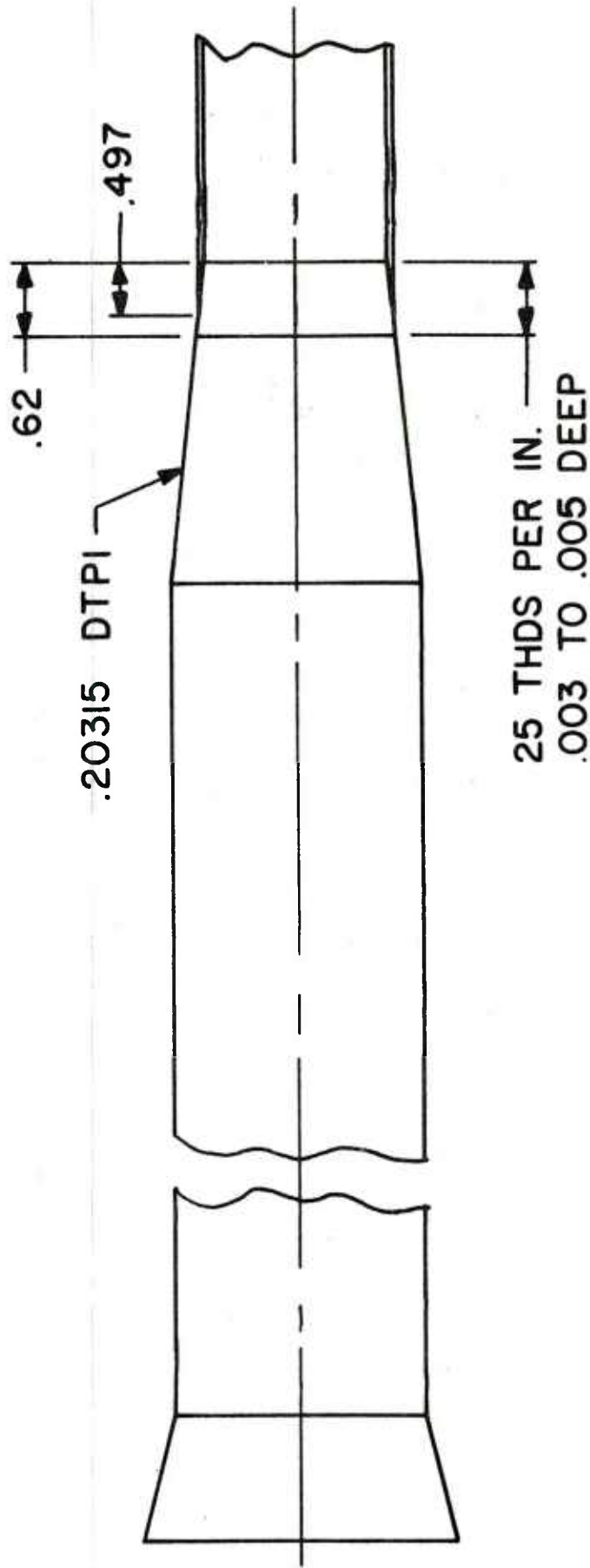


M185 STANDARD CONE



Note: The steep forcing cone design was incorporated in all U.S. 155-mm M185 cannons.

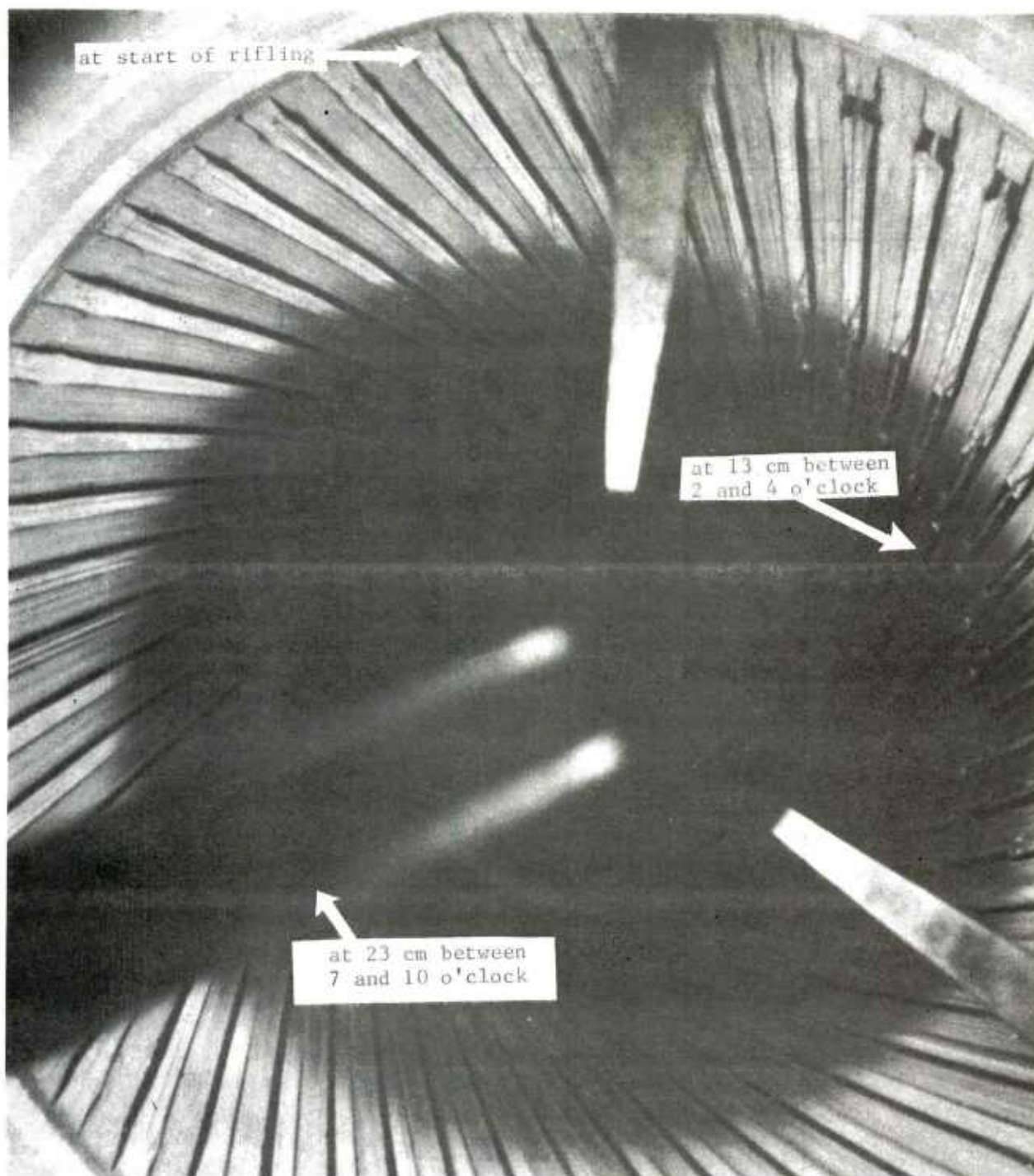
Figure 2. M185 cannon tube forcing cone modification



- GROOVED STEEP CONE ANGLE

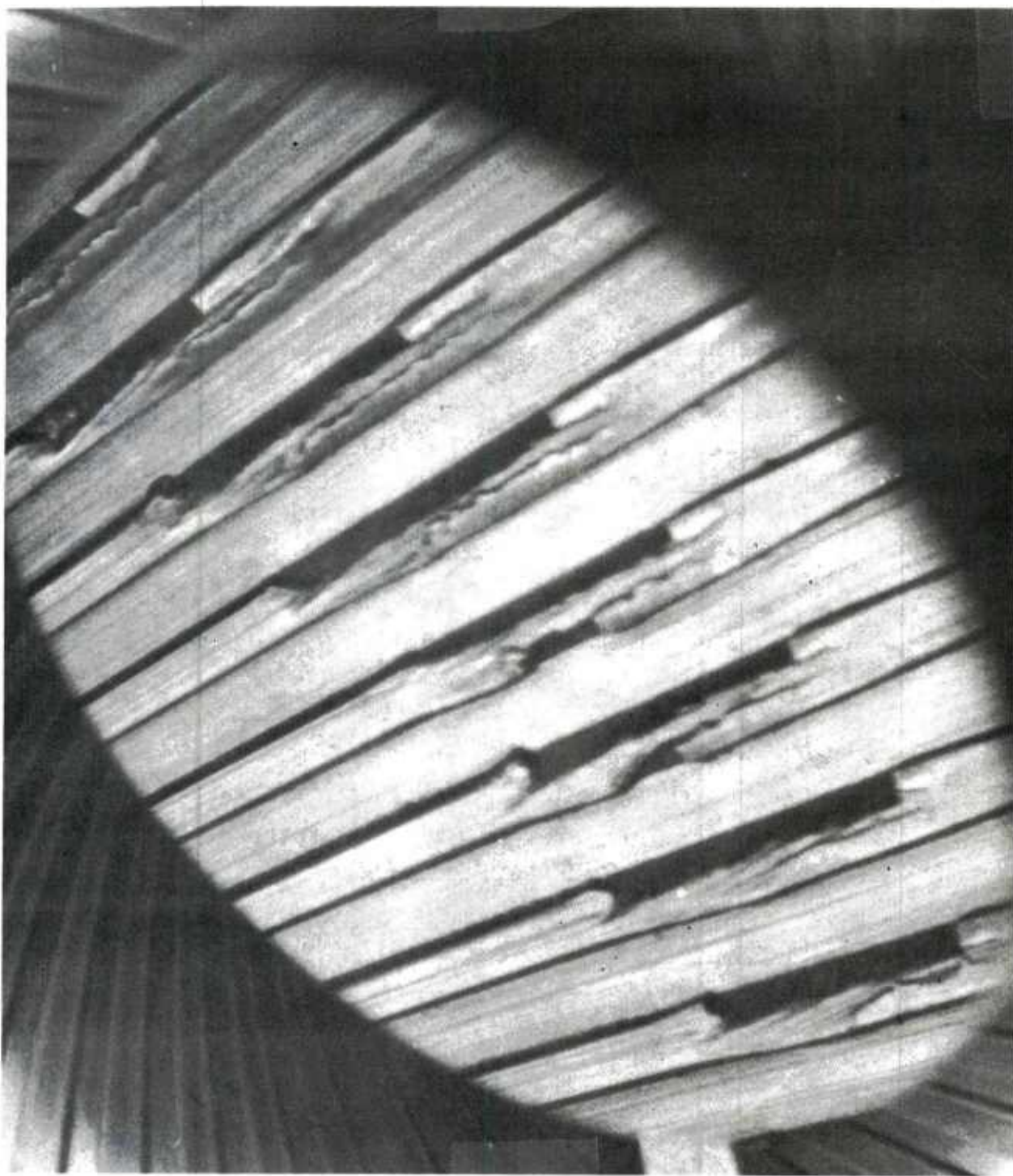
Note: The steep forcing cone design was incorporated in all U.S. 155-mm M185 cannons.

Figure 3. M185 cannon tube grooved forcing cone modification



a. Damage at start of rifling, at 13 cm, and at 23 cm

Figure 4. Damage to tube S/N 25460



b. Enlargement showing damage at 13 cm between 2 and 4 o'clock

Figure 4. (cont)

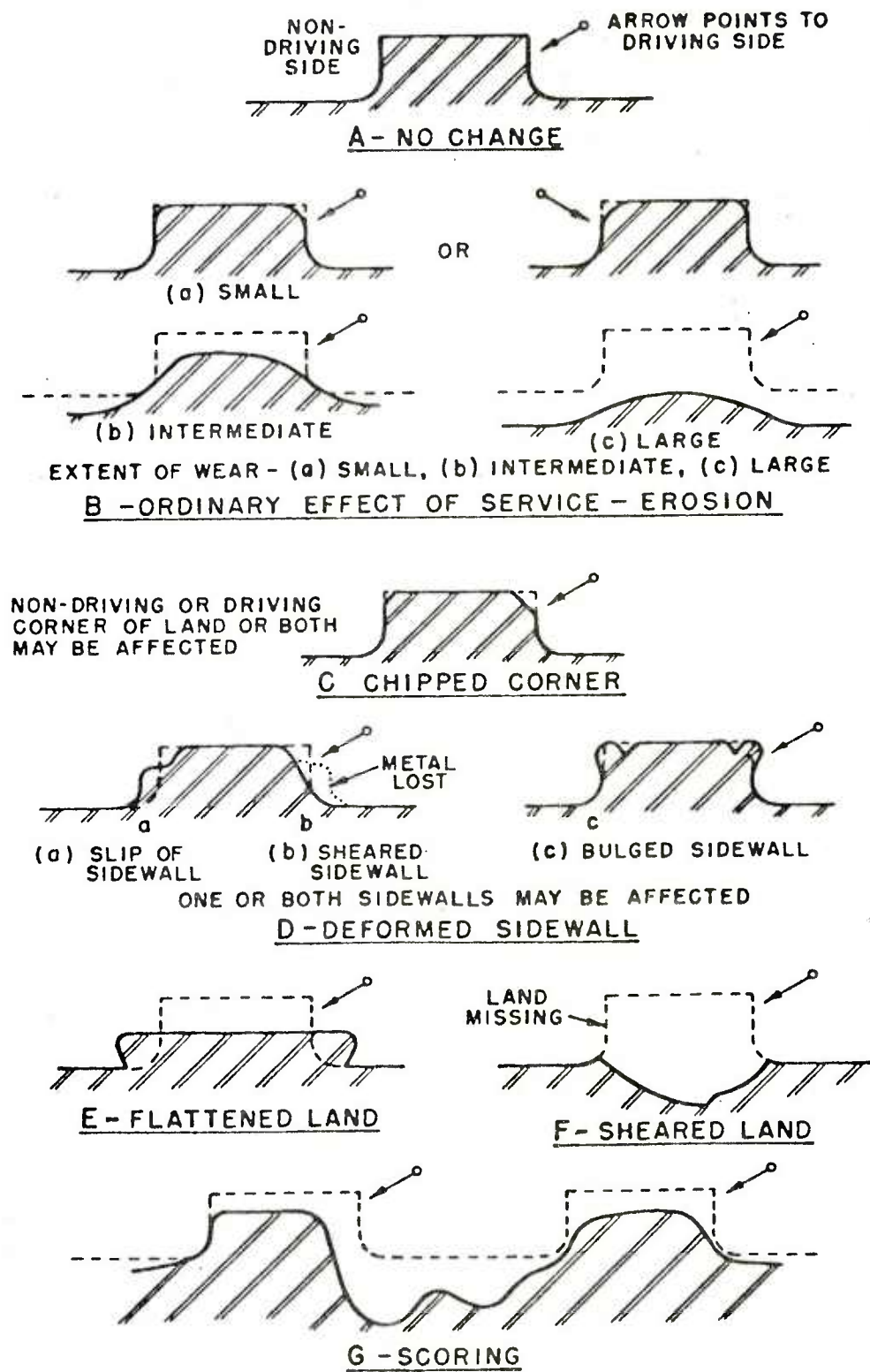


Figure 5. Nomenclature for worn or deformed rifling. Transverse sections normal to axis of gun tube

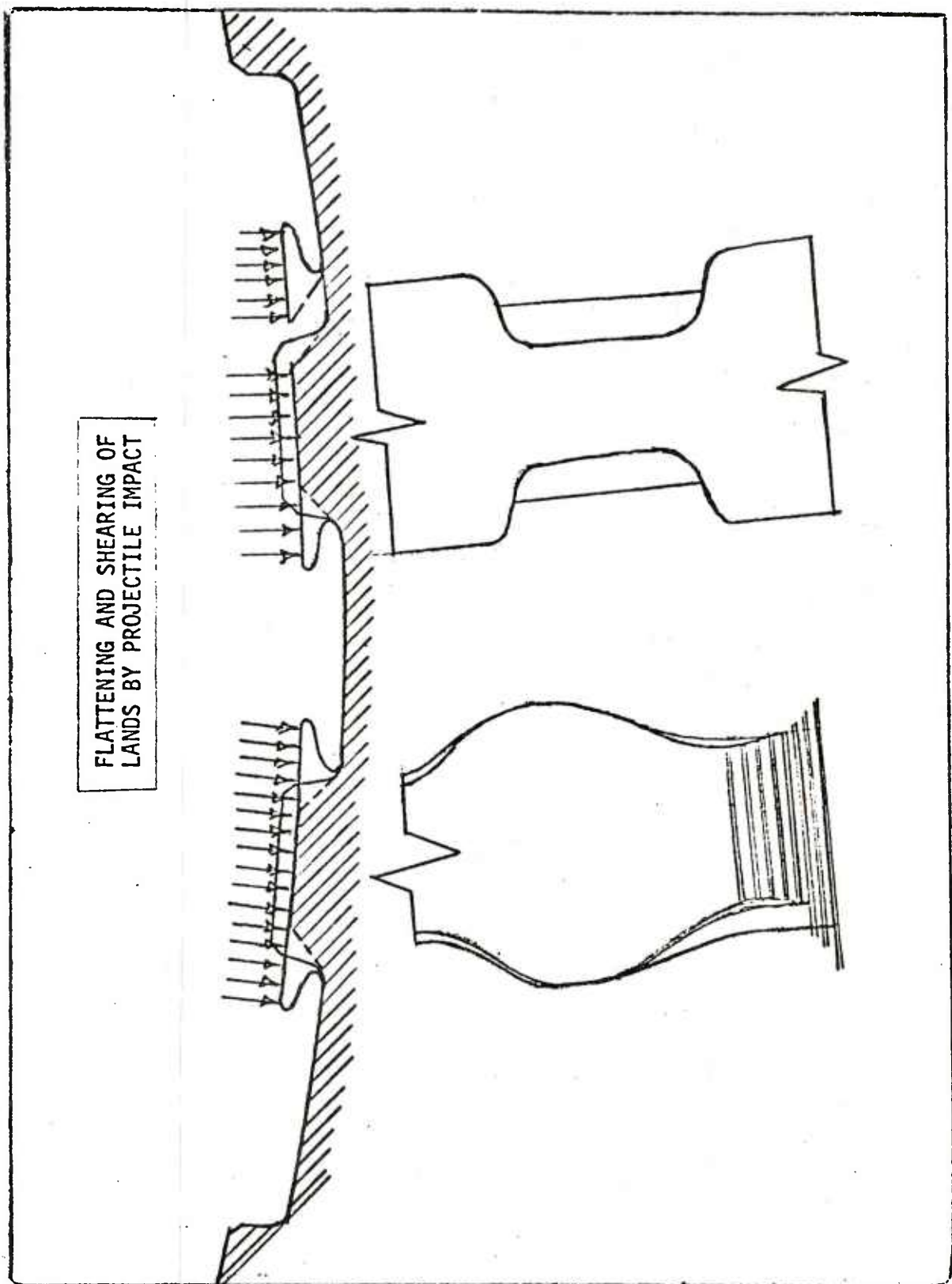


Figure 6. Mechanism of land stripping--fragments sheared down

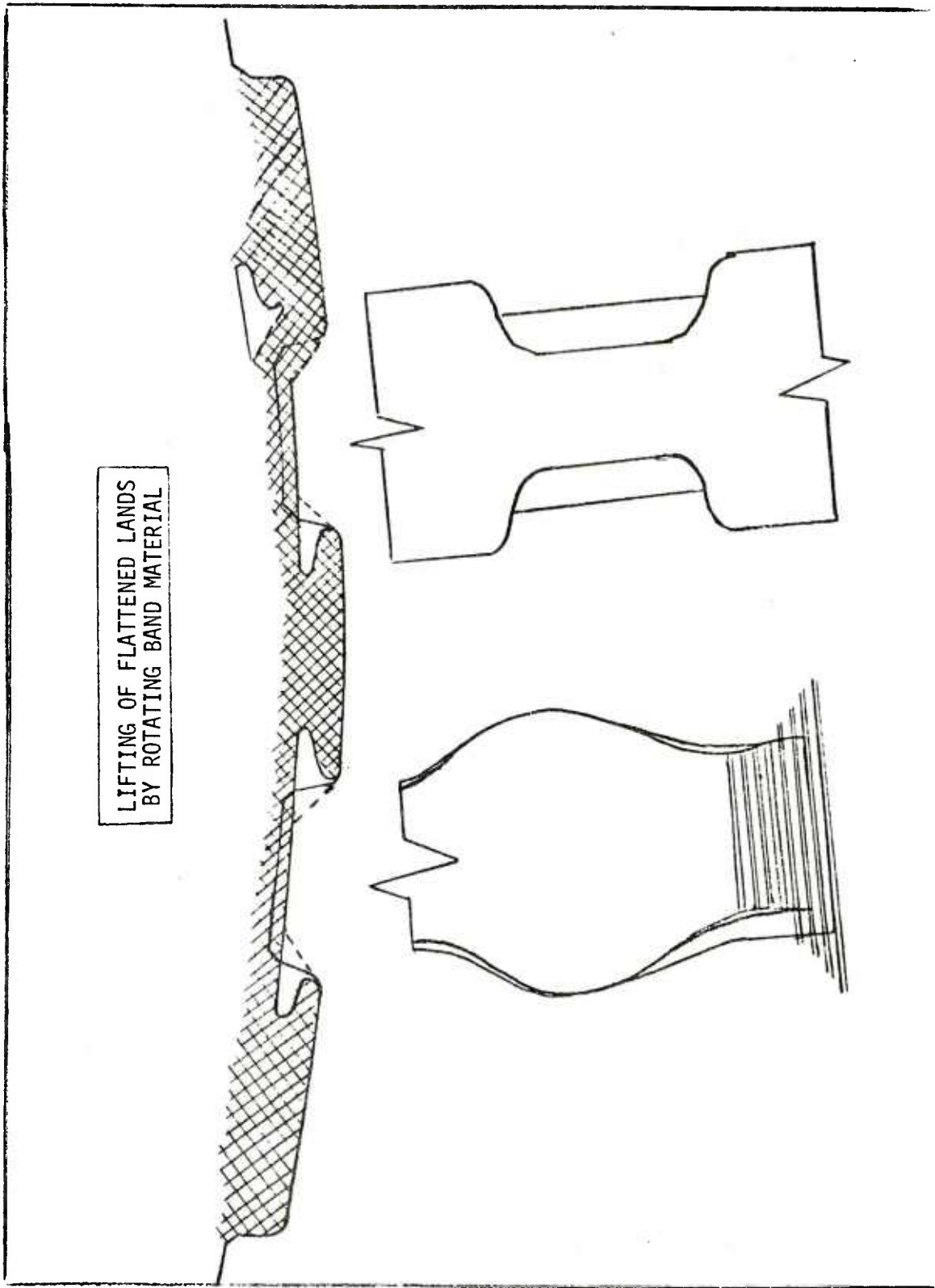
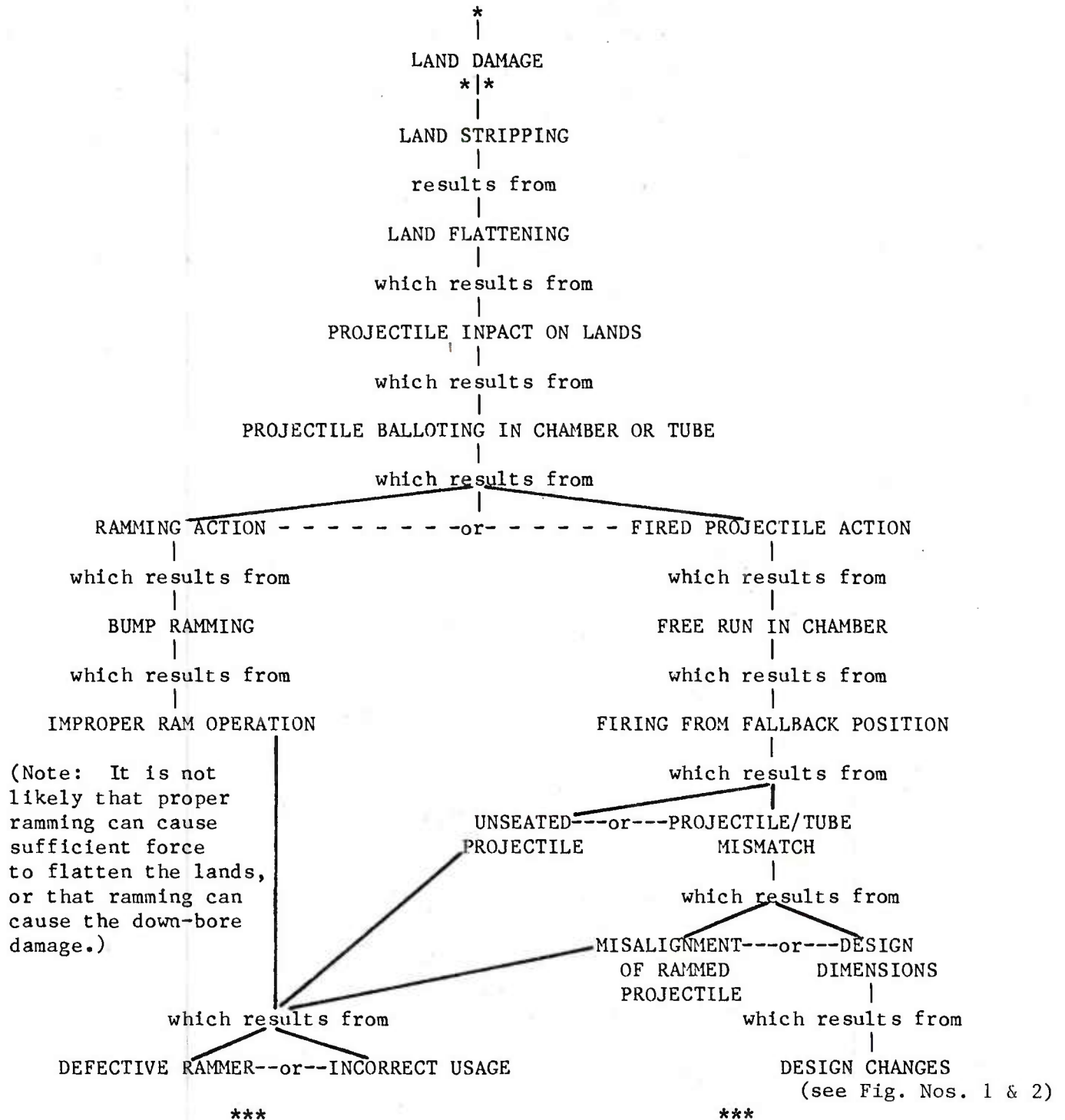


Figure 7. Mechanism of land stripping--fragments lifted



The root cause in this fault tree appears to be either in the dimensions of the rotating band/forcing cone or in the operation of the rammer.

Figure 8. Land damage fault tree

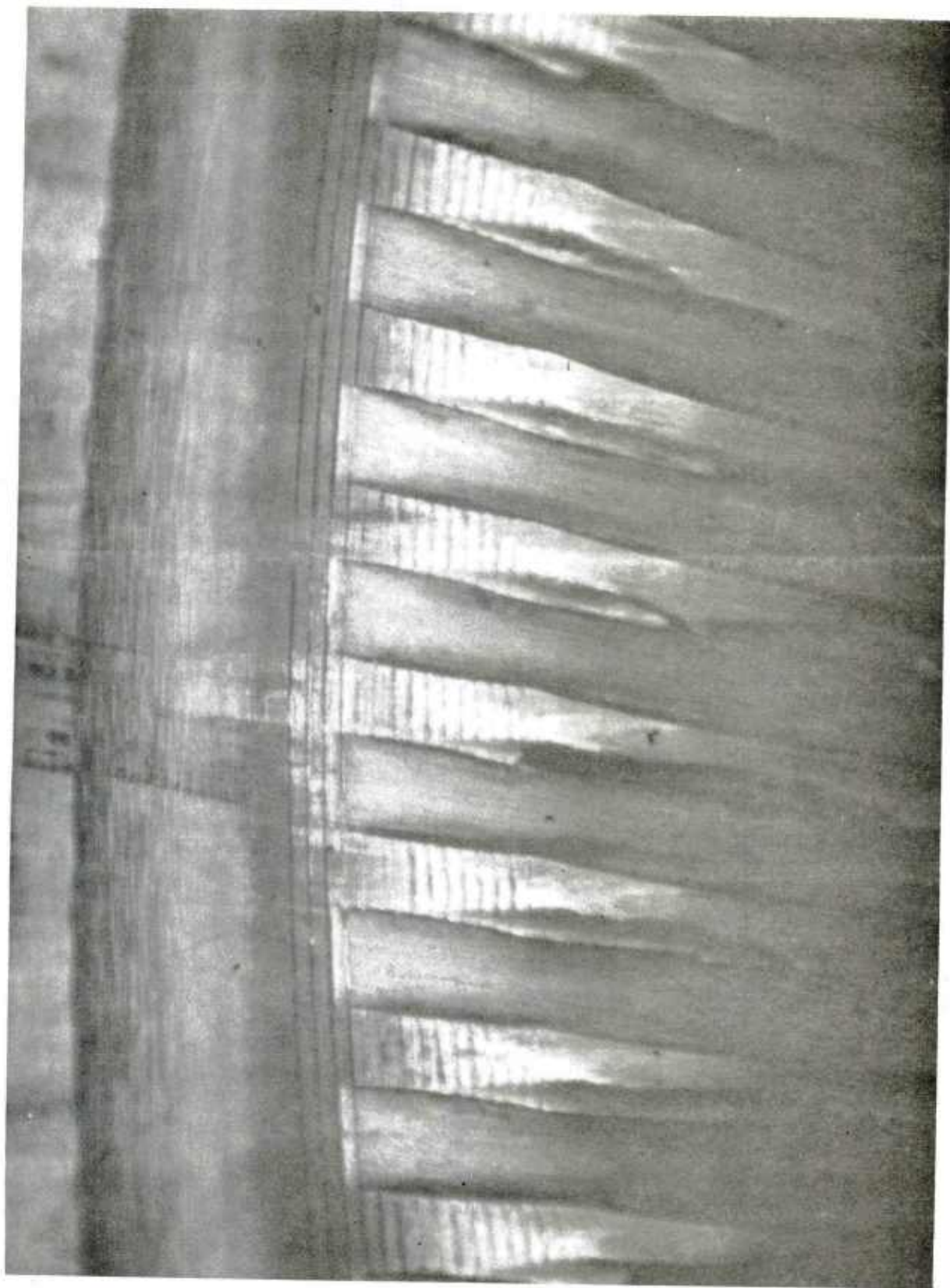


Figure 9. Rifling damage to tube S/N 24715 after tube round 9--12 o'clock position



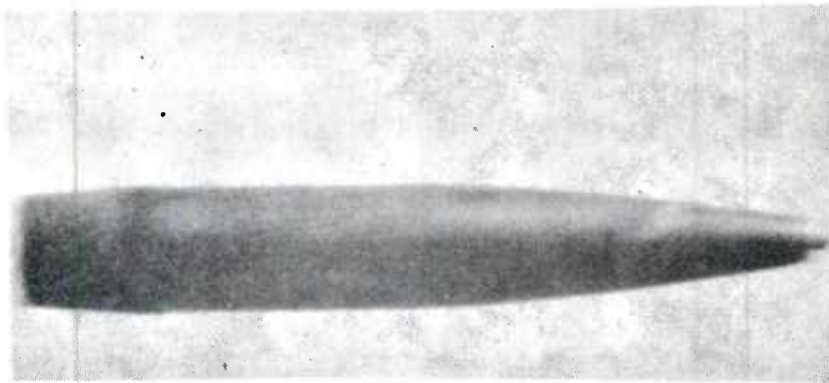
a. Projectile 9 fired 1 April 1981

Figure 10. Recovered projectile--fallback test

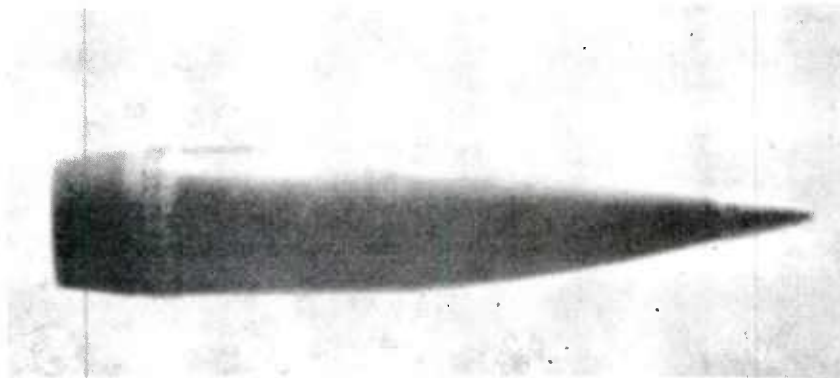


b. Projectile 2 fired 31 March 1981

Figure 10. (cont)



Round No. 9 fired from tube No. 24715.
Note that the windshield is missing
from the fuze. The projectile is not
proportioned properly in this photo-
graph because the muzzle velocity was
not as high as expected.



View of projectile which showed no
abnormalities in the smear photographs.

Tube No. 28317, Tube Round No. 13

Figure 11. Smear camera photographs of projectile's muzzle exit

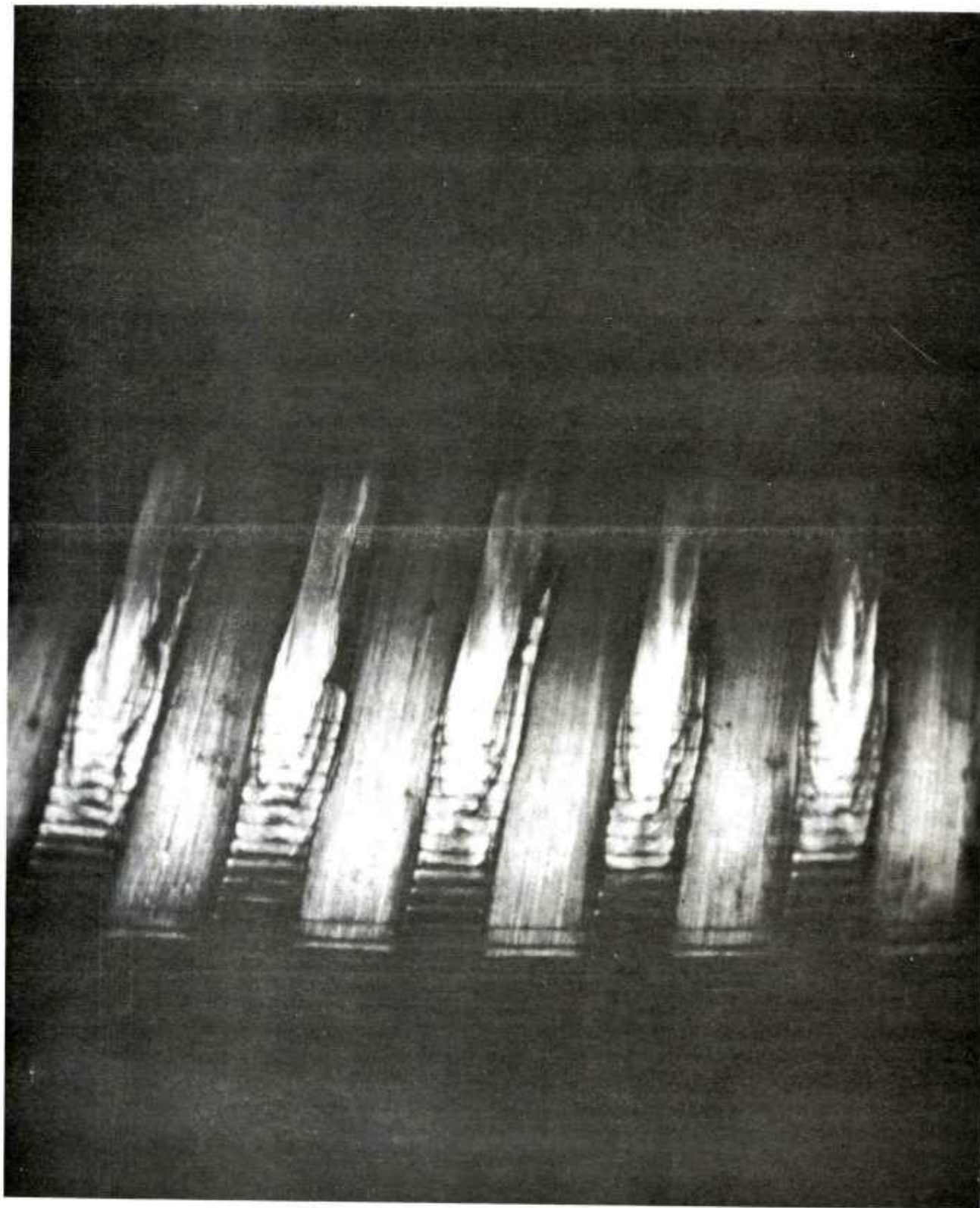
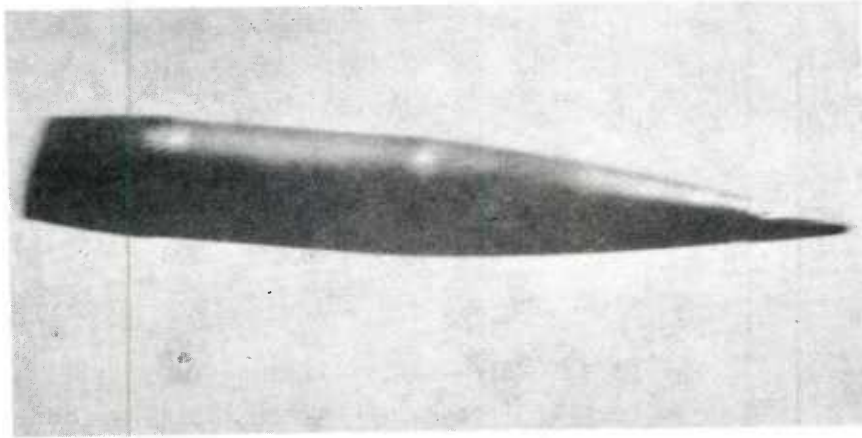


Figure 12. Tube S/N 28317 at end of fallback test--3 o'clock position



Round No. 4 fired from
tube No. 28317 showing
projectile instability
near the muzzle.



Round No. 26 fired from
tube No. 28317. Note
that the windshield is
missing from the fuze
and is behind the pro-
jectile when this
photograph was taken.

Figure 13. Smear camera photographs of flight instability and fuze damage

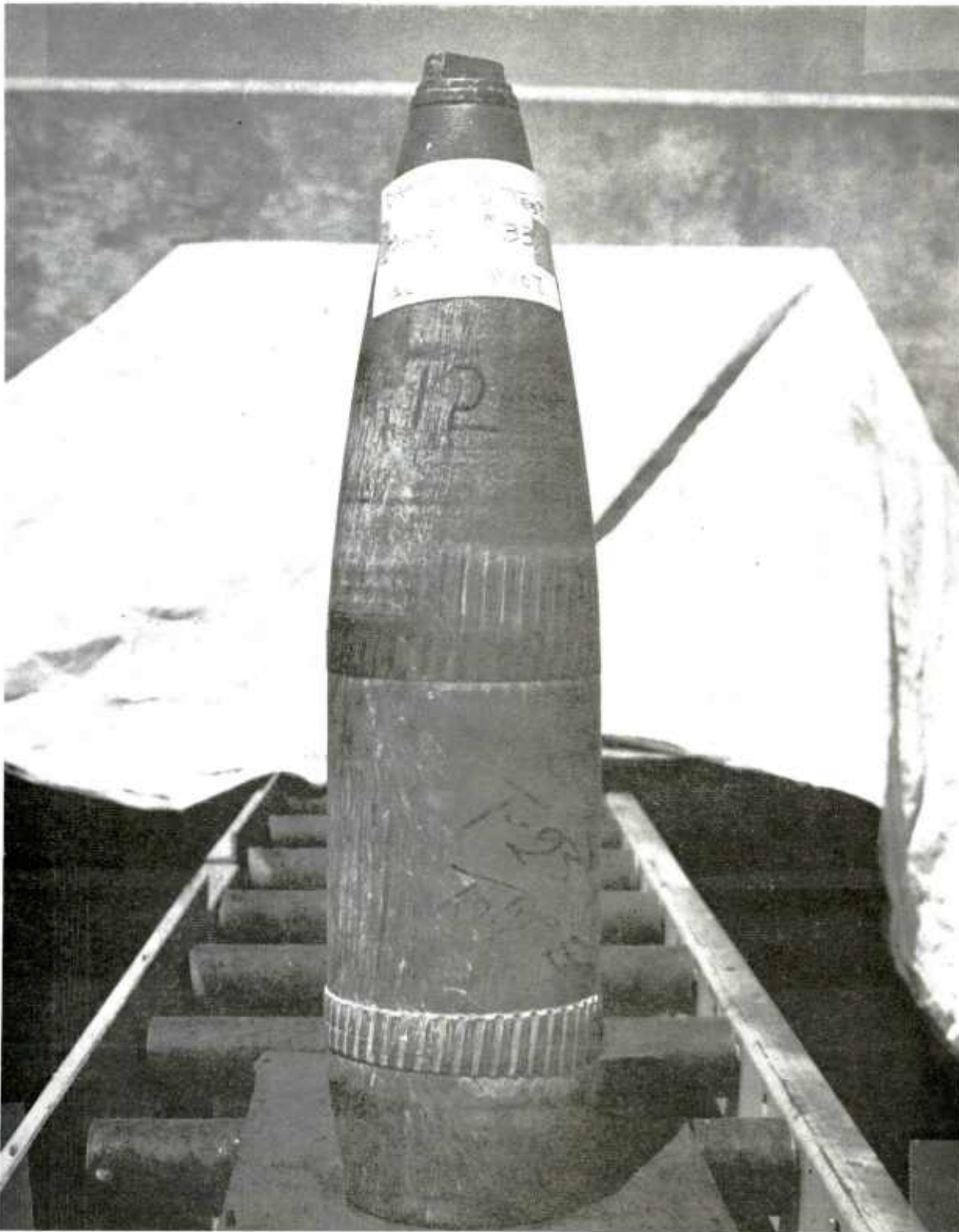
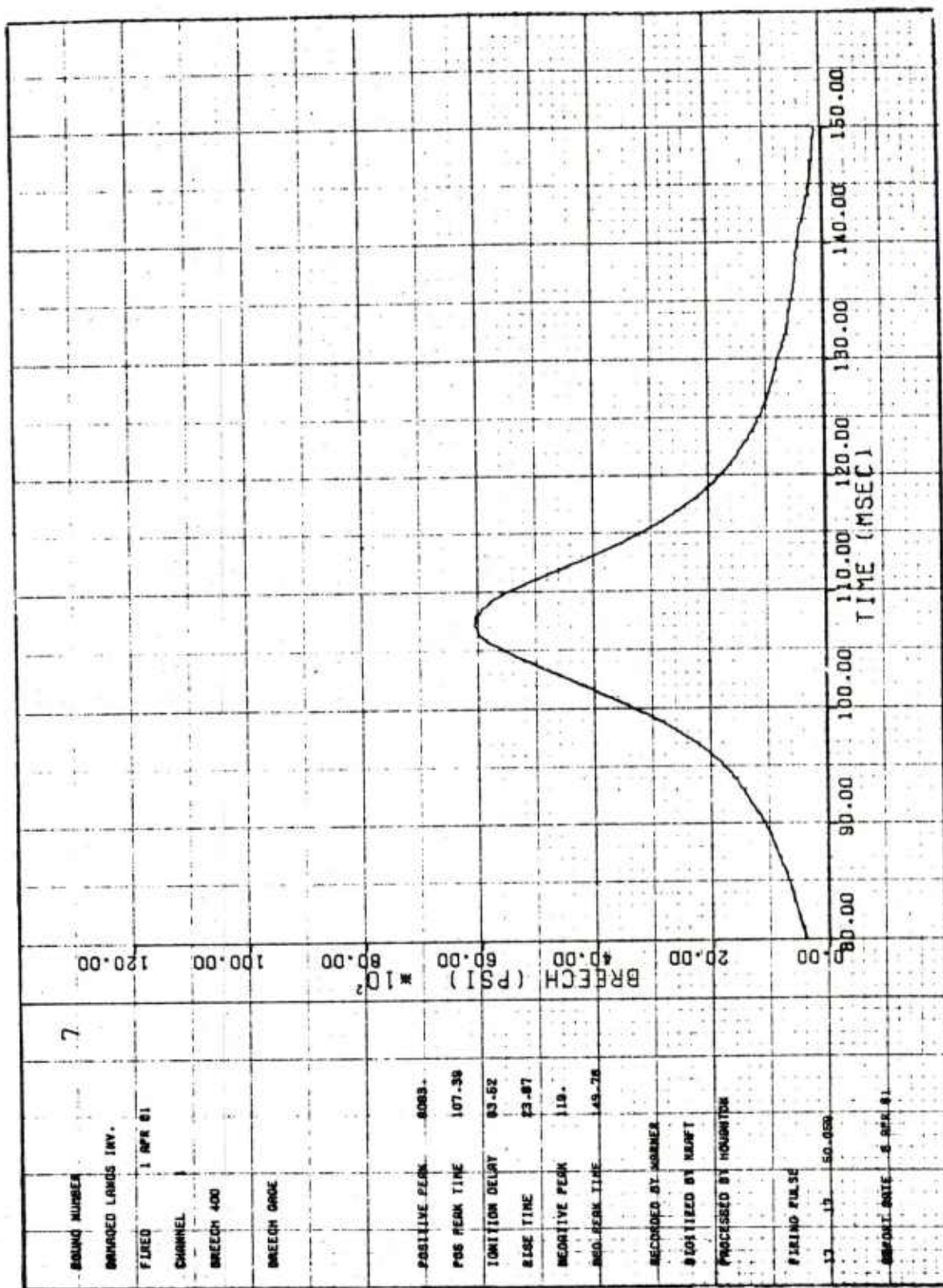
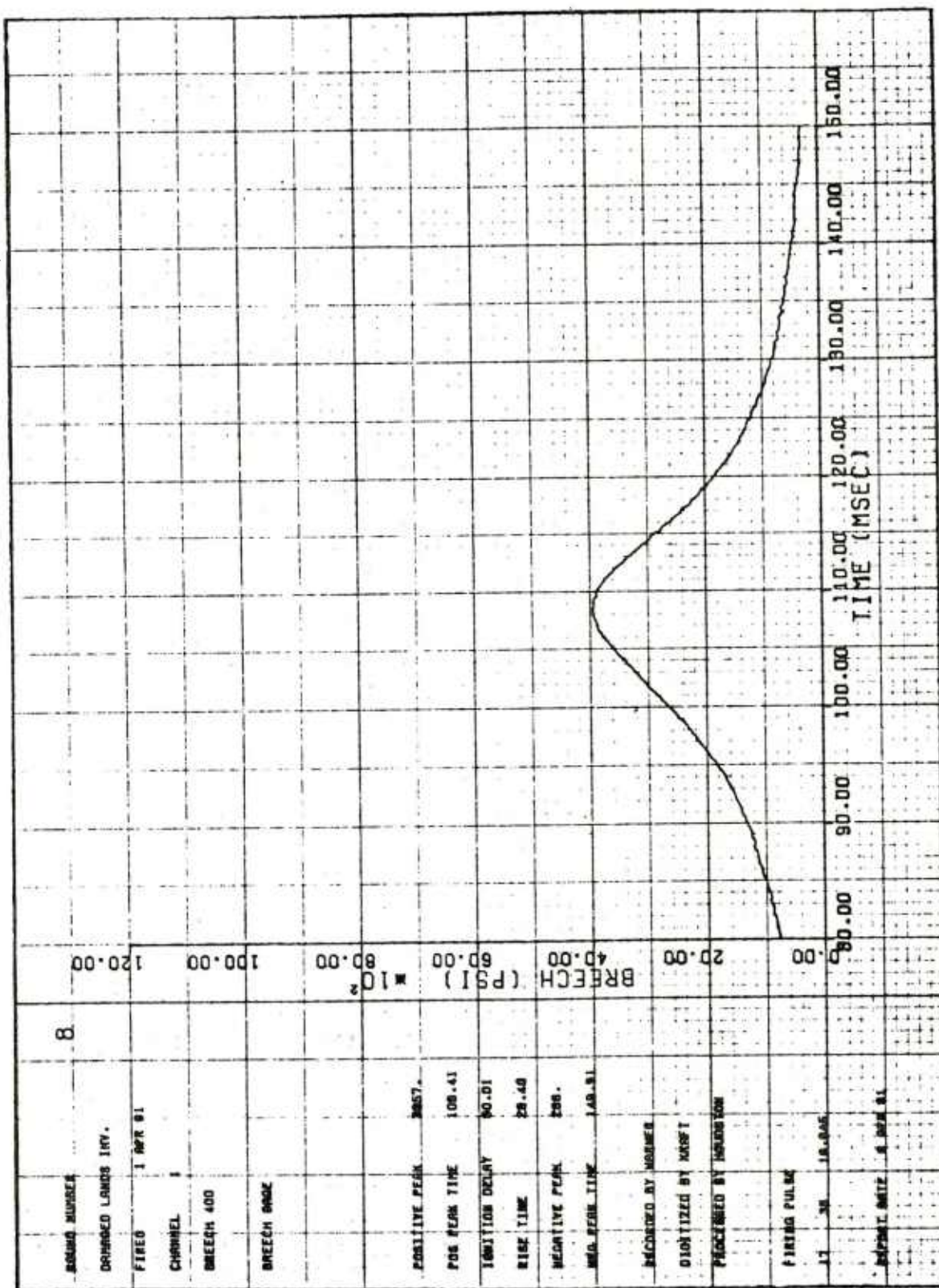


Figure 14. Tube round no. 23 fired from tube S/N 28317. Note the engraving on the ogive, front bourrelet and the body from contact with the rifling.



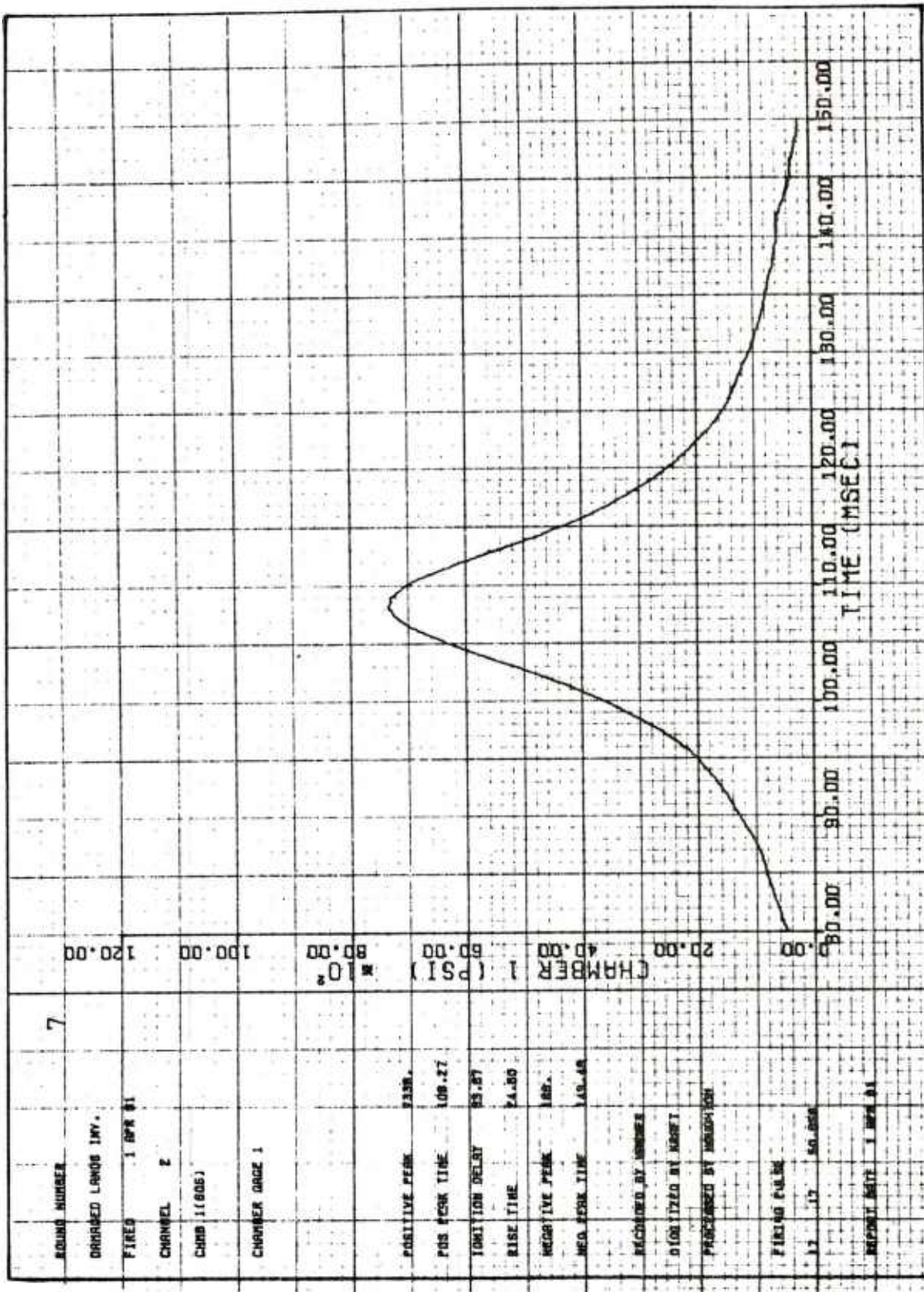
a. Breech--round 7

Figure 15. Breech and chamber pressure curves--tube S/N 24715



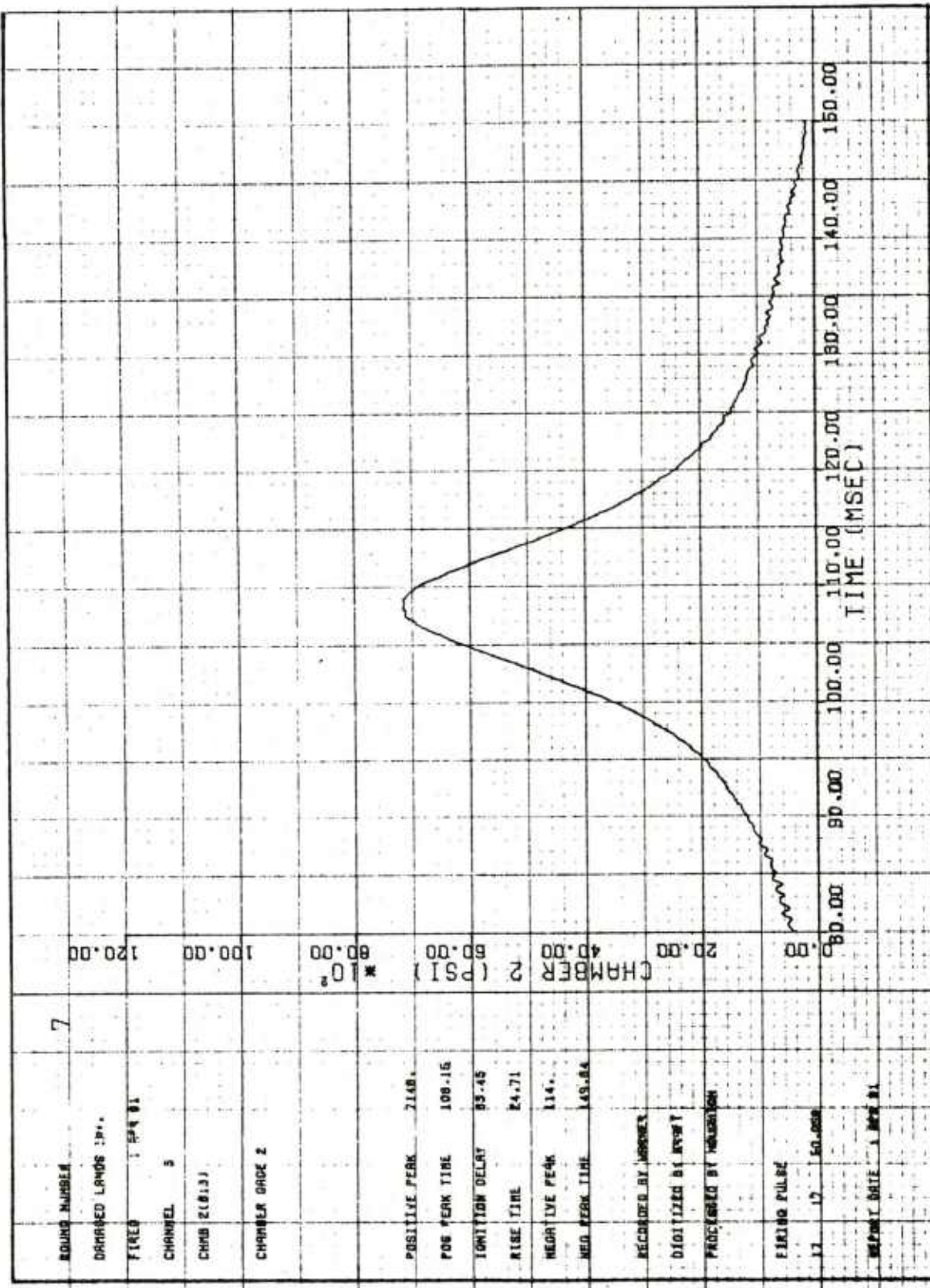
b. Breech--round 8

Figure 15. (cont)



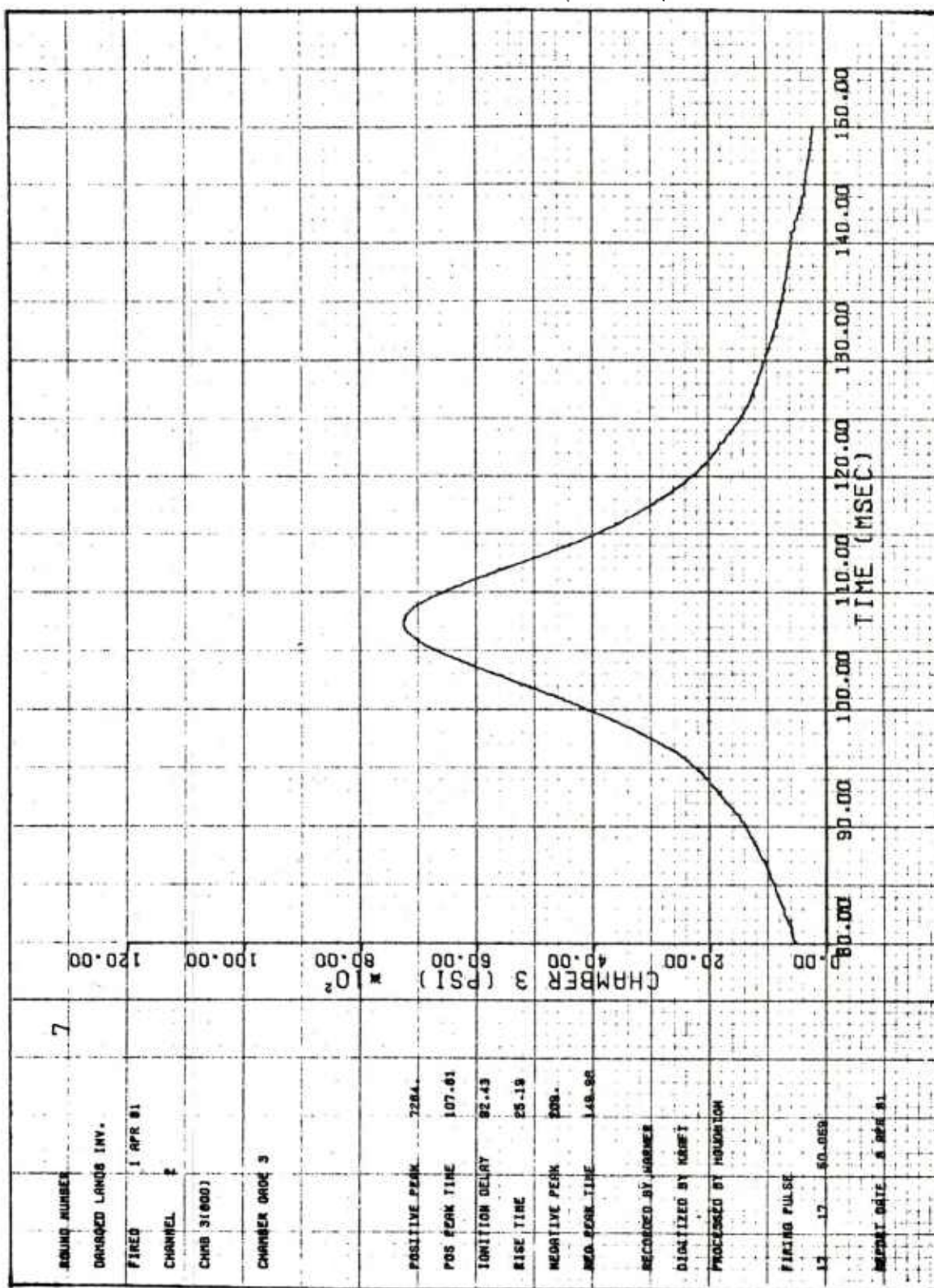
c. Chamber--position no. 1--round 7

Figure 15. (cont)



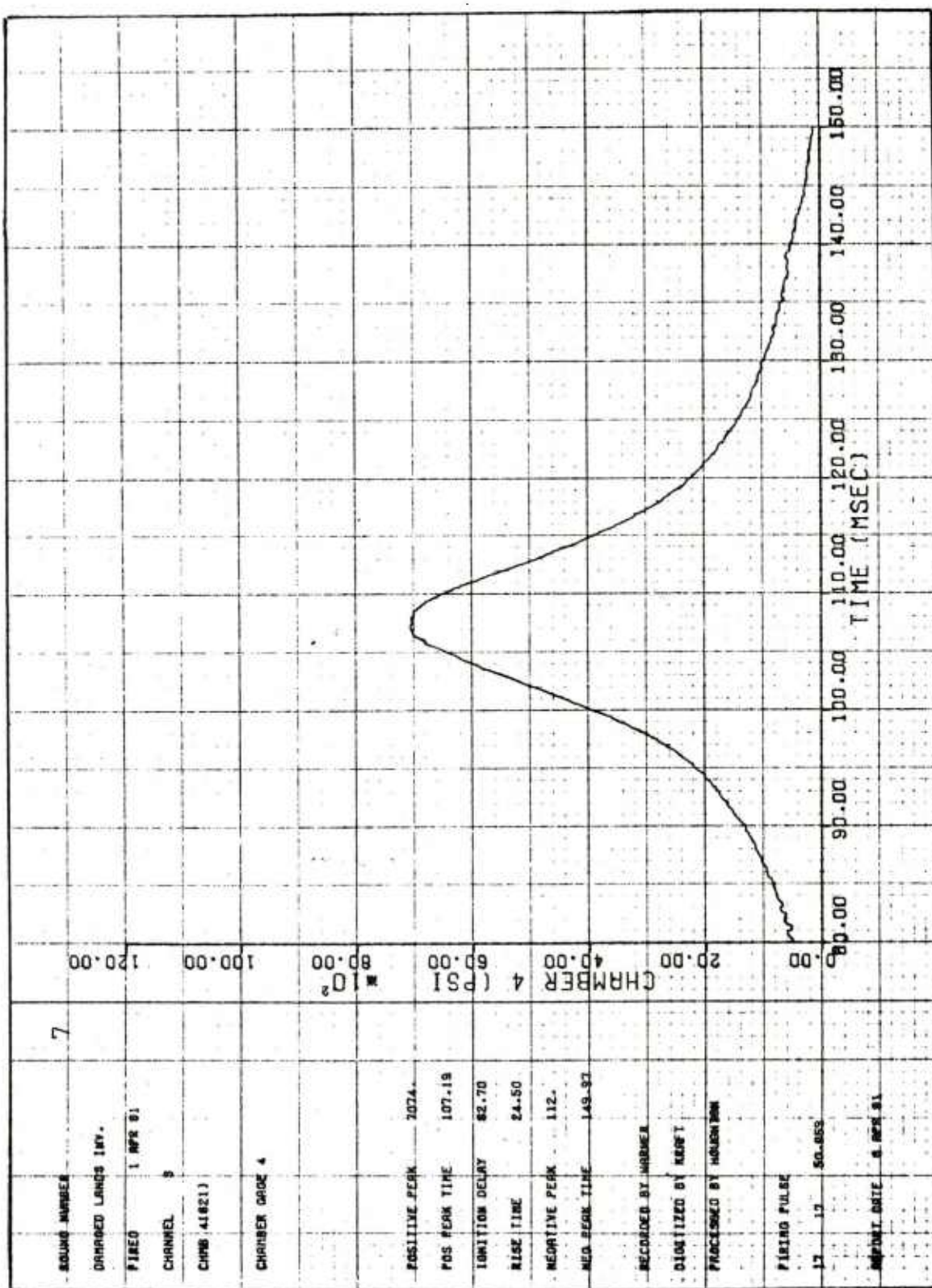
d. Chamber--position no. 2--round 7

Figure 15. (cont)



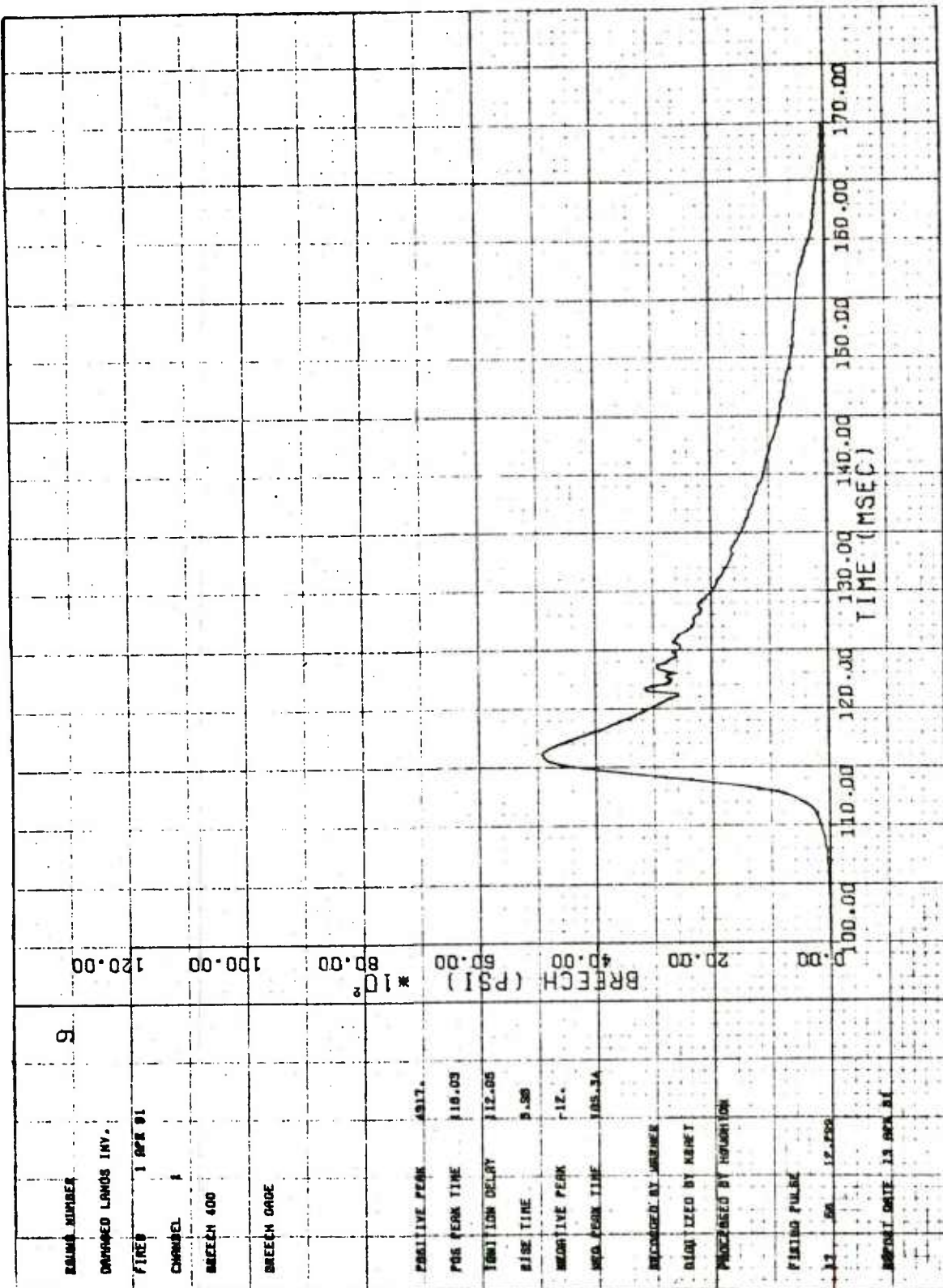
e. Chamber--position no. 3--round 7

Figure 15. (cont)



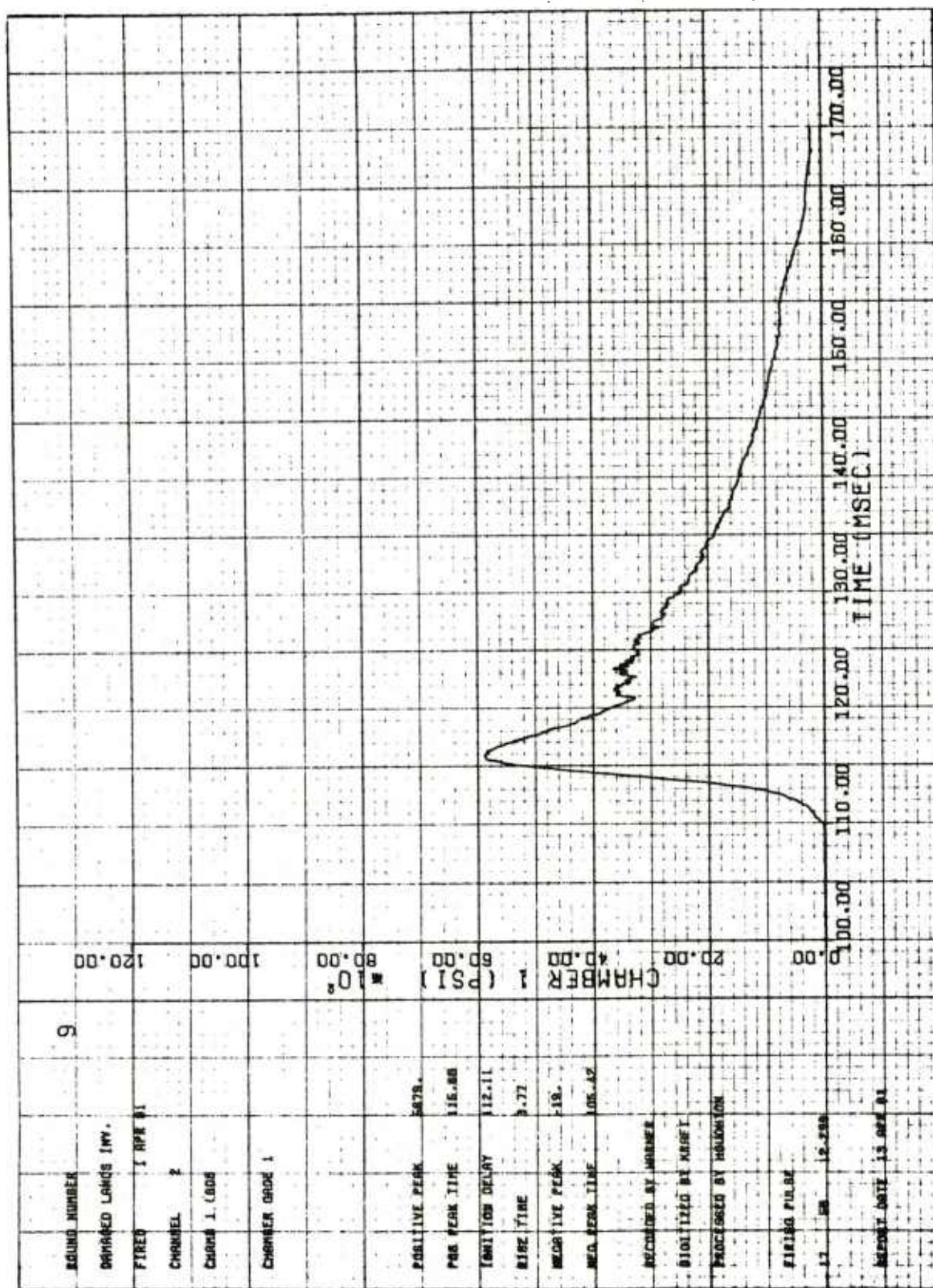
f. Chamber--position no. 4--round 7

Figure 15. (cont)



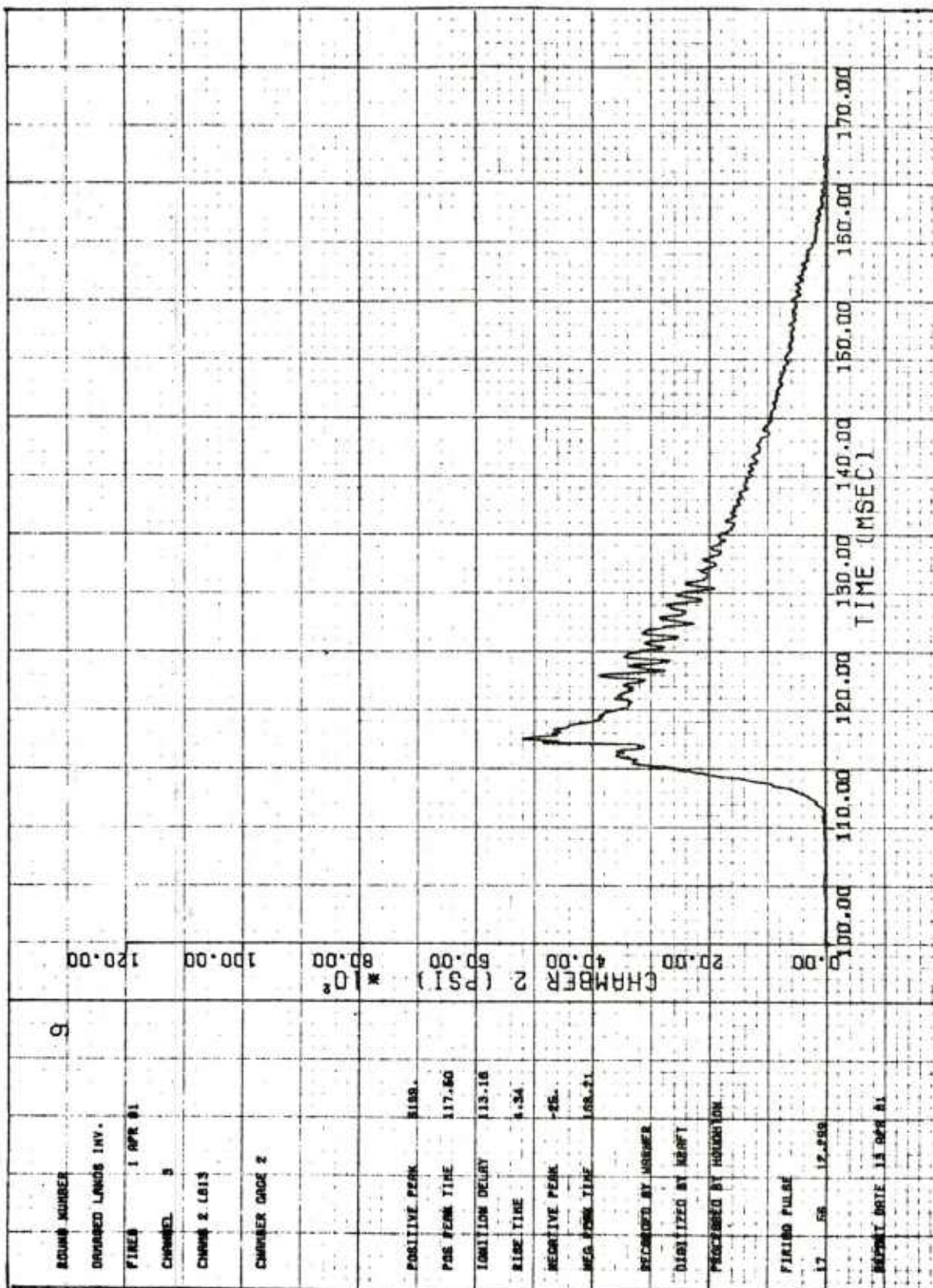
g. Breech--round 9

Figure 15. (cont)



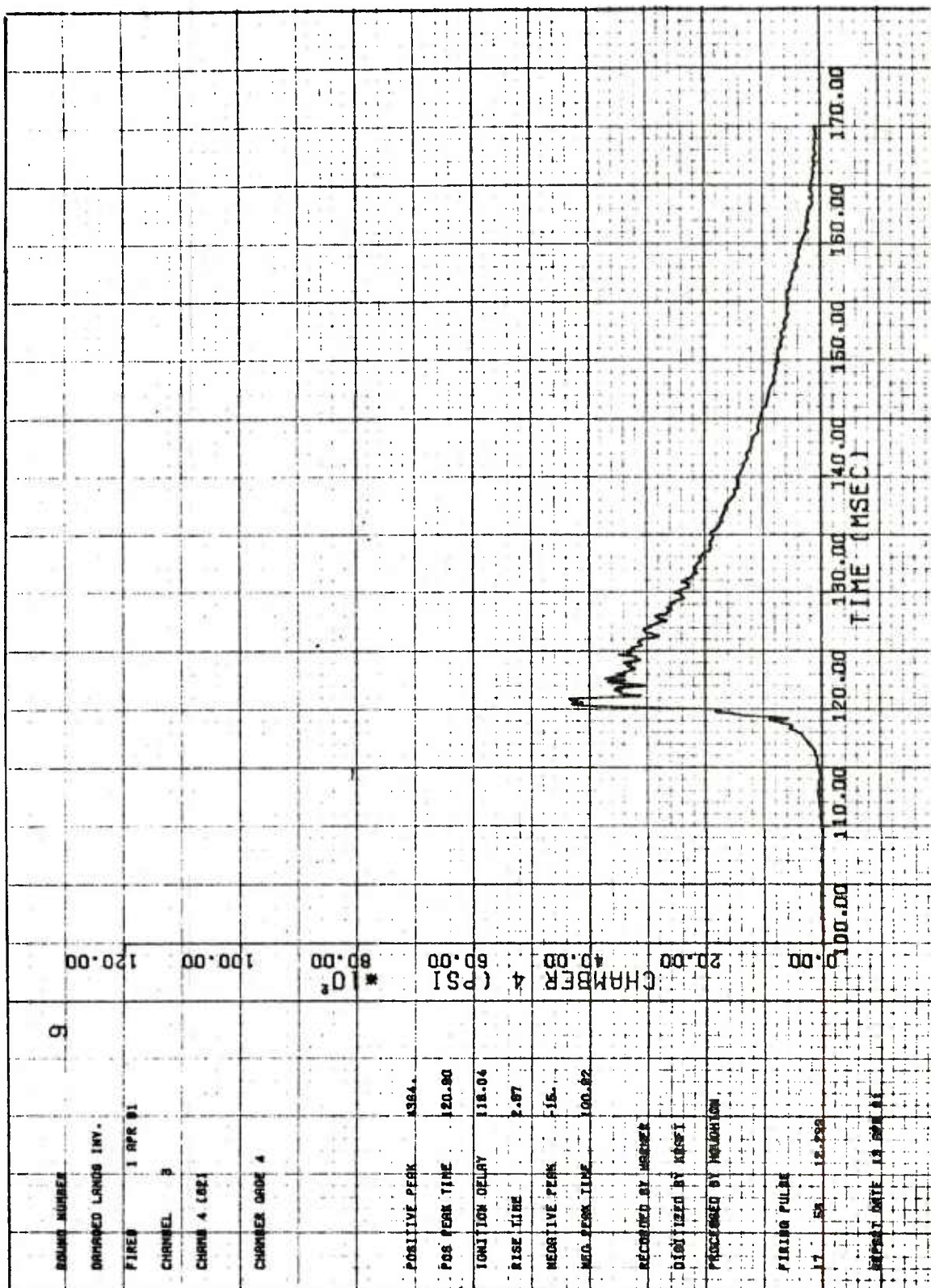
h. Chamber--position no. 1--round 9

Figure 15. (cont)



i. Chamber--position no. 2--round 9

Figure 15. (cont)



k. Chamber--position no. 4--round 9

Figure 15. (cont)

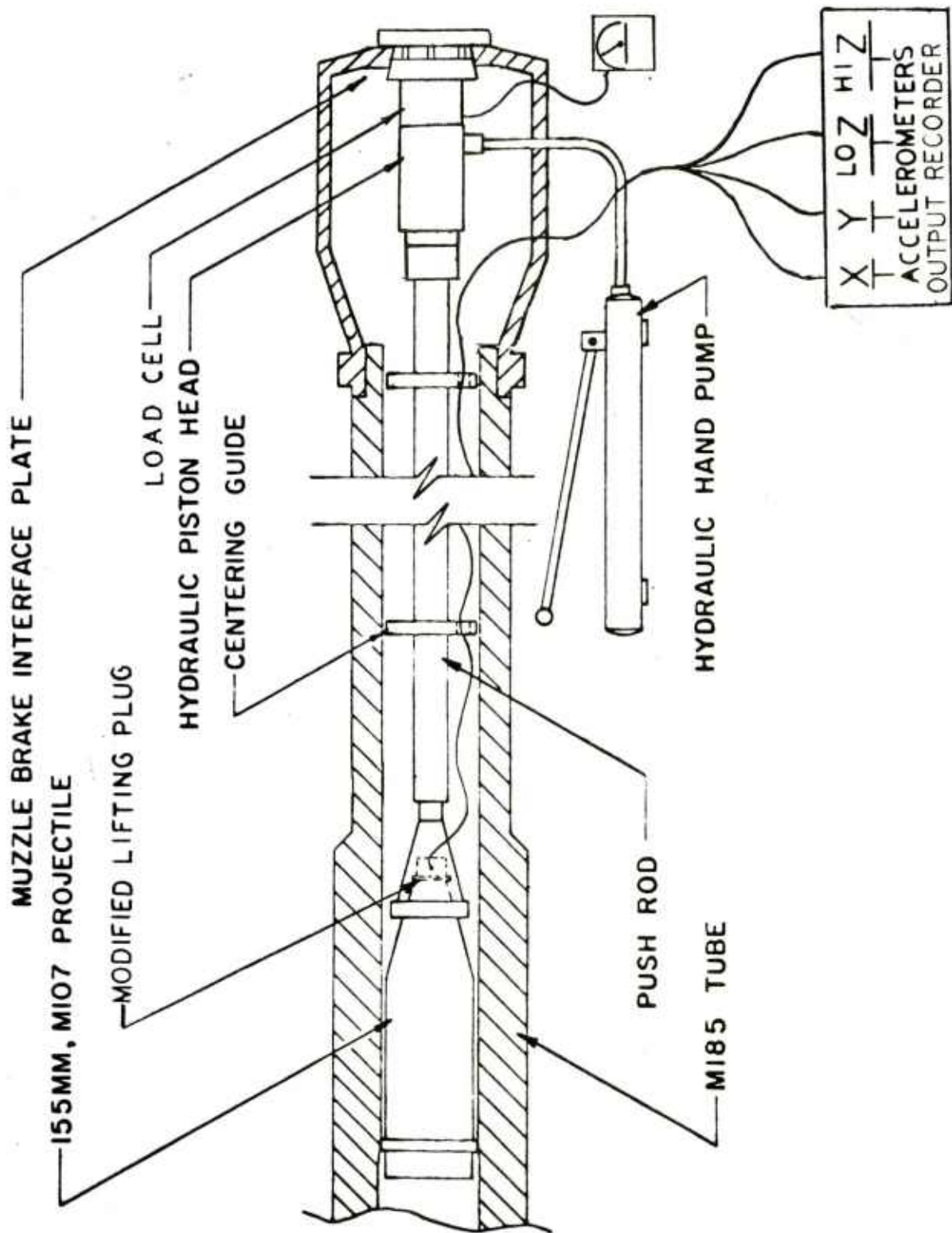


Figure 16. Pictorial schematic of Deram tool

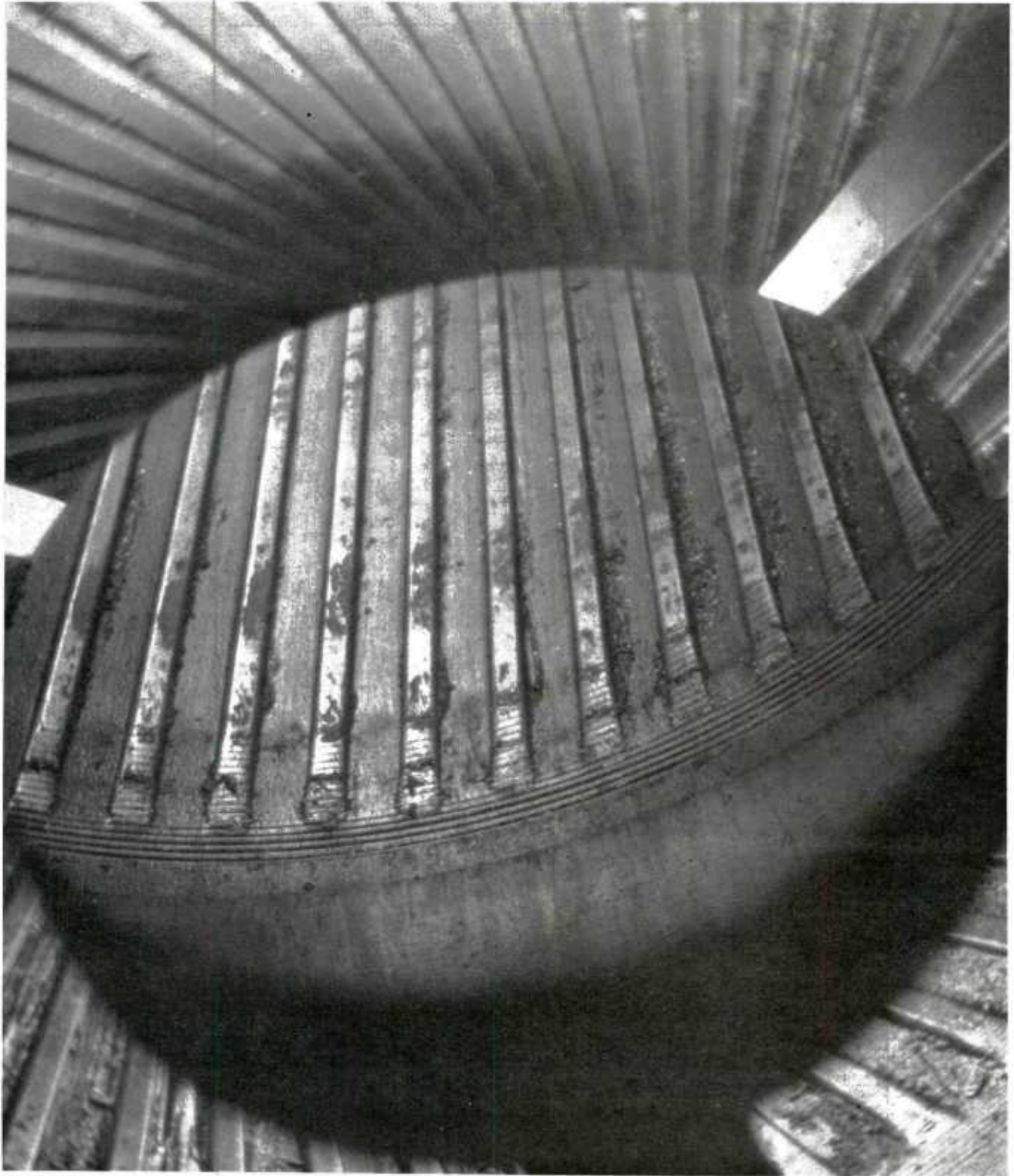


Figure 17. M185 cannon tube S/N 26066 after ramming test--shows debris but no damage

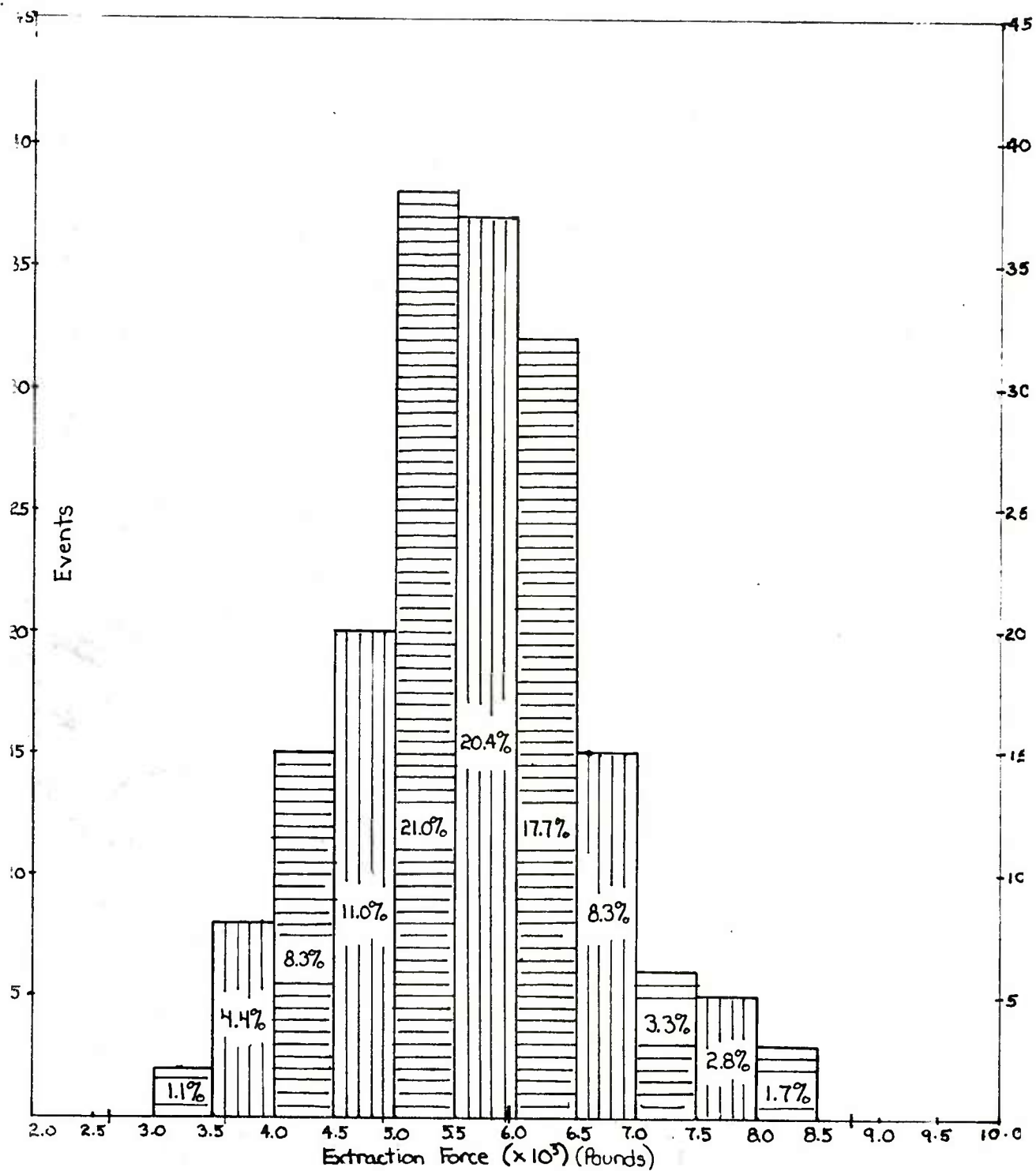
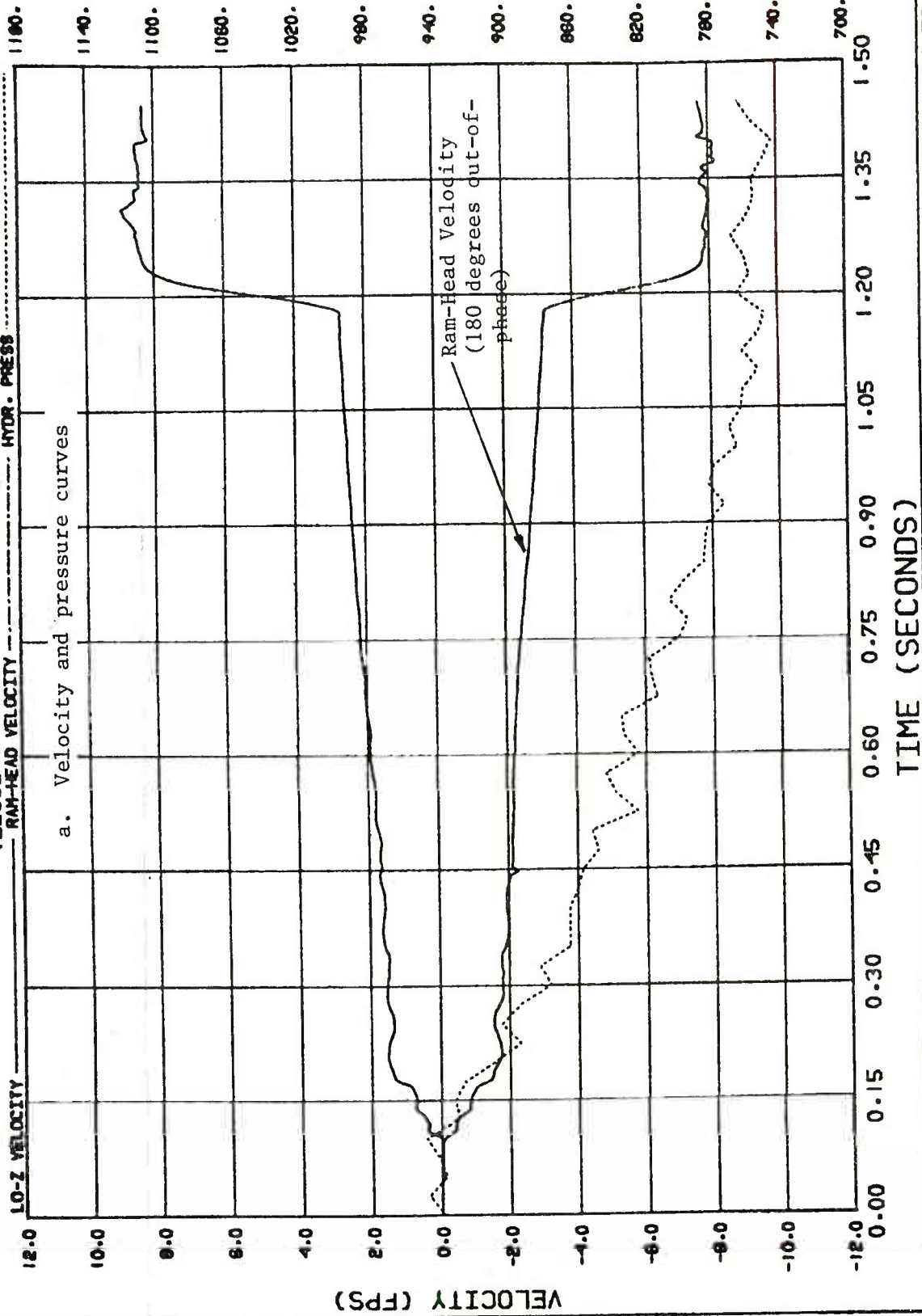


Figure 18. Extraction force--700 mil QE case

M185-DAM1

TEST NO. 4
VELOCITY/HYDR. PRESS (300 MILS)

RAM-HEAD VELOCITY ----- HYDR. PRESS -----



HYDRA VERSION 1.4.00

- 8 -

10/05/82 09:59:32

Figure 19. Ramming test 4--velocity and pressure and acceleration curves

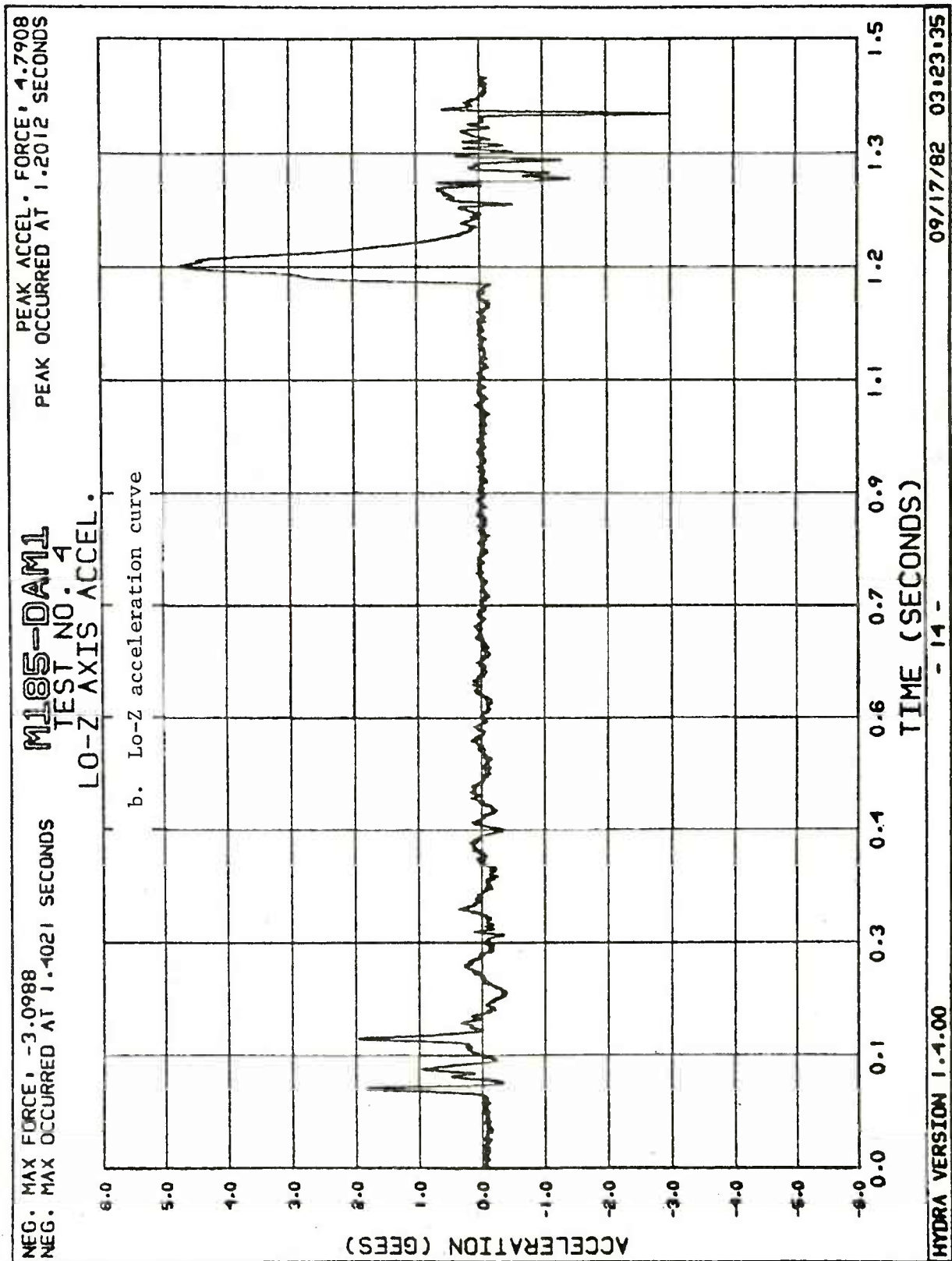


Figure 19. (cont)

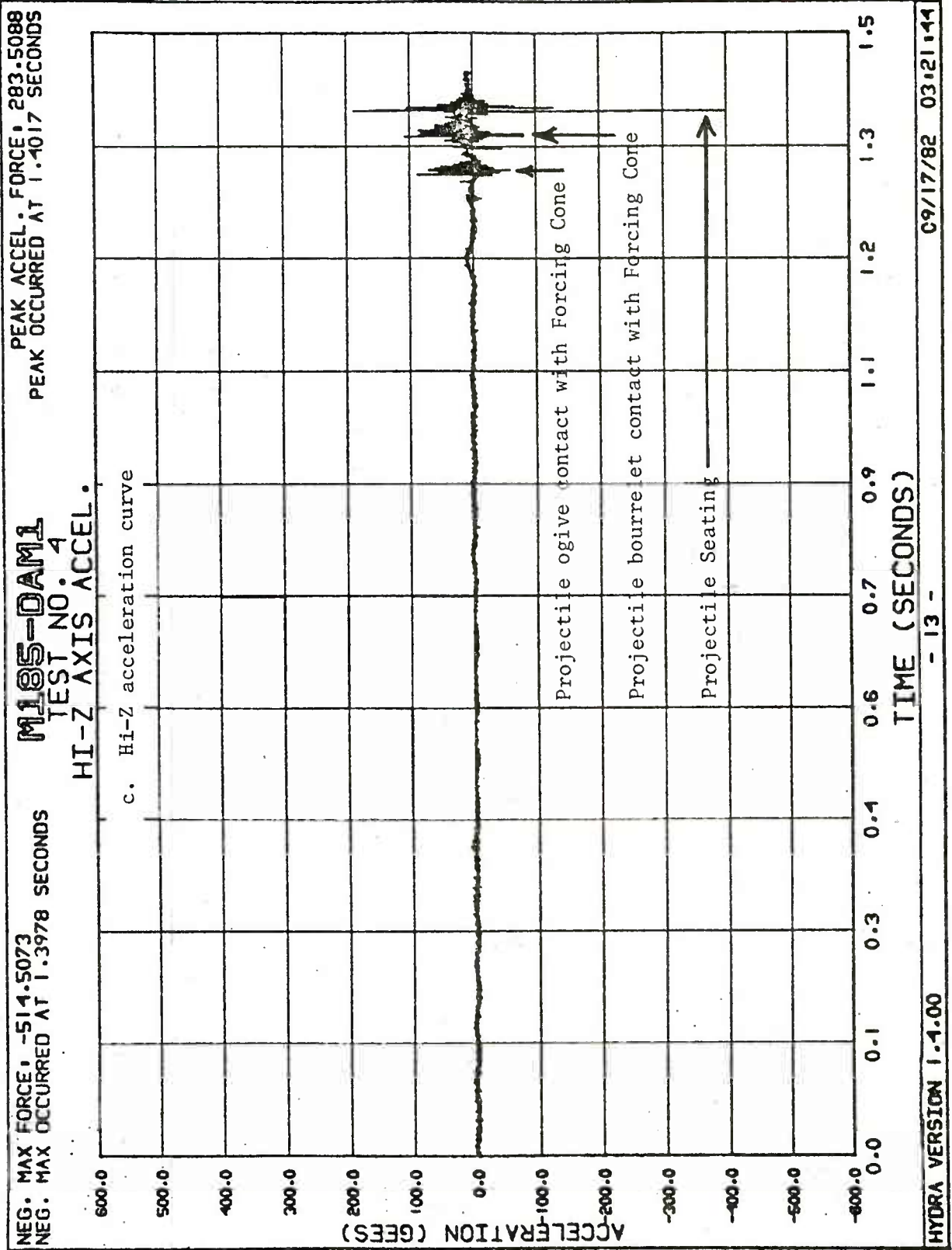


Figure 19. (cont)

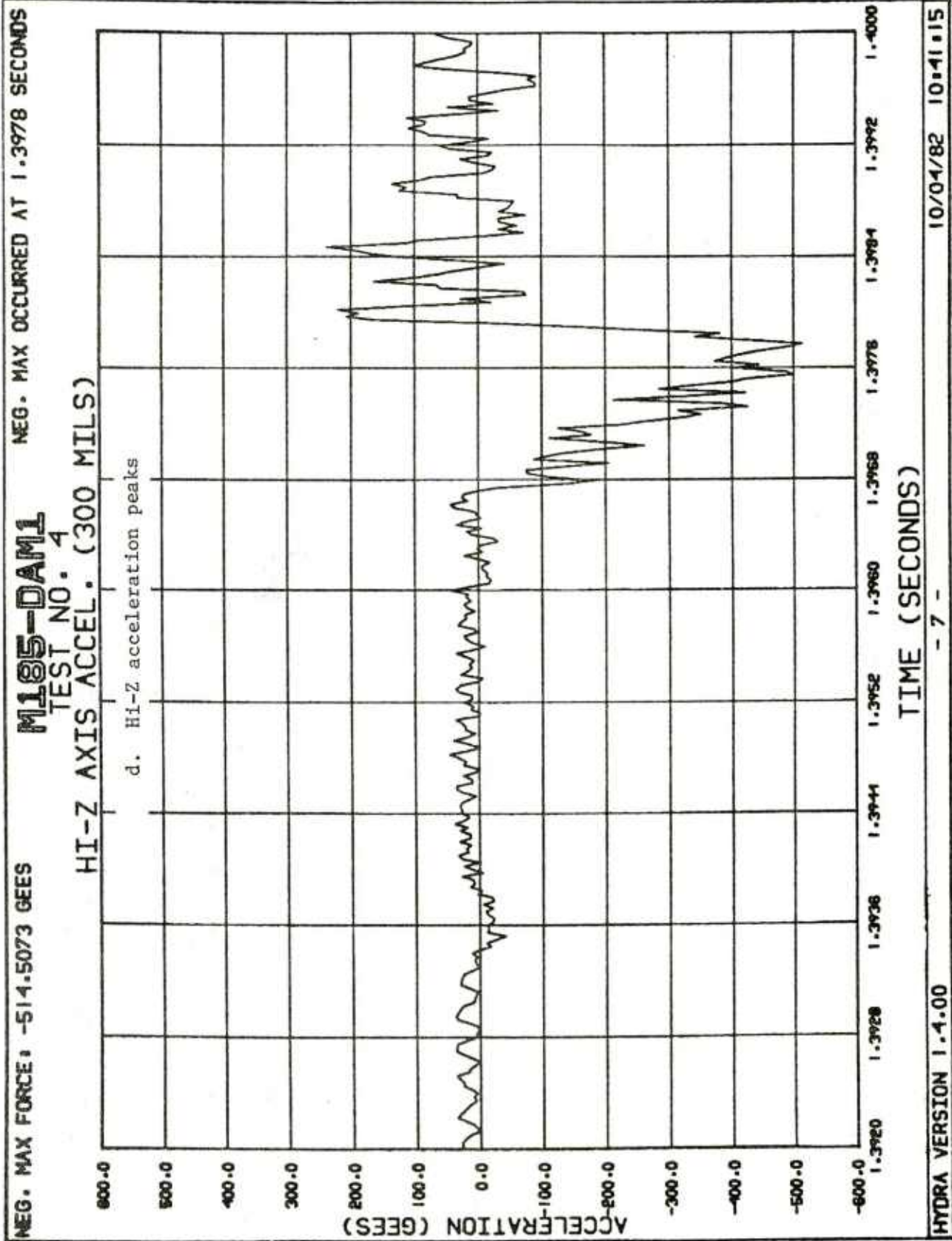


Figure 19. (cont)

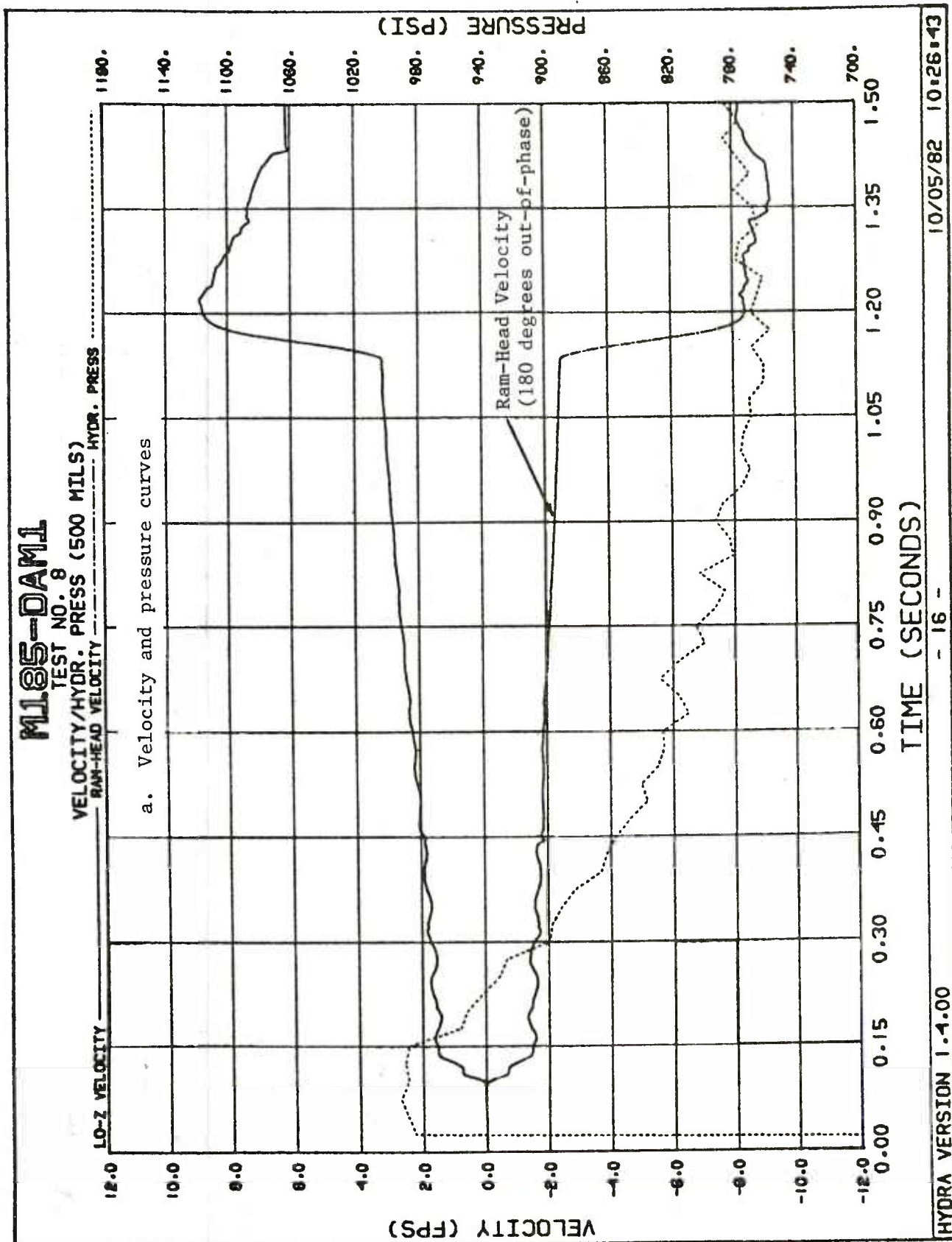


Figure 20. Ramming test 8

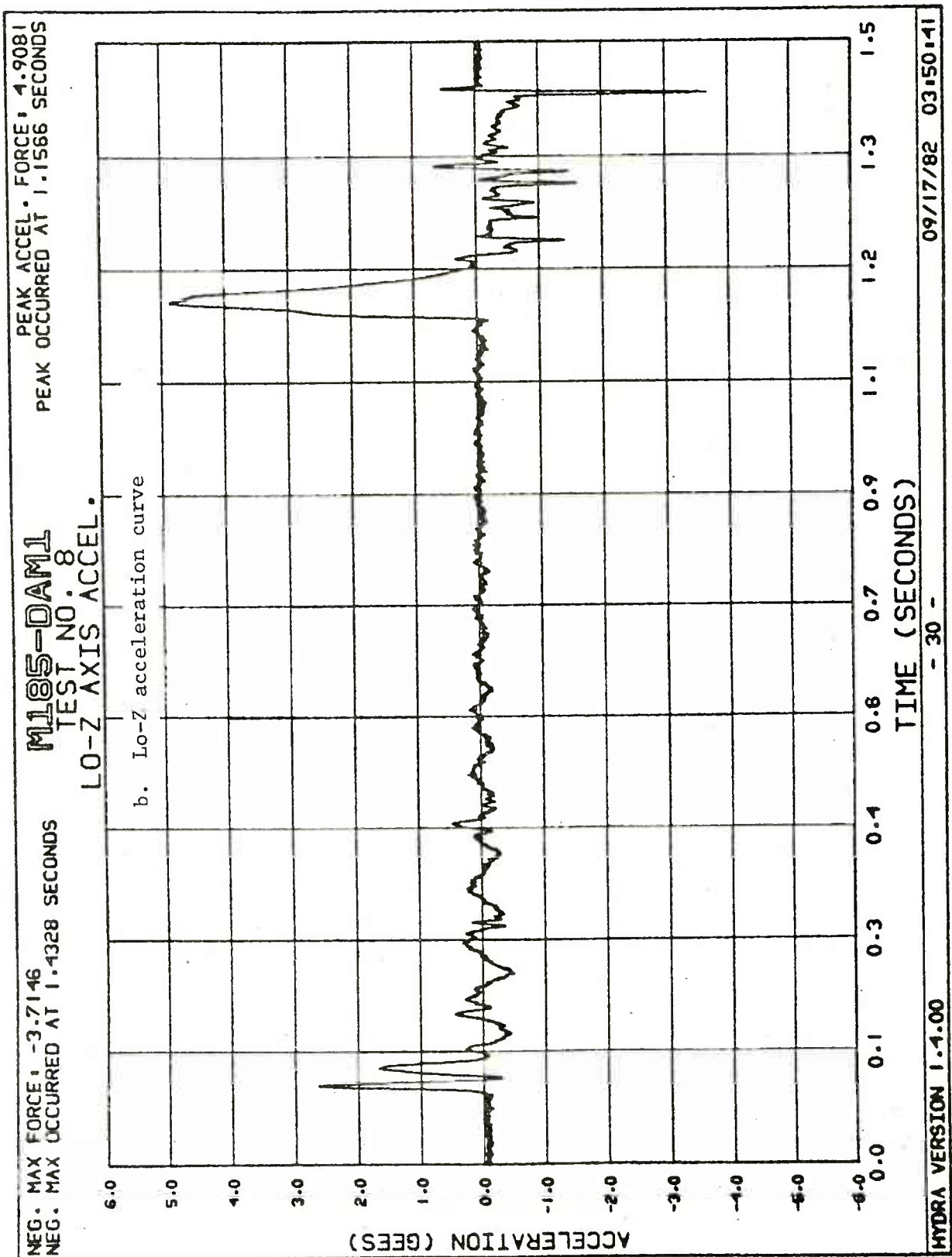


Figure 20. (cont)

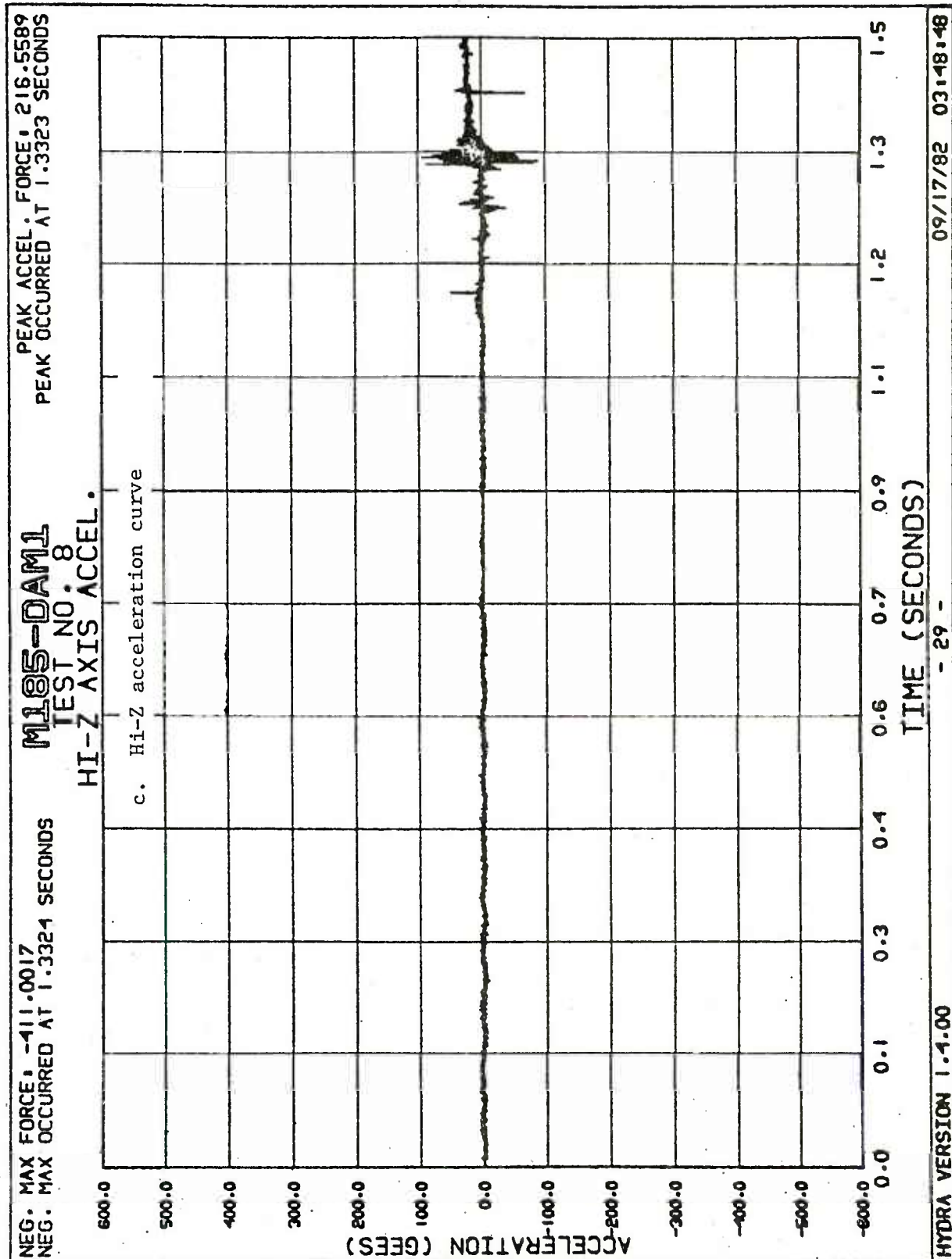


Figure 20. (cont)

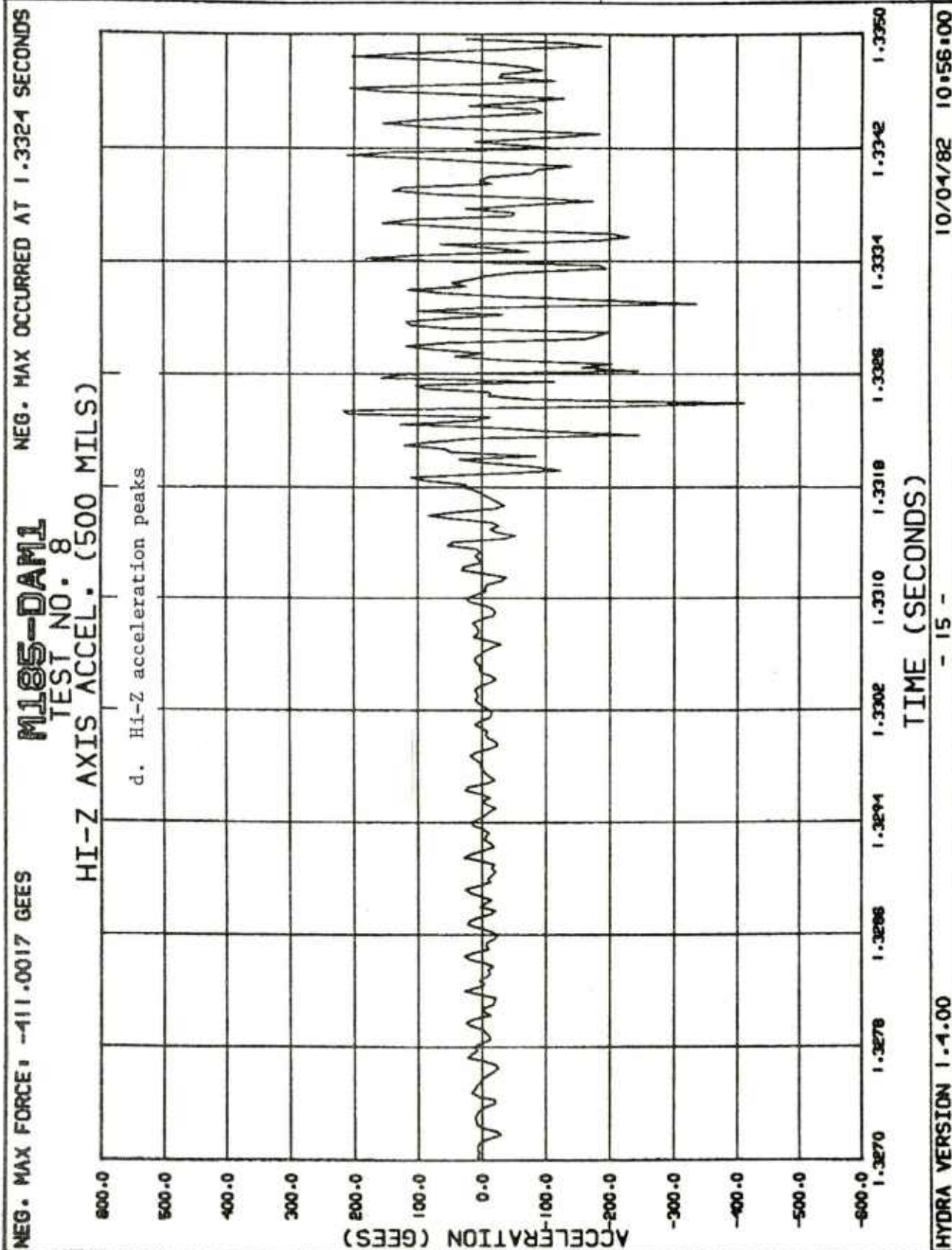
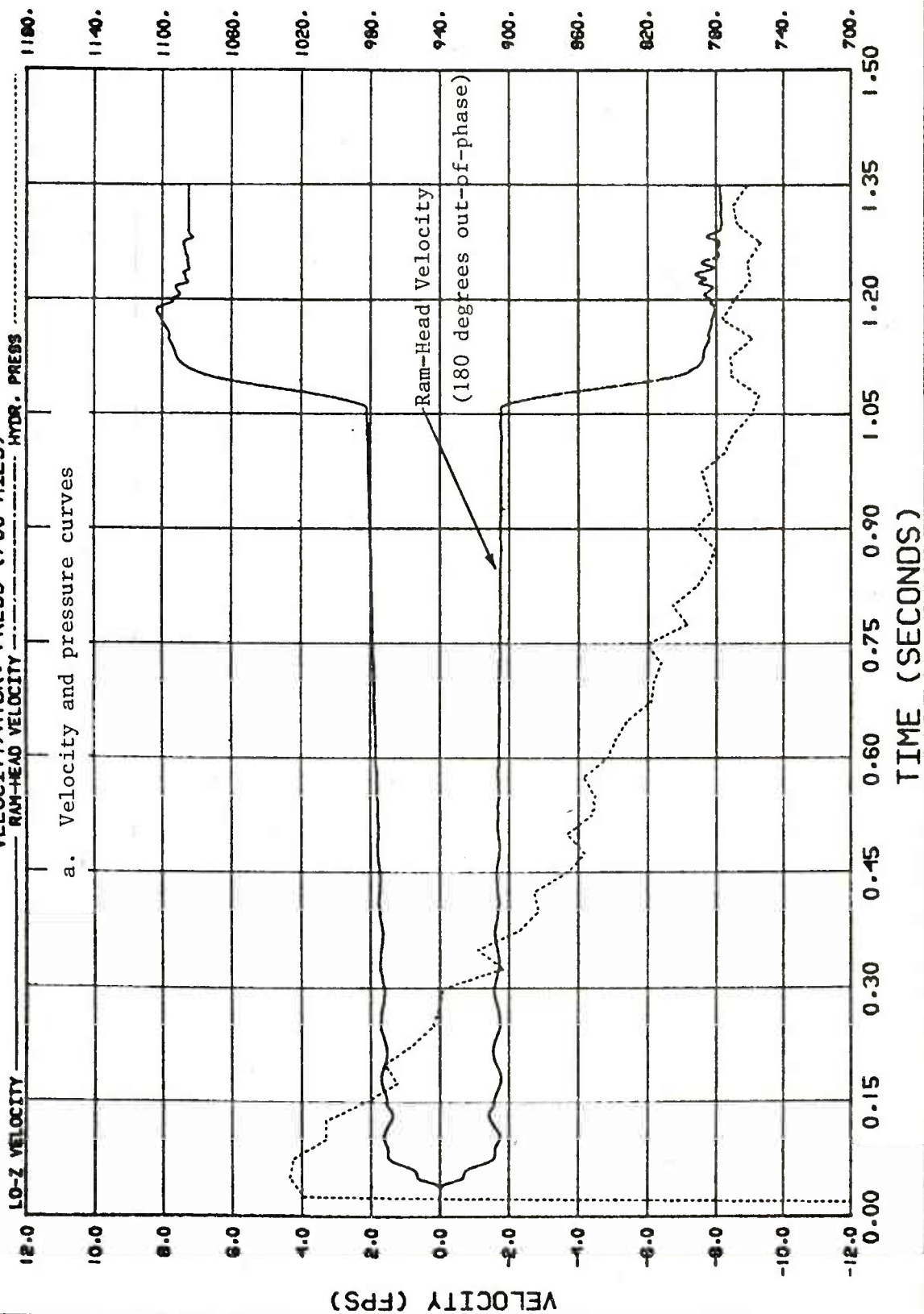


Figure 20. (cont)

M185-DAM1

TEST NO. 12
VELOCITY/HYDR. PRESS (700 MILS)



HYDRA VERSION 1.4.00

- 24 -

10/06/82 11:56:50

Figure 21. Ramming test 12

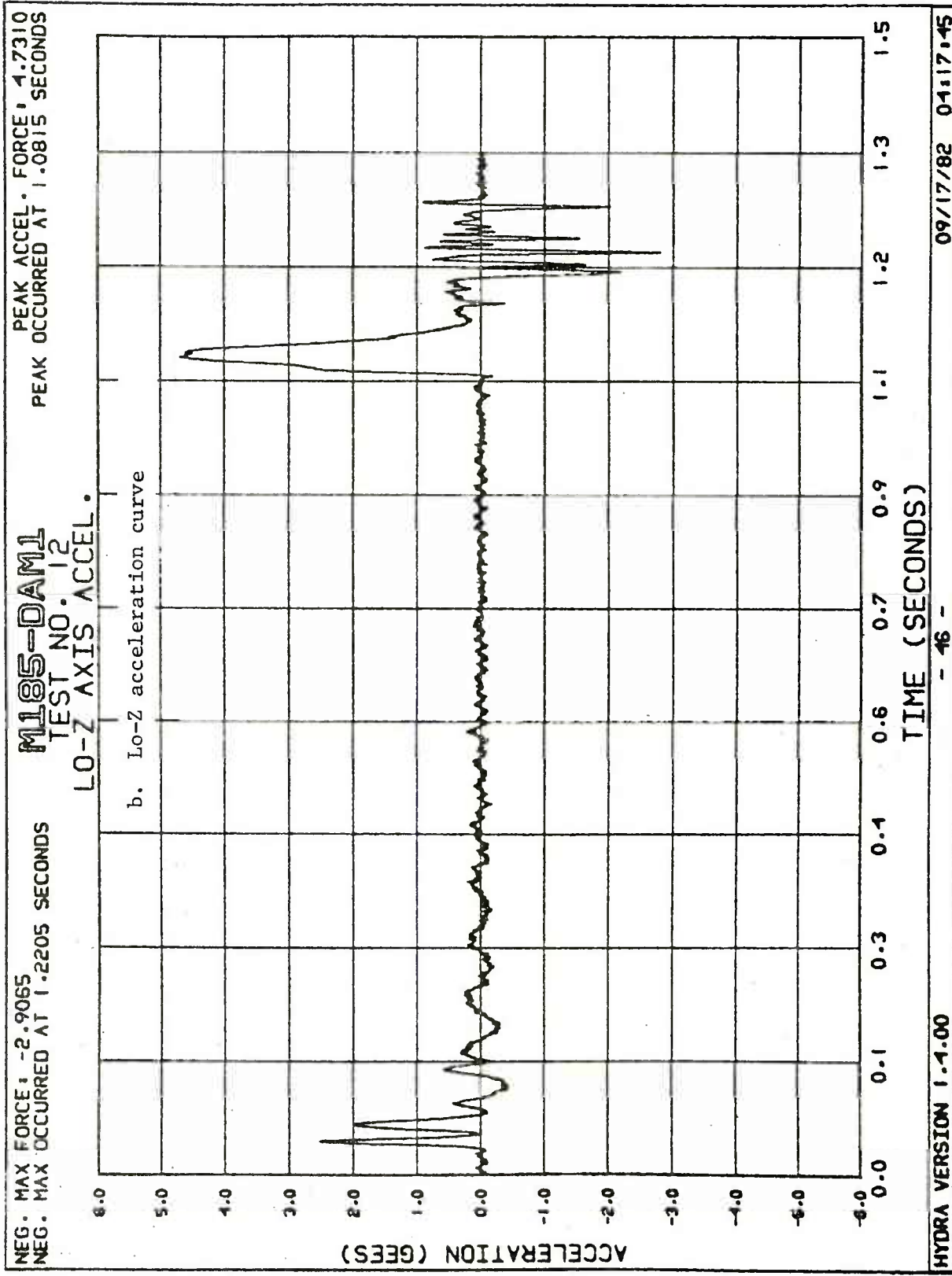


Figure 21. (cont)

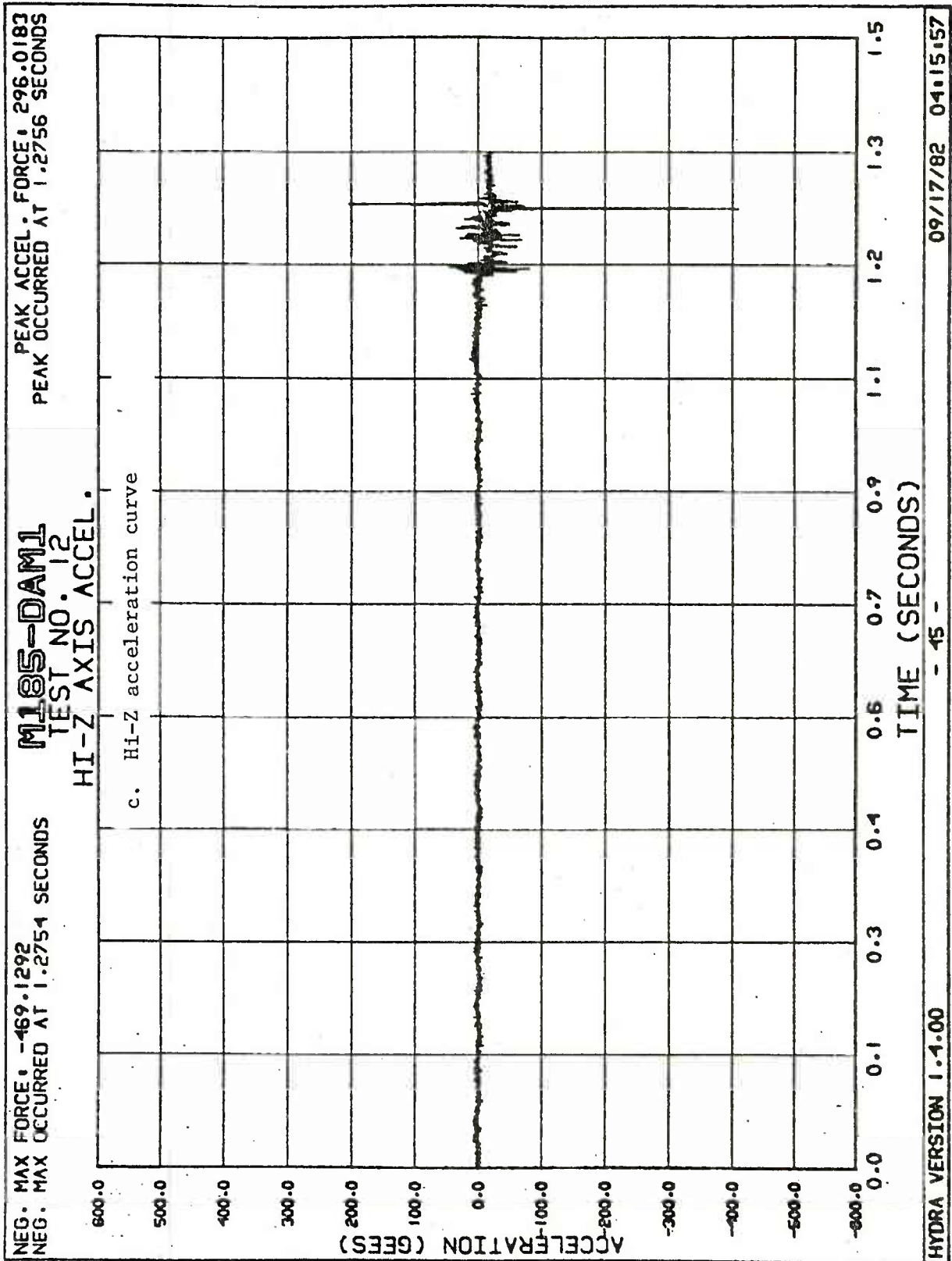


Figure 21. (cont)

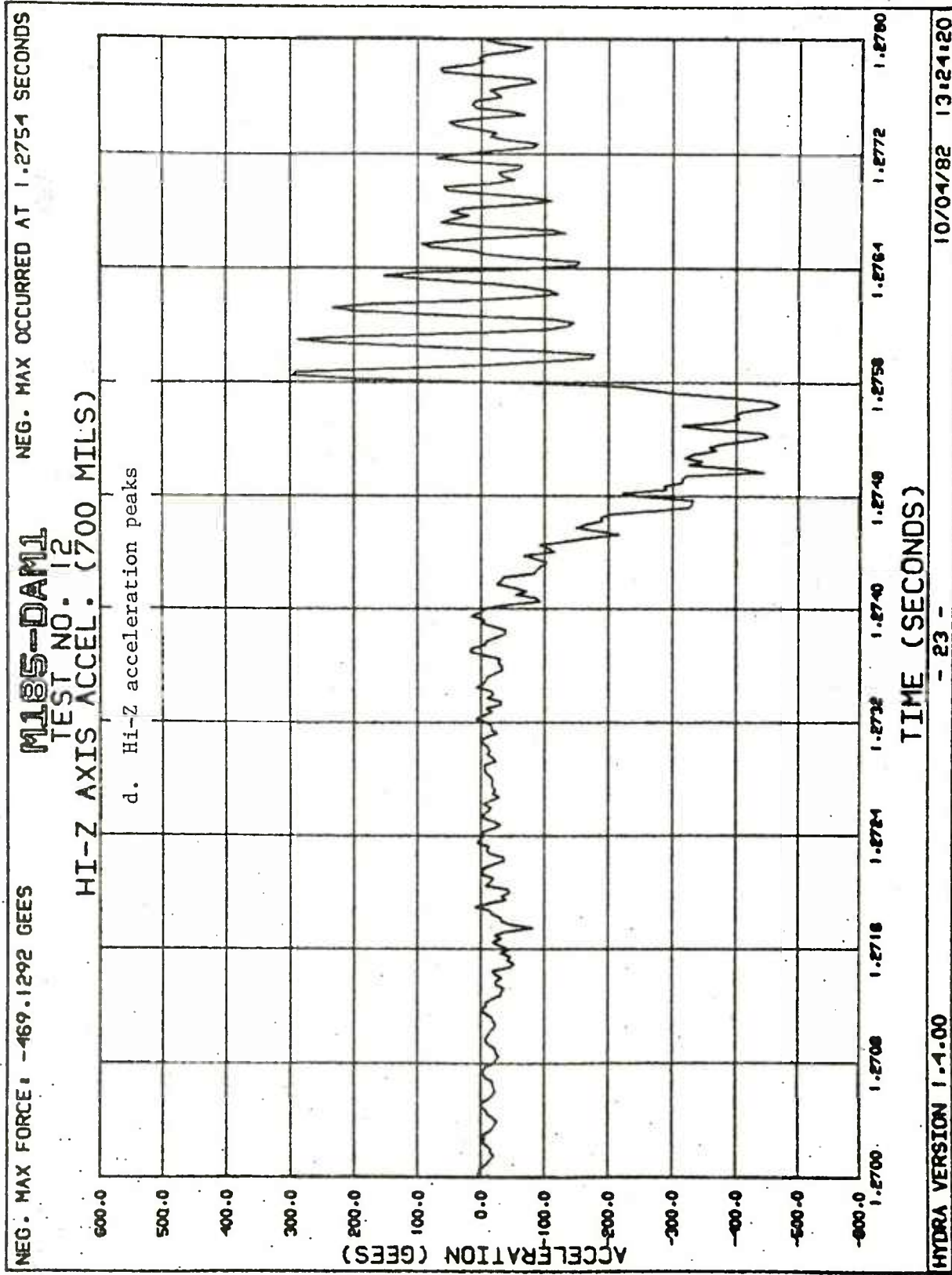


Figure 21. (cont)

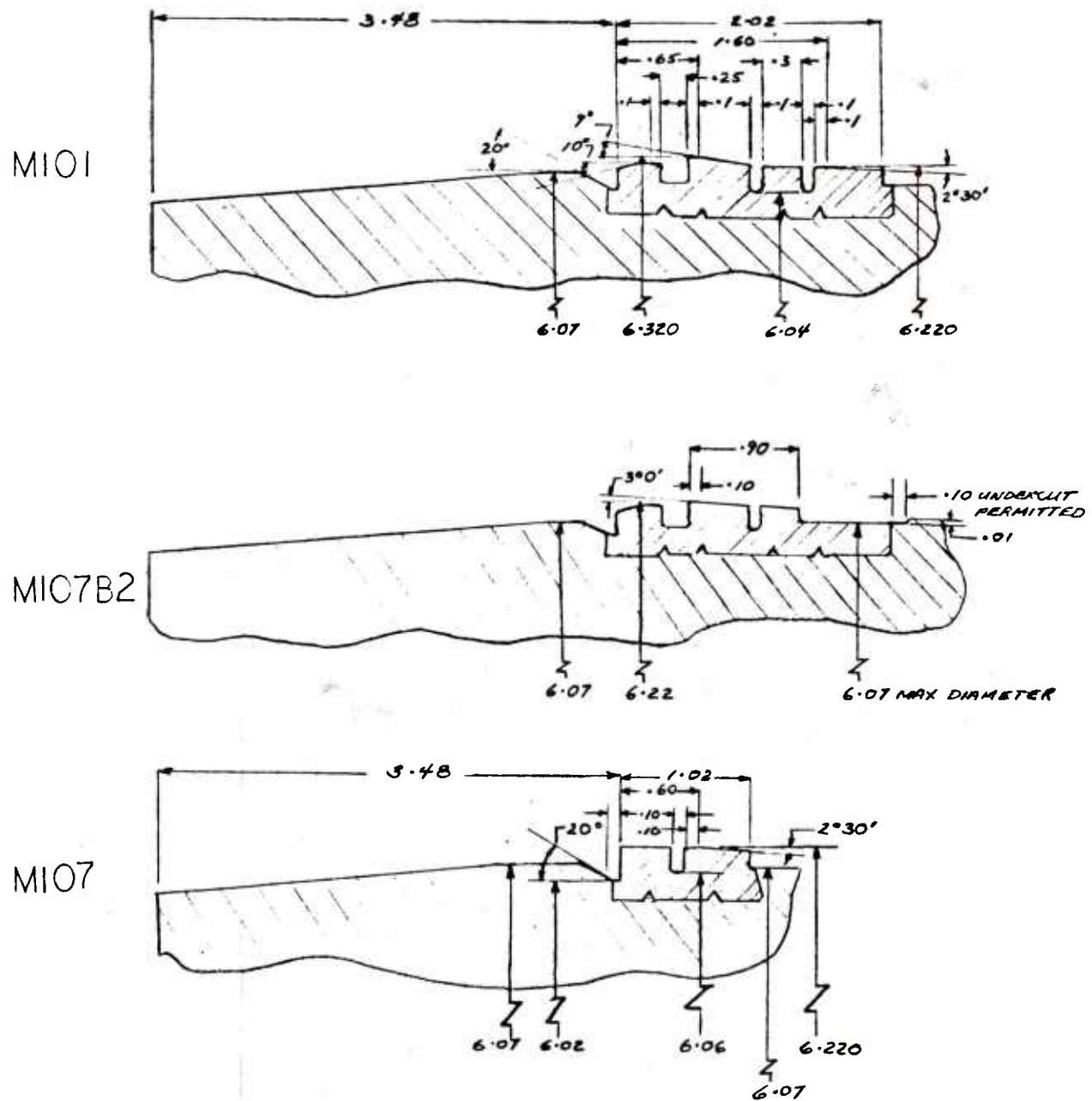
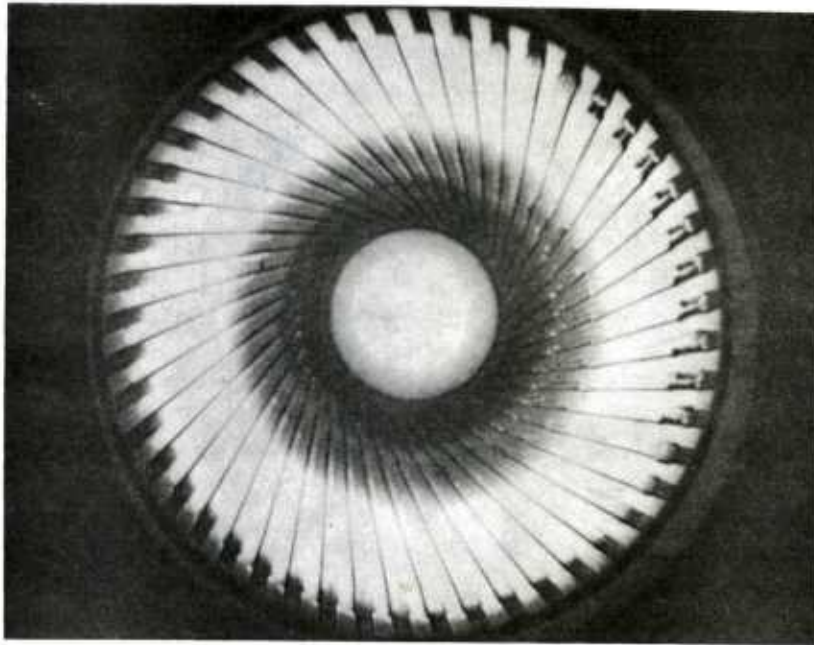
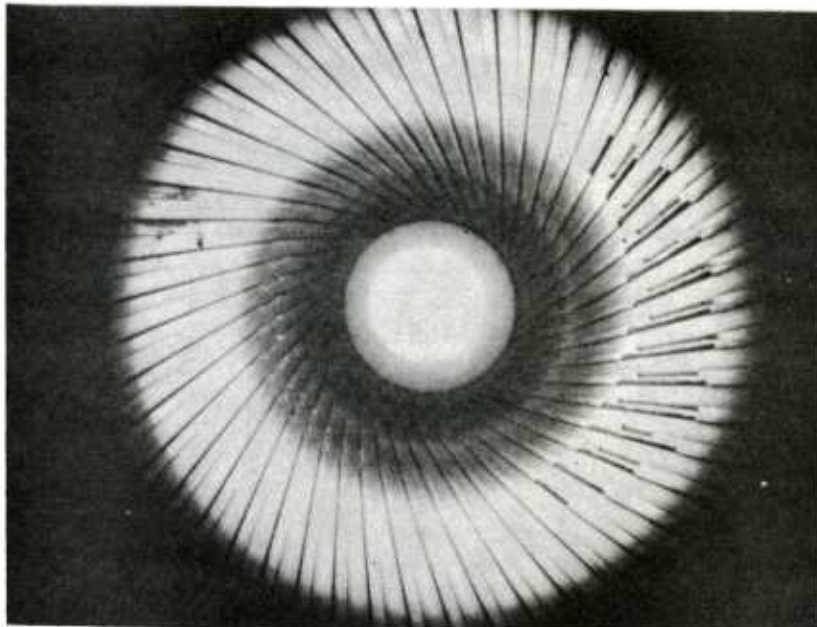


Figure 22. Rotating band configurations--all dimensions nominal

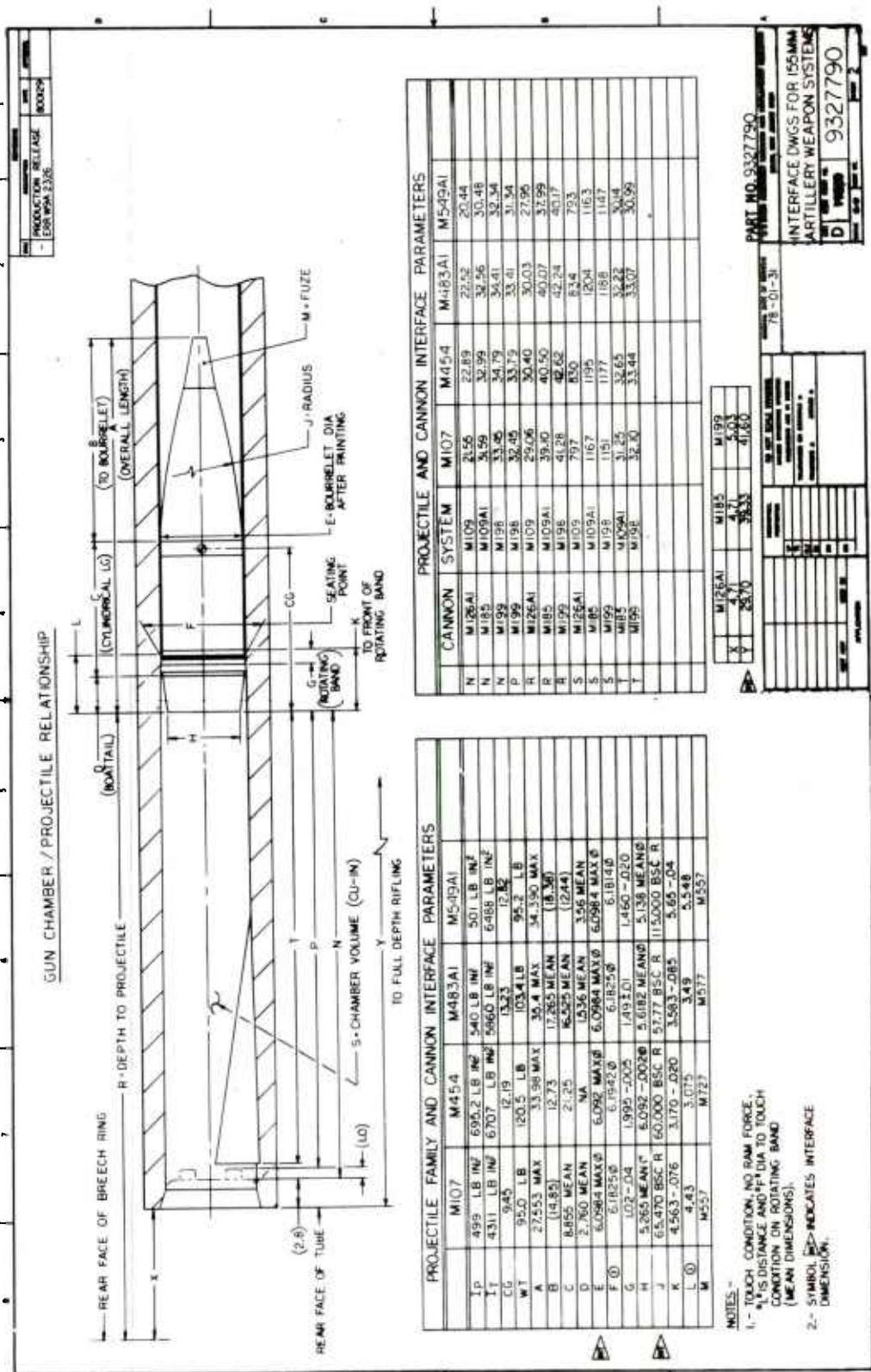


a. Origin of rifling general view after firing 458 rounds



b. Condition of rifling 42 to 48 inches general view after firing 458 rounds

Figure 23. M185 cannon tube S/N 25460 at start of degradation test



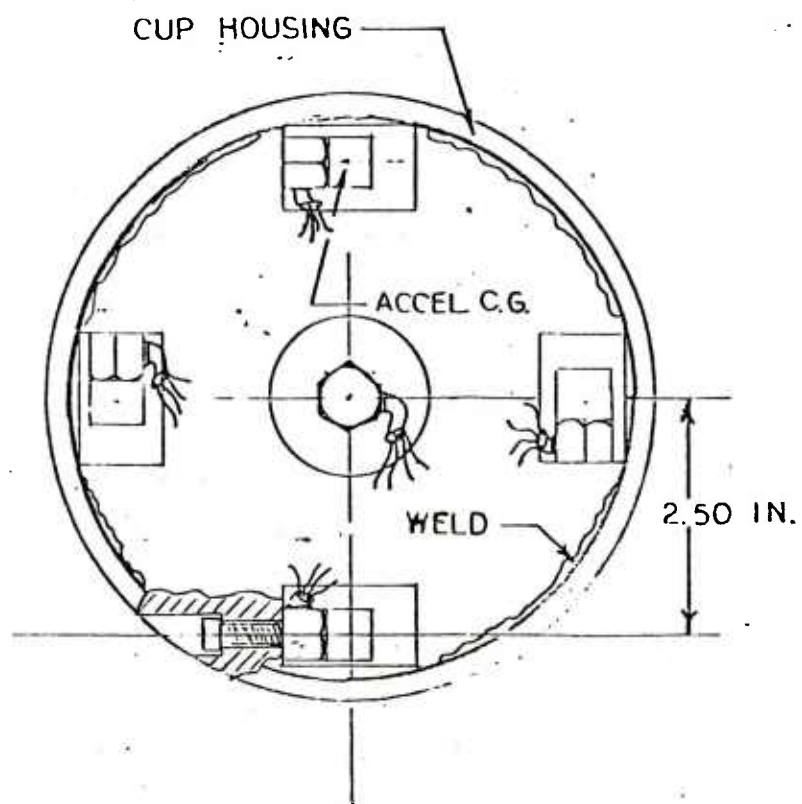


Figure 25. Collector cup with accelerometers---top view

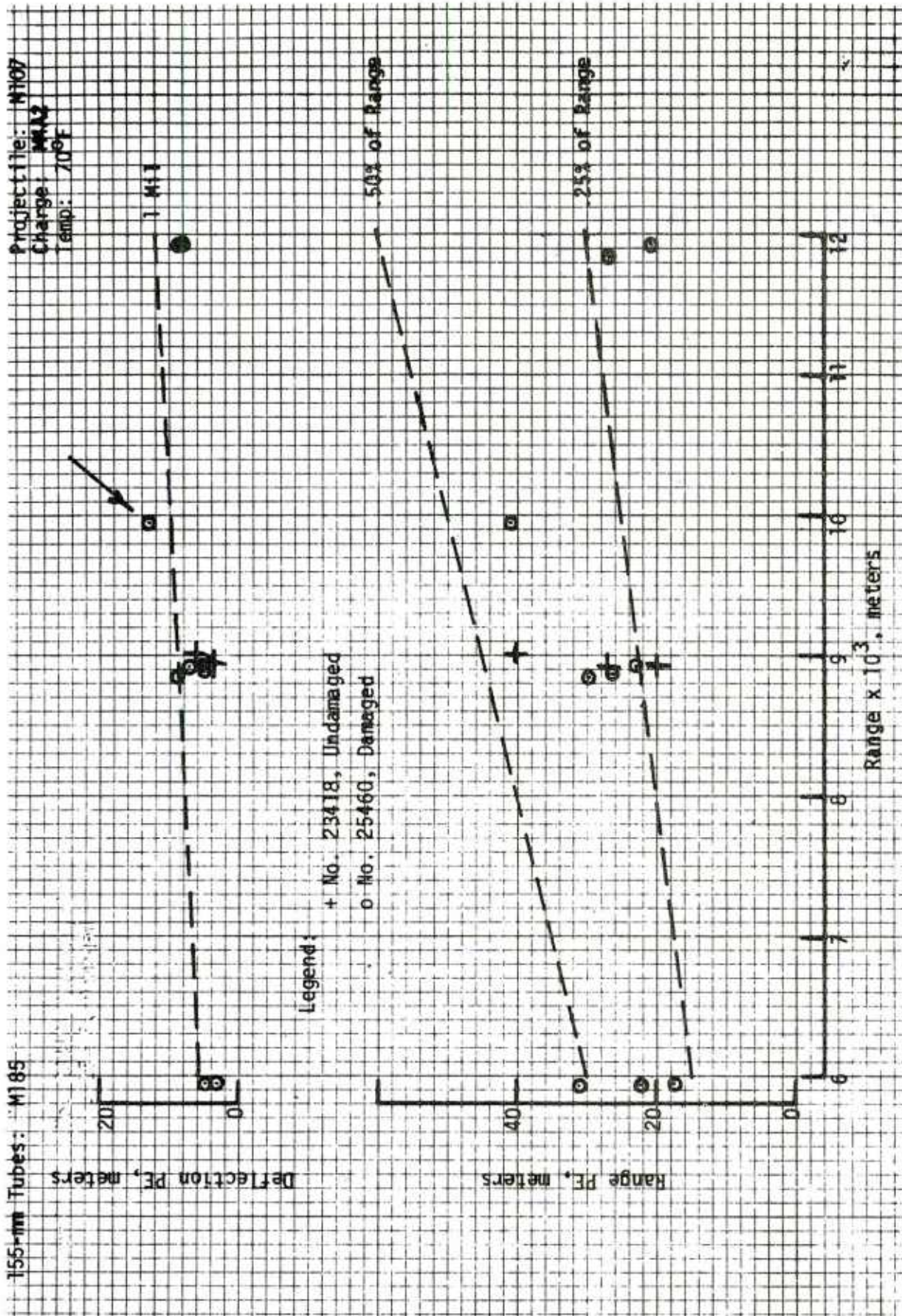
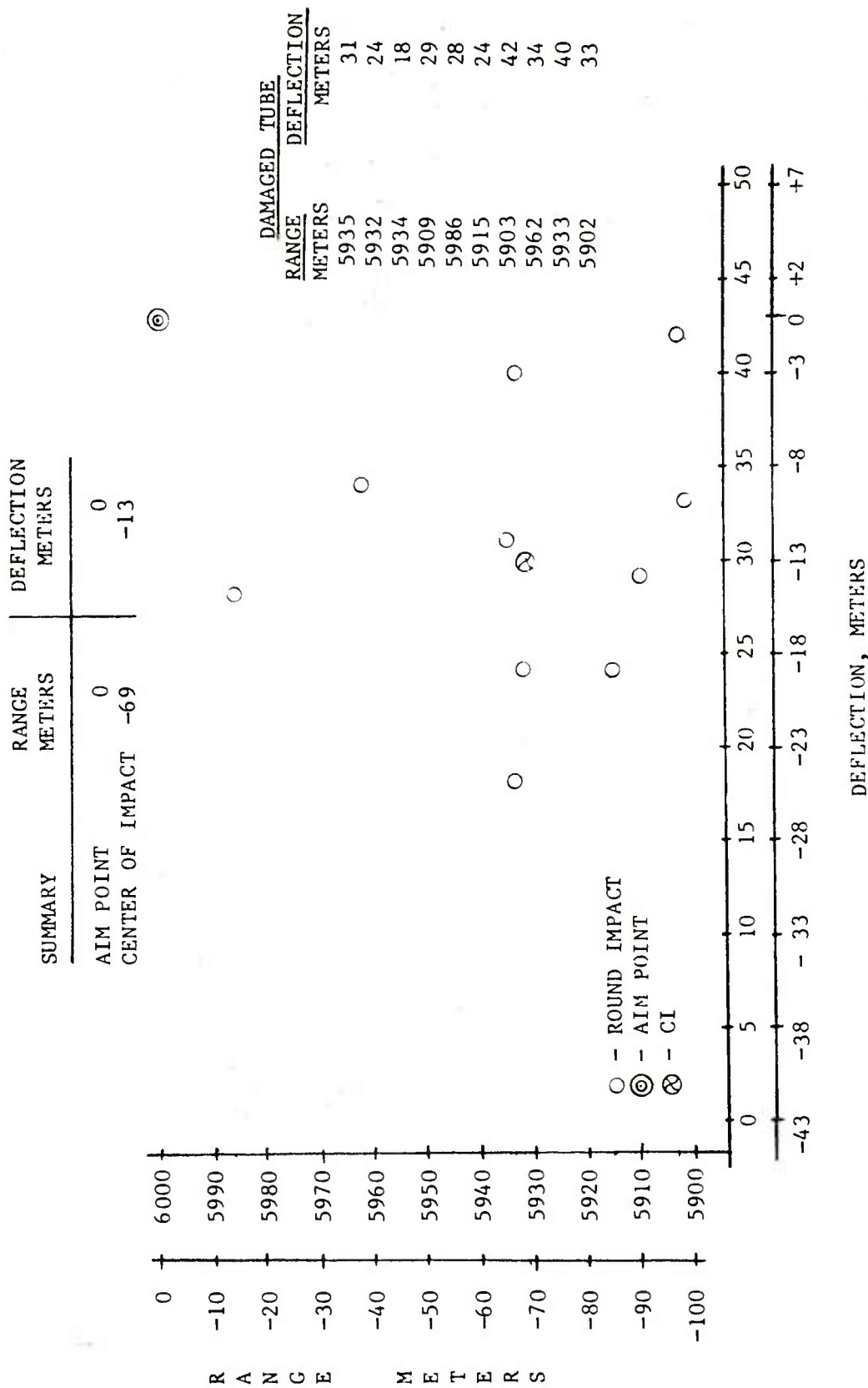


Figure 26. Range and deflection PE versus range

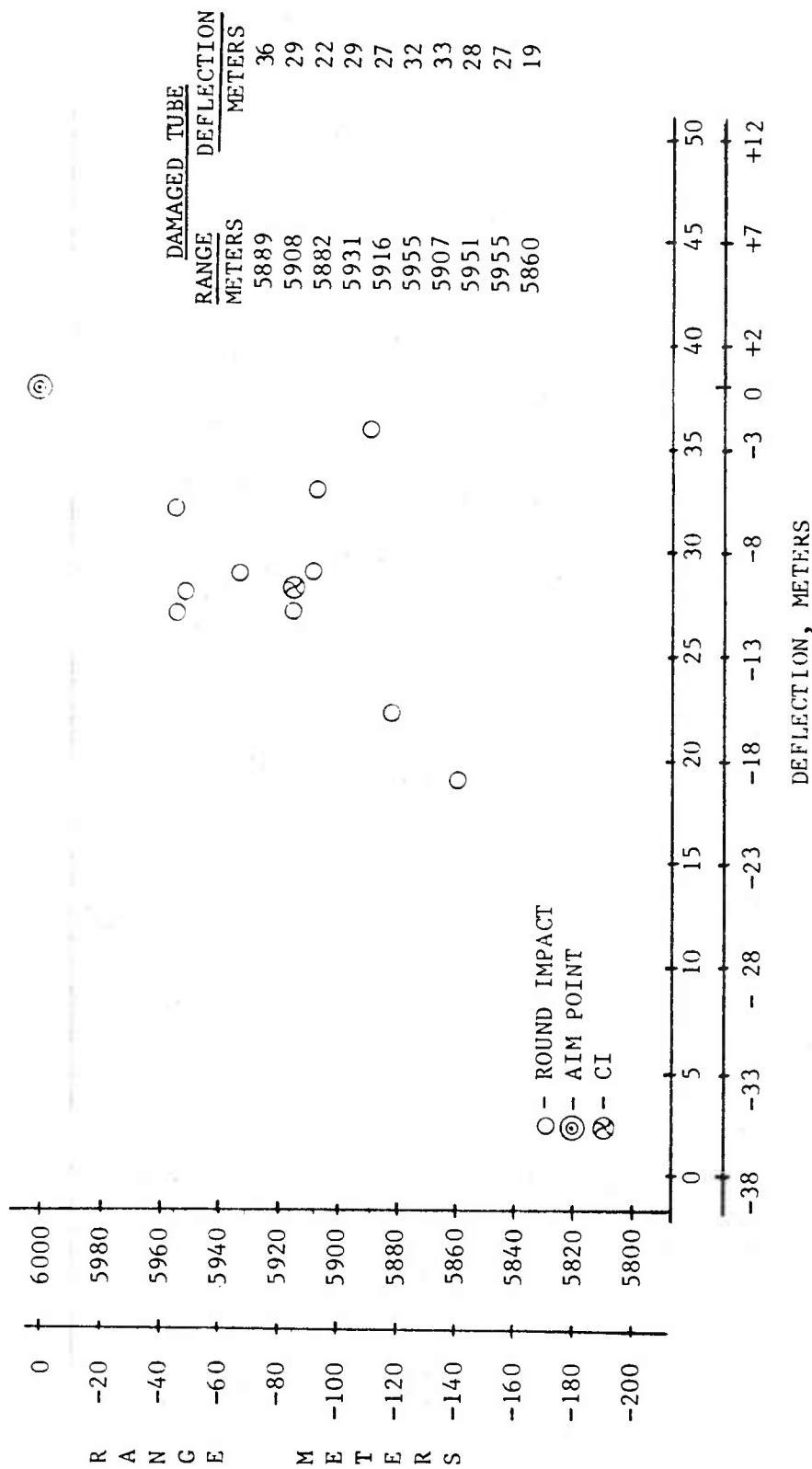


NOTES: 1. RANGES CORRECTED TO SERVICE VELOCITY, TO STANDARD ICAO METRO AND TO STANDARD PROJECTILE WEIGHT OF 95.00 POUNDS. DEFLECTIONS CORRECTED TO STANDARD ICAO METRO.

2. CENTER OF IMPACT IS A STATISTICAL DETERMINATION BASED ON INDIVIDUAL POUND COORDINATES.

Figure 27. Range firings with damaged tube S/N 25460--6000 meters

SUMMARY	RANGE METERS	DEFLECTION METERS
AIM POINT	0	0
CENTER OF IMPACT	-85	-10

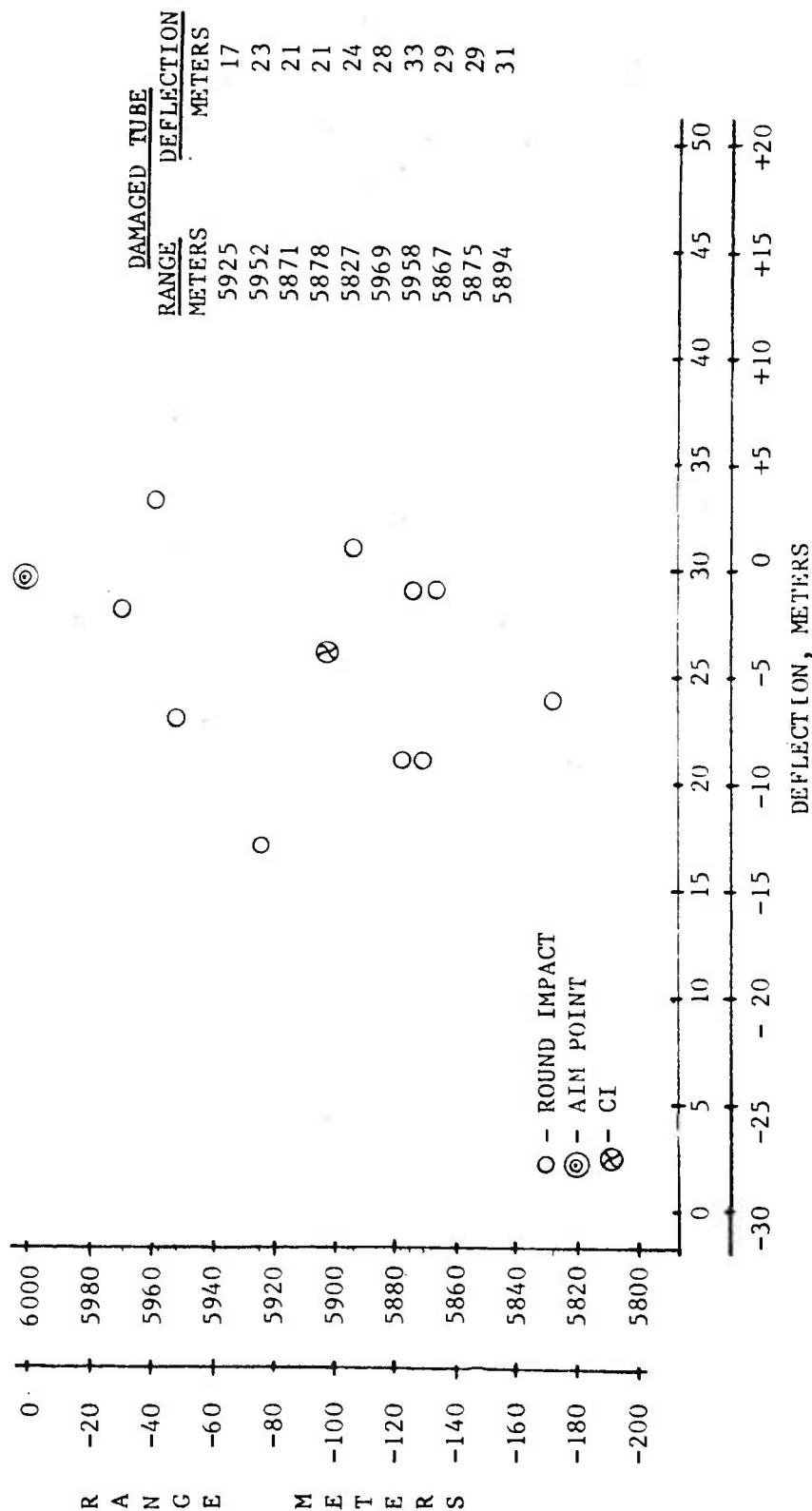


- NOTES:
1. RANGES CORRECTED TO SERVICE VELOCITY, TO STANDARD ICAO METRO AND TO STANDARD PROJECTILE WEIGHT OF 95.00 POUNDS. DEFLECTIONS CORRECTED TO STANDARD ICAO METRO.
 2. CENTER OF IMPACT IS A STATISTICAL DETERMINATION BASED ON INDIVIDUAL ROUND COORDINATES.

b. Zone 6--QE 205.4 mils

Figure 27. (cont)

SUMMARY	RANGE METERS	DEFLECTION METERS
AIM POINT	0	0
CENTER OF IMPACT	-98	-4



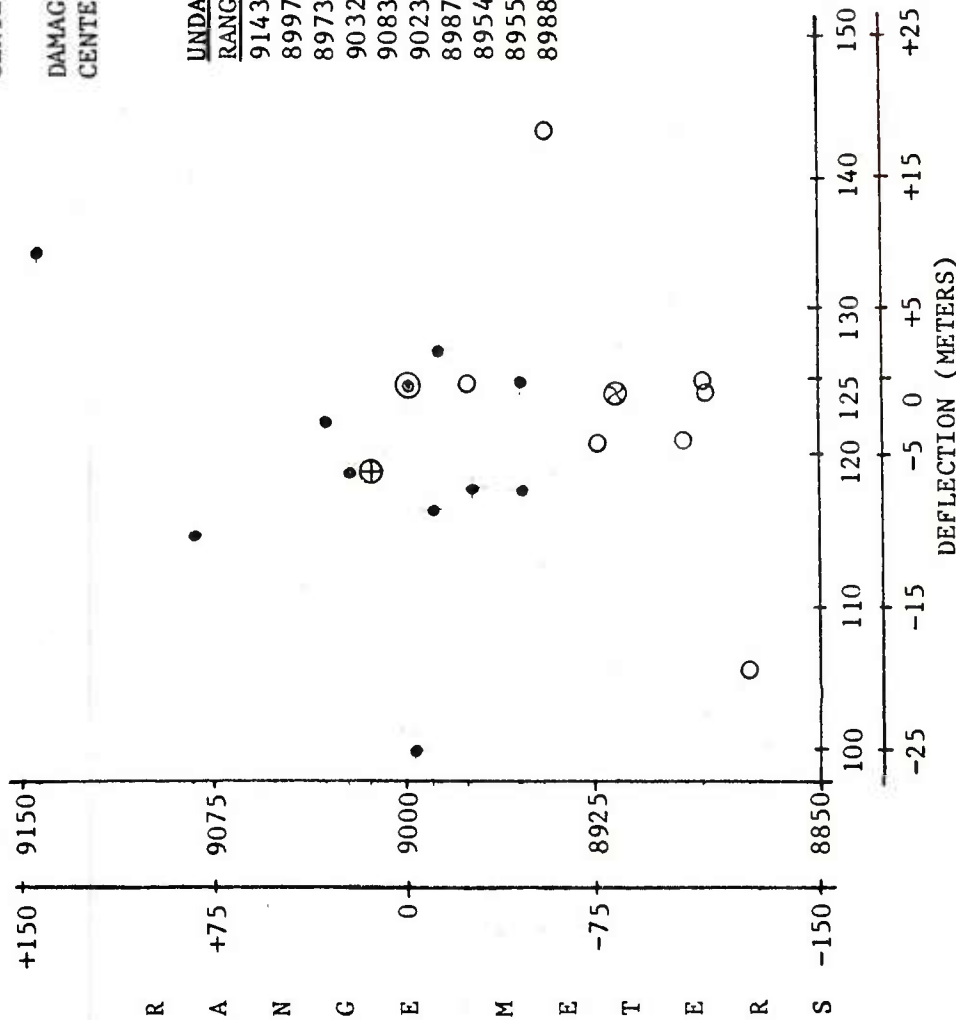
- NOTES: 1. RANGES CORRECTED TO SERVICE VELOCITY, TO STANDARD ICAO METRO AND TO STANDARD PROJECTILE WEIGHT OF 95.00 POUNDS. DEFLECTIONS CORRECTED TO STANDARD ICAO METRO.
2. CENTER OF IMPACT IS A STATISTICAL DETERMINATION BASED ON INDIVIDUAL ROUND COORDINATES.

c. Zone 7--QE 141.0 mils

Figure 27. (cont)

LEGEND

- ROUND IMPACT (UNDAMAGED)
- ⊕ CENTER OF IMPACT (UNDAMAGED)
- ⊙ AIM POINT (COMMON)
- ROUND IMPACT (DAMAGED)
- ⊗ CENTER OF IMPACT (DAMAGED)



NOTES:

1. RANGES CORRECTED TO SERVICE VELOCITY, TO STANDARD ICAO METRO AND TO STANDARD PROJECTILE WEIGHT OF 95.00 POUNDS. DEFLECTIONS CORRECTED TO STANDARD ICAO METRO.
2. CENTER OF IMPACT IS A STATISTICAL DETERMINATION BASED ON INDIVIDUAL ROUND COORDINATES.

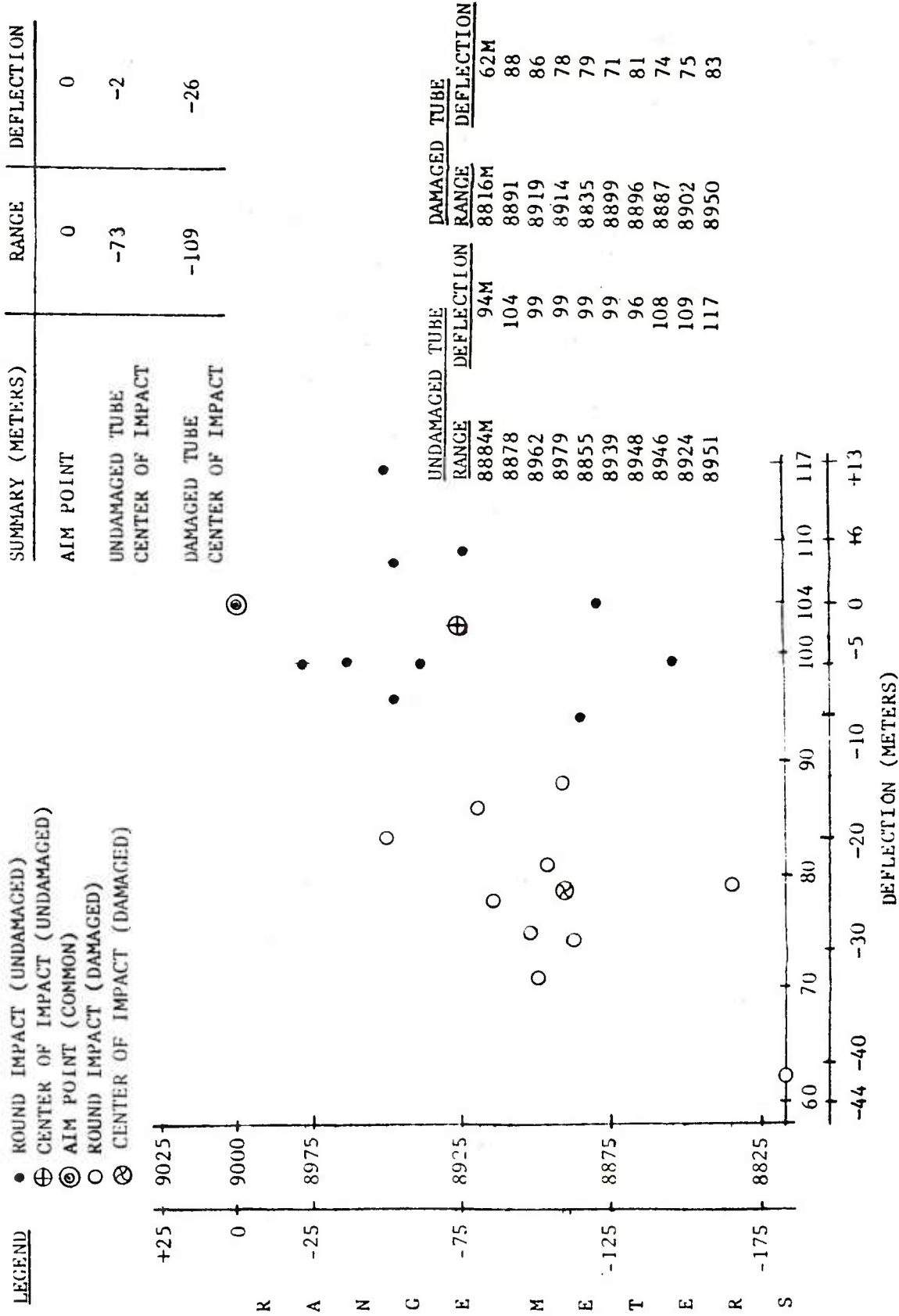
a. Zone 5--QE 513 mils

Figure 28. Comparison of range firings--undamaged tube S/N 25460 versus damaged tube S/N 25460--9000 meters

SUMMARY (METERS)	RANGE	DEFLECTION
AIM POINT	0	0
UNDAMAGED TUBE CENTER OF IMPACT	+14	-6
DAMAGED TUBE CENTER OF IMPACT	-83	-1

UNDAMAGED TUBE		DAMAGED TUBE	
RANGE	DEFLECTION	RANGE	DEFLECTION
9143M	134M	* 8939M	-68M
8997	100	* 8977	100
8973	118	* 8895	109
9032	122	8975	125
9083	114	8945	143
9023	119	8896	125
8987	127	8894	124
8954	118	8924	121
8955	125	8879	106
8988	117	8903	121

* APG DID NOT CONSIDER
THESE STATISTICALLY
VALID UNIFORMITY GROUPS

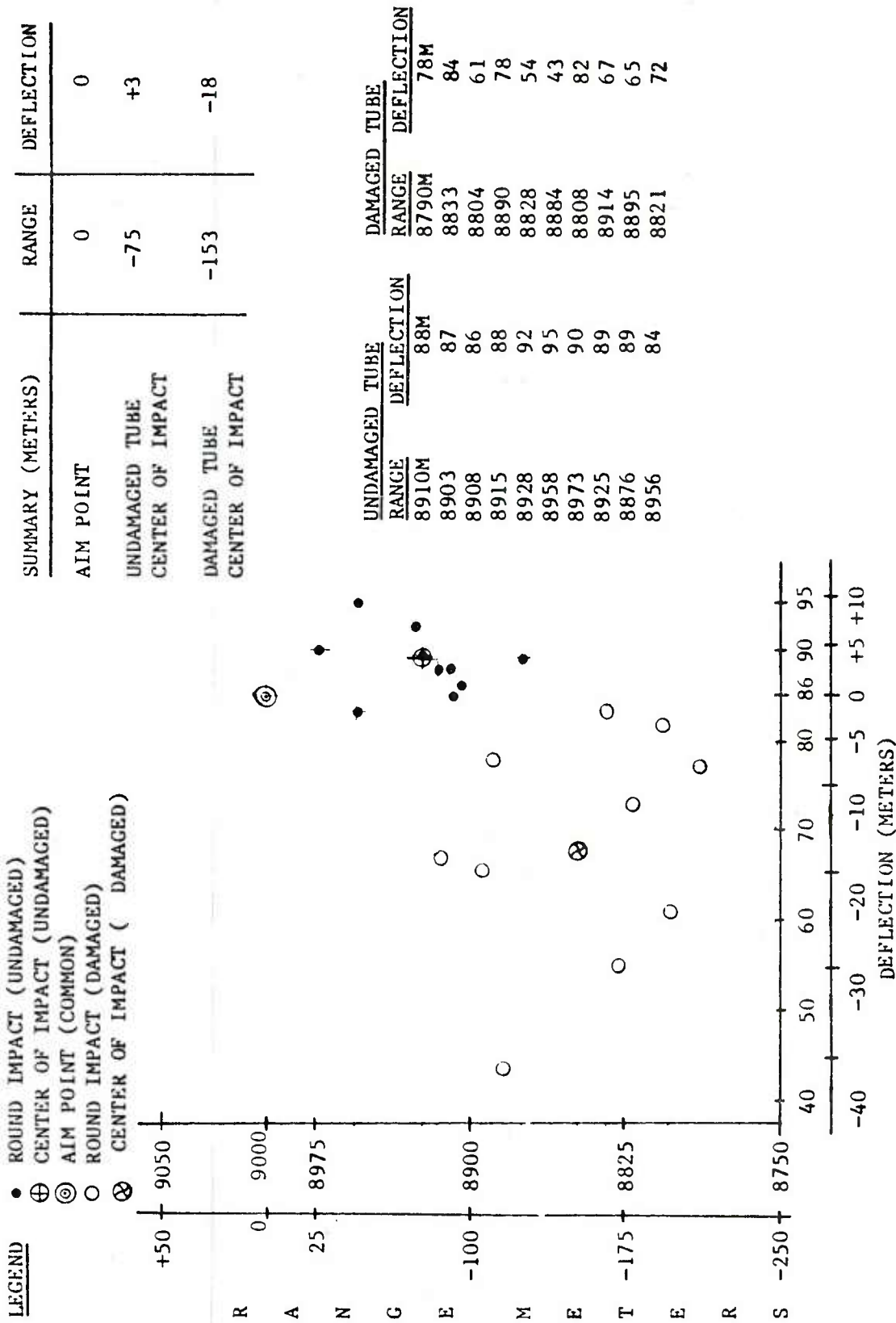


NOTES:

1. RANGES CORRECTED TO SERVICE VELOCITY, TO STANDARD ICAO METRO AND TO STANDARD PROJECTILE WEIGHT OF 95.00 POUNDS. DEFLECTIONS CORRECTED TO STANDARD ICAO METRO.
2. CENTER OF IMPACT IS A STATISTICAL DETERMINATION BASED ON INDIVIDUAL ROUND COORDINATES.

b. Zone 6--QE 372 mils

Figure 28. (cont)

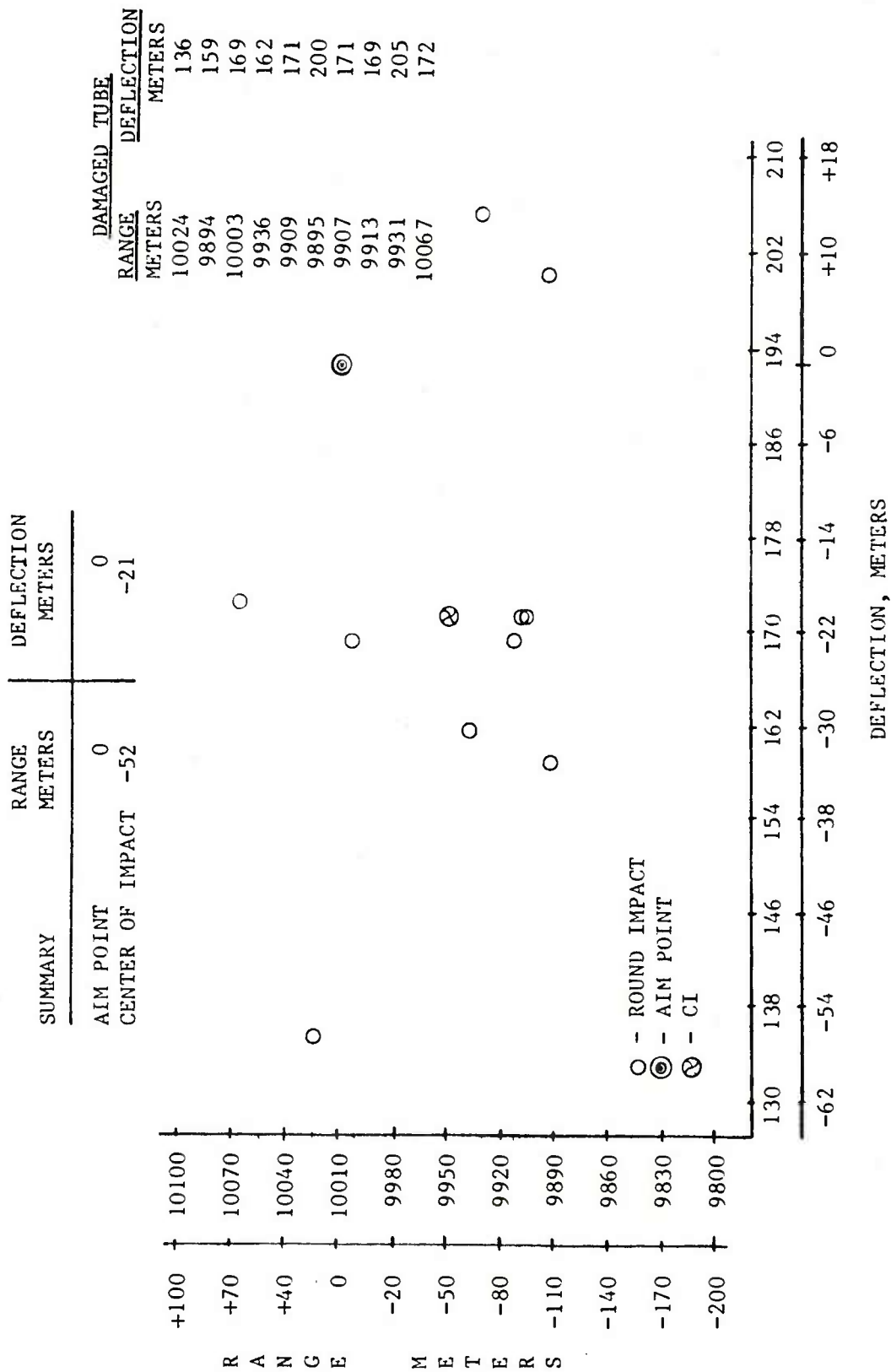


NOTES:

1. RANGES CORRECTED TO SERVICE VELOCITY, TO STANDARD ICAO METRO AND TO STANDARD PROJECTILE WEIGHT OF 95.00 POUNDS. DEFLECTIONS CORRECTED TO STANDARD ICAO METRO.
2. CENTER OF IMPACT IS A STATISTICAL DETERMINATION BASED ON INDIVIDUAL ROUND COORDINATES.

c. Zone 7--QE 267 mils

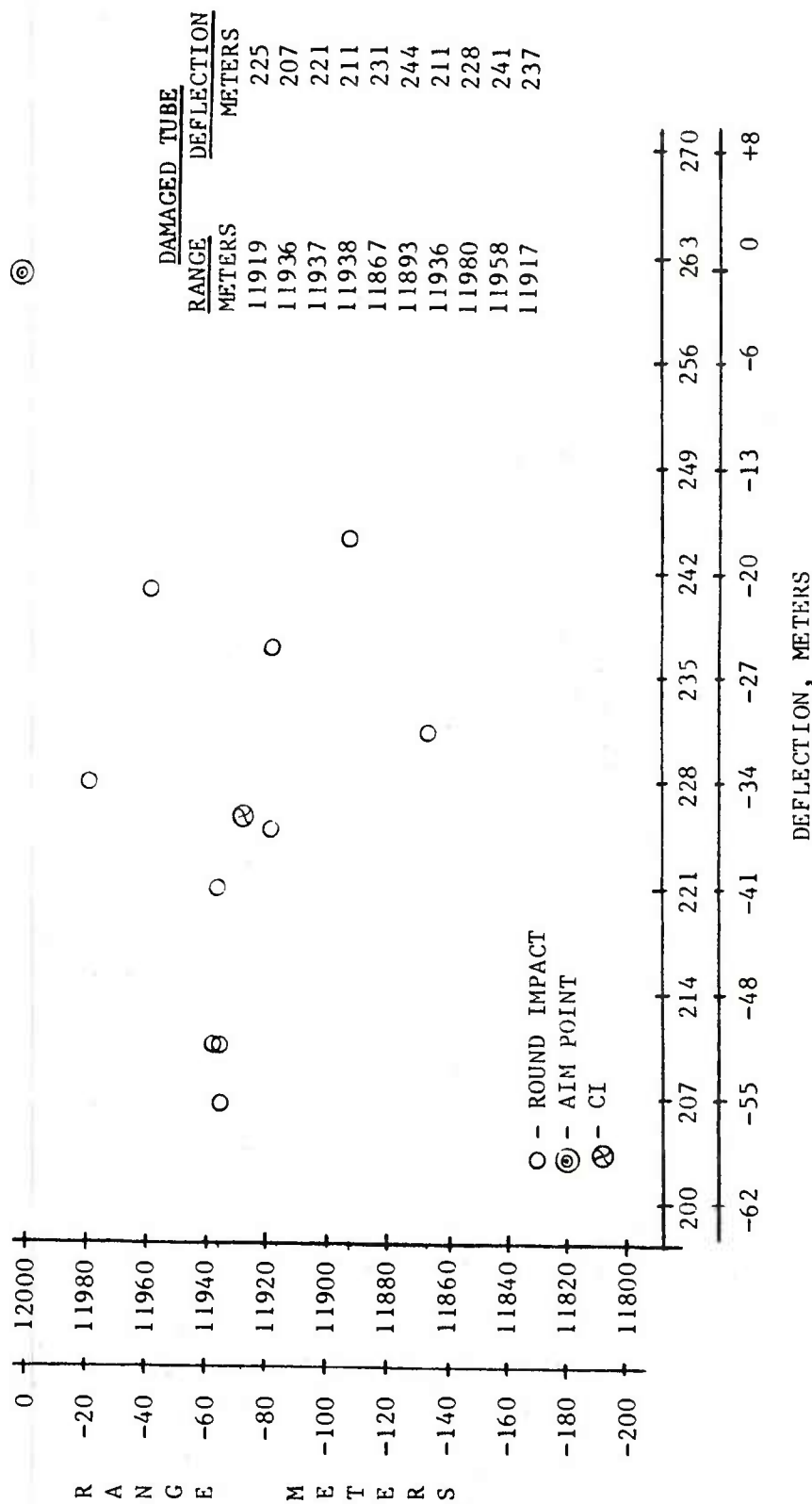
Figure 28. (cont)



- NOTES:
1. RANGES CORRECTED TO SERVICE VELOCITY, TO STANDARD ICAO METRO AND TO STANDARD PROJECTILE WEIGHT OF 95.00 POUNDS. DEFLECTIONS CORRECTED TO STANDARD ICAO METRO.
 2. CENTER OF IMPACT IS A STATISTICAL DETERMINATION BASED ON INDIVIDUAL ROUND COORDINATES.

Figure 29. Range firings with damaged tube S/N 25460--10,000 meters

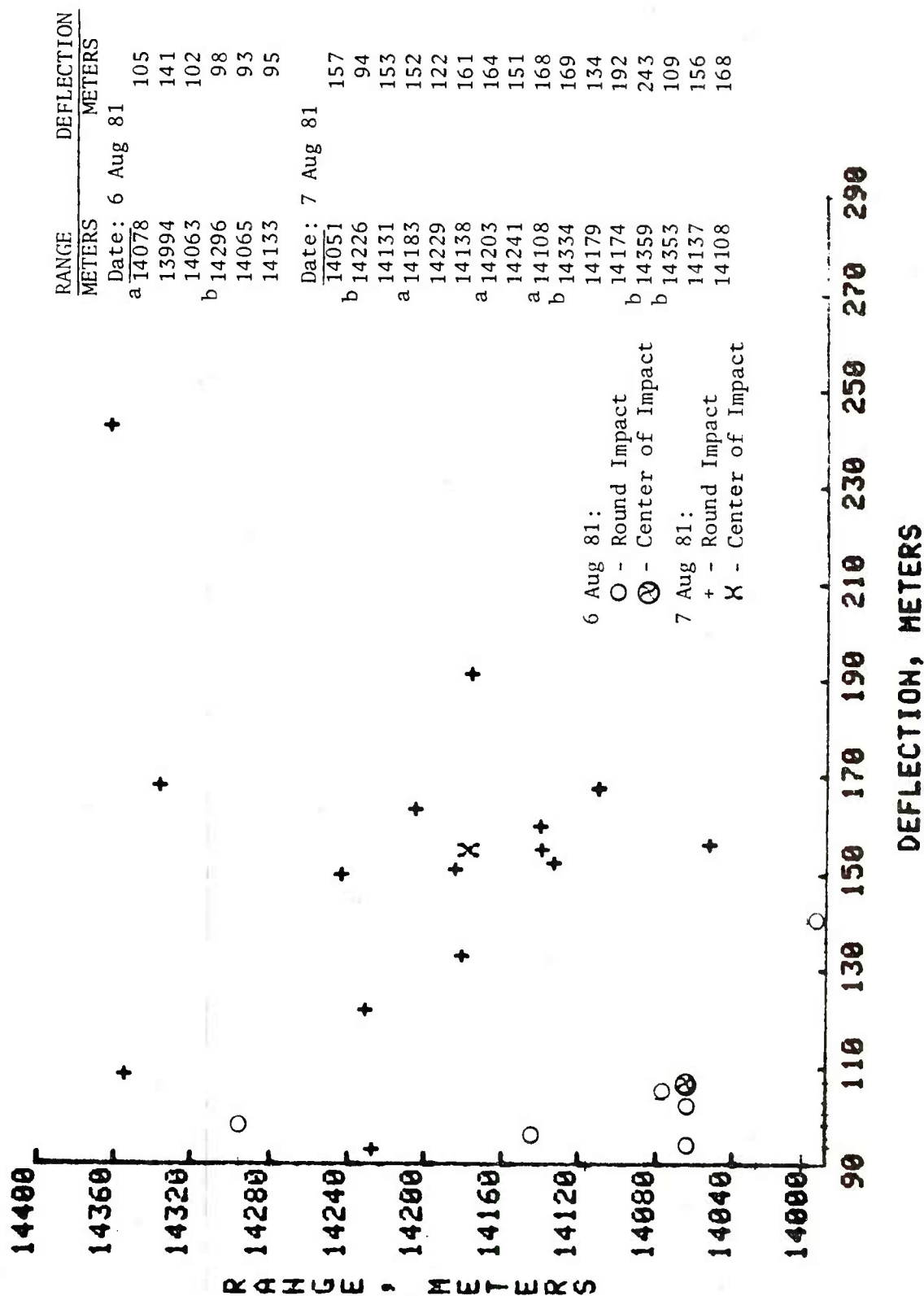
SUMMARY	RANGE METERS	DEFLECTION METERS
AIM POINT	0	0
CENTER OF IMPACT	-72	-36



- NOTES:
1. RANGES CORRECTED TO SERVICE VELOCITY, TO STANDARD ICAO METRO AND TO STANDARD PROJECTILE WEIGHT OF 95.00 POUNDS. DEFLECTIONS CORRECTED TO STANDARD ICAO METRO.
 2. CENTER OF IMPACT IS A STATISTICAL DETERMINATION BASED ON INDIVIDUAL ROUND COORDINATES.

a. Zone 6--QE 650 mils

Figure 30. Range firings with damaged tube S/N 25460--12,000 meters



a. IR times lost
 b. Round malfunctioned - no air burst

Figure 31. Range firings with damaged tube S/N 25460--M577 fuze and M483A1 projectile

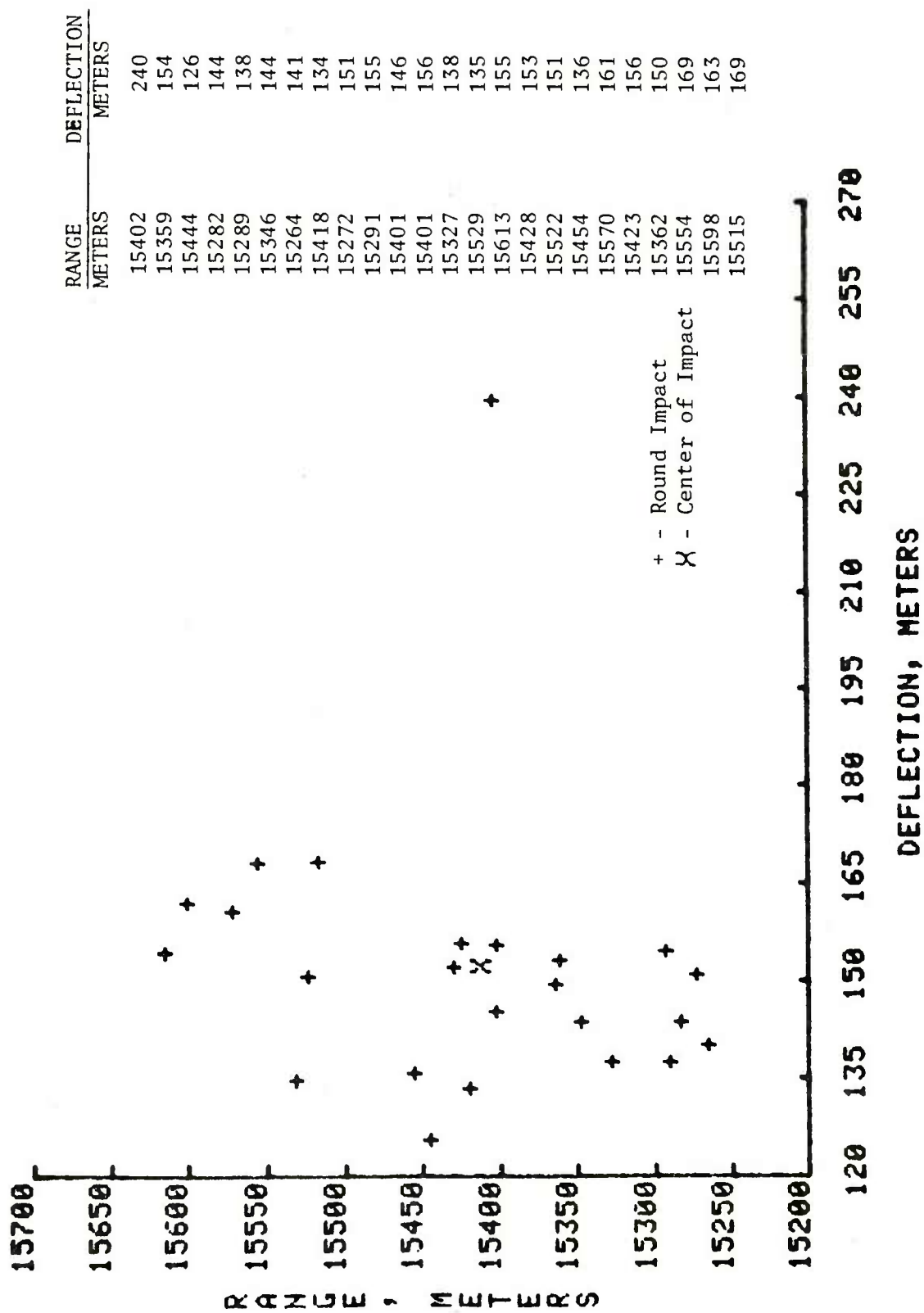
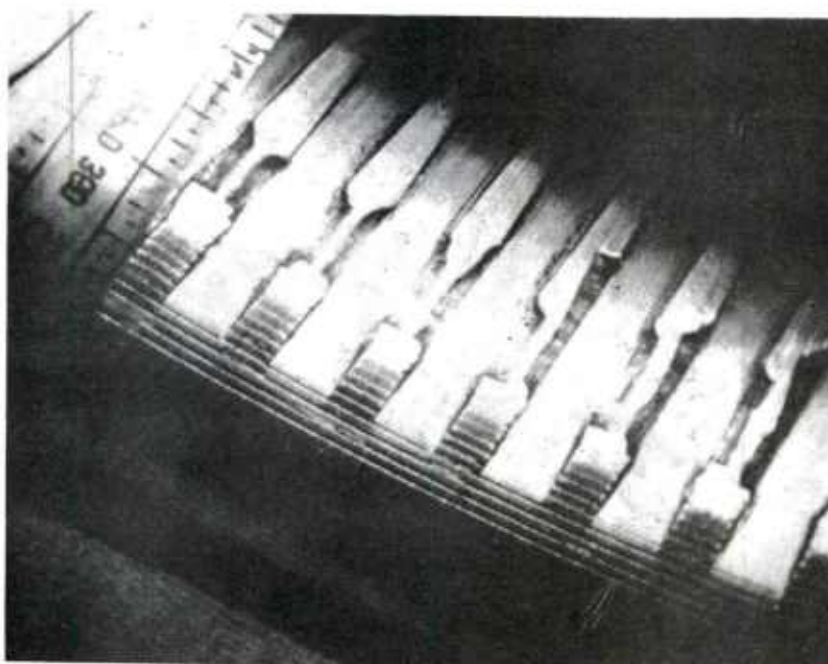
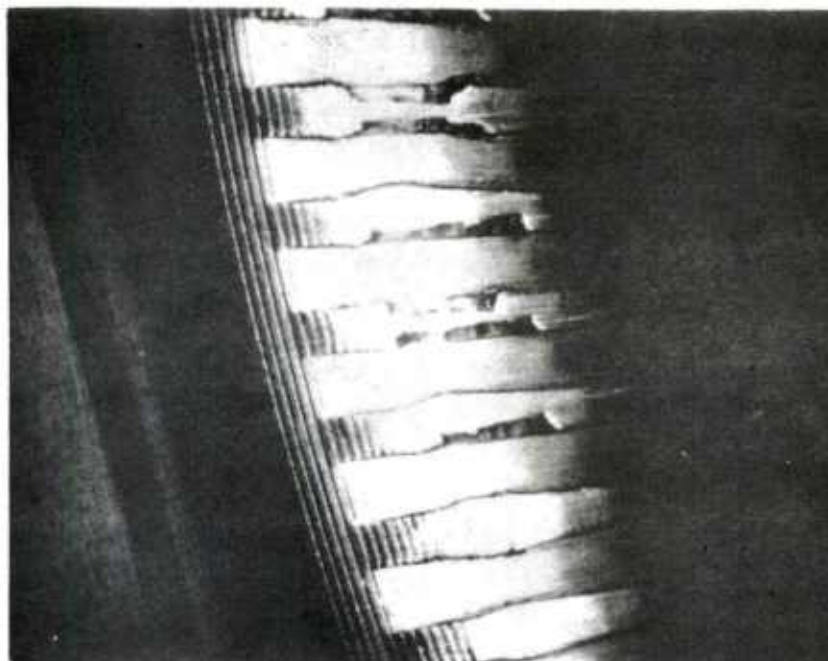
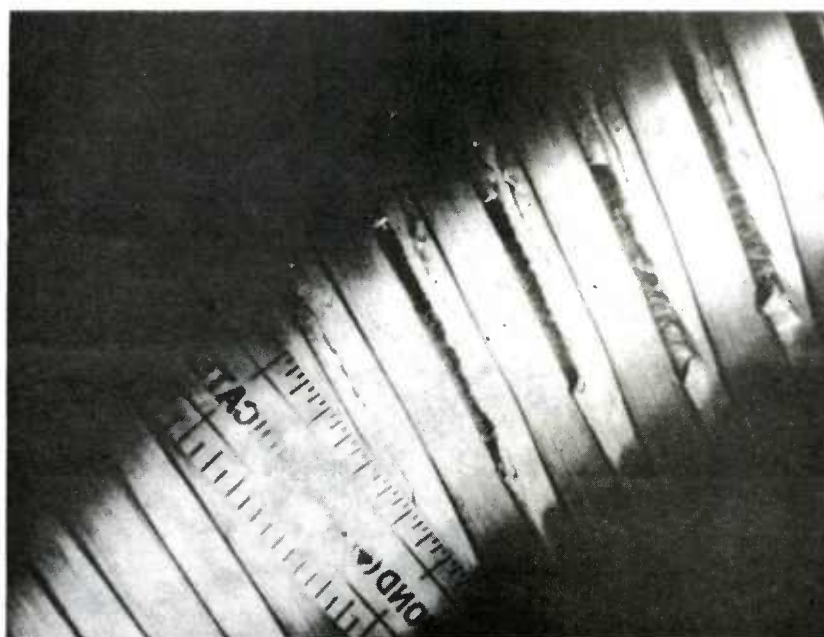
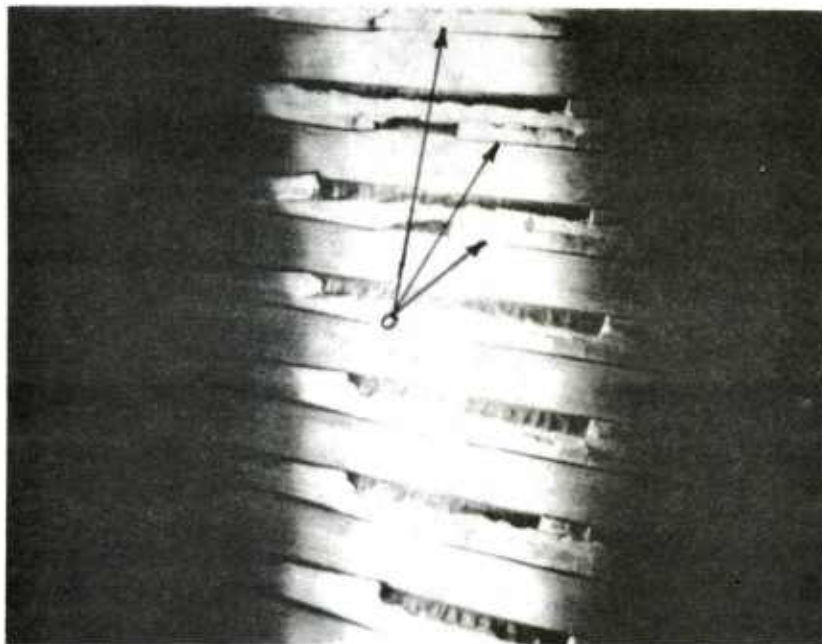


Figure 32. Range firings with damaged tube S/N 25460-M549 projectile, rocket off



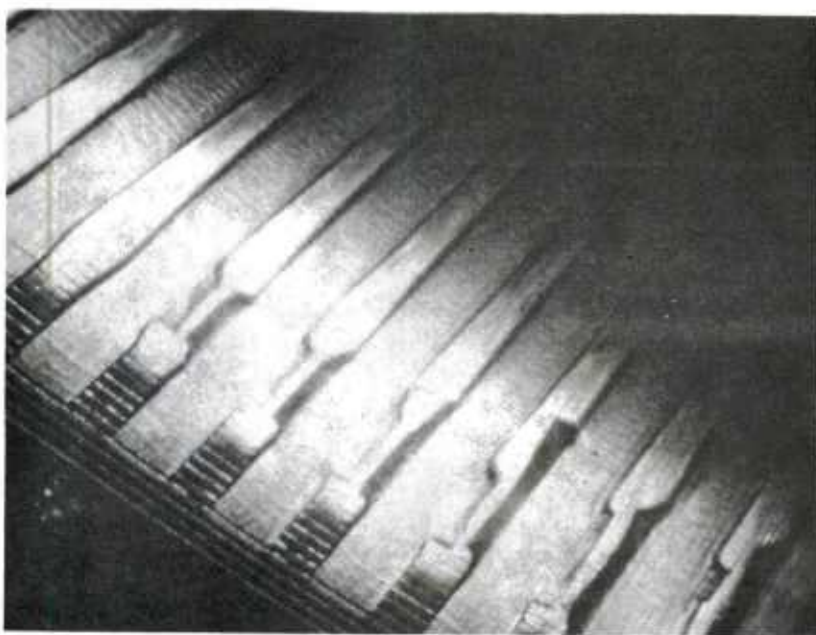
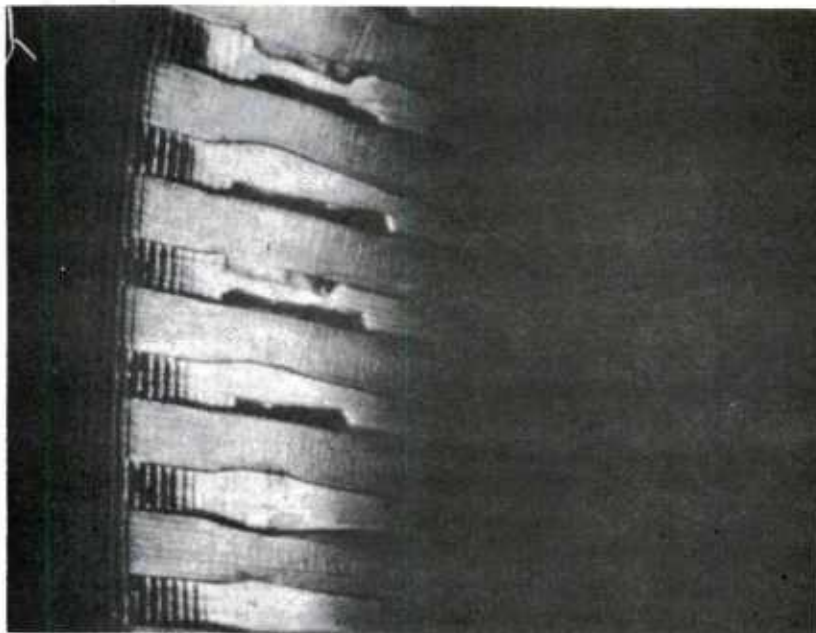
a. Origin of rifling 1 to 3 o'clock

Figure 33. 155-mm M185 howitzer tube S/N 25460 at start of degradation test after firing 458 rounds



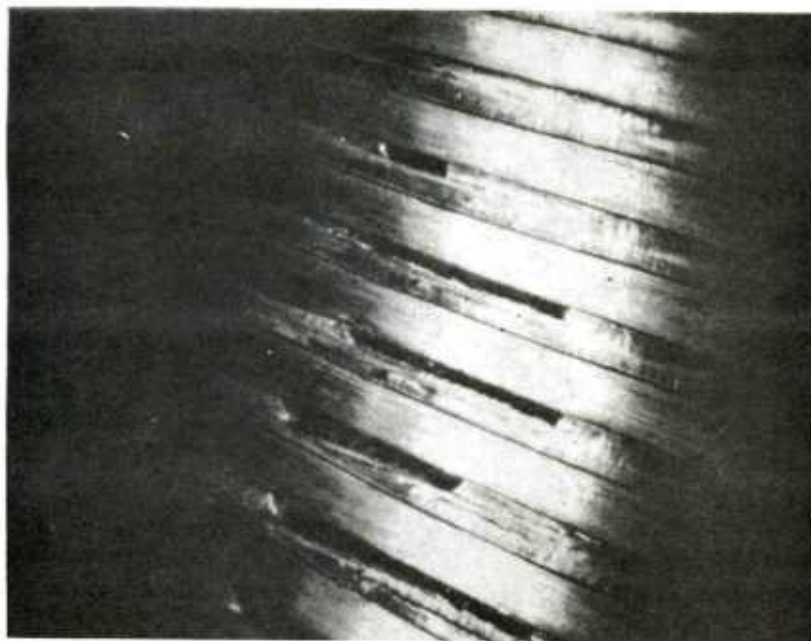
b. Condition of rifling 44.75 to 48 in. 6:30 to 9:30 o'clock

Figure 33. (cont)



a. Origin of rifling 1 to 3 o'clock after firing 611 rounds

Figure 34. 155-mm M185 howitzer tube S/N 25460



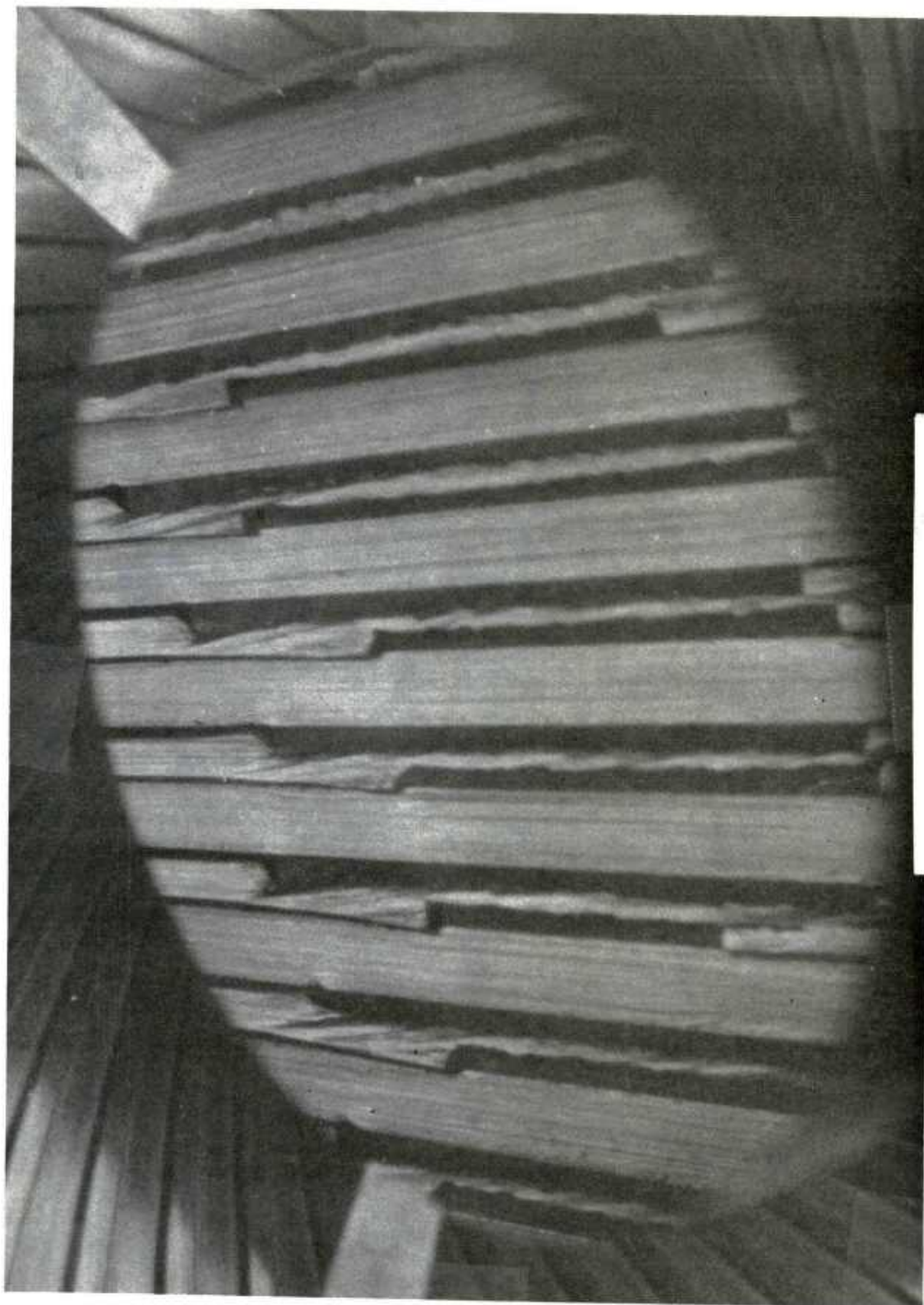
b. Condition of rifling 44.75 to 48 in. 6:30 to 9:30 o'clock after firing 522 rounds

Figure 34. (cont)



a. At origin of rifling

Figure 35. Type of rifling damage not warranting condemnation of the tube



b. Near origin of rifling

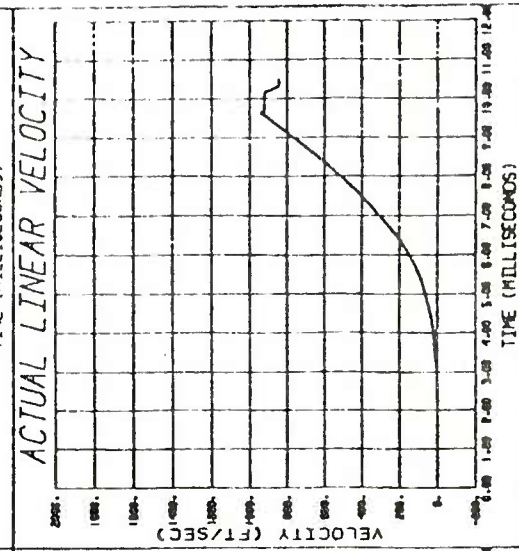
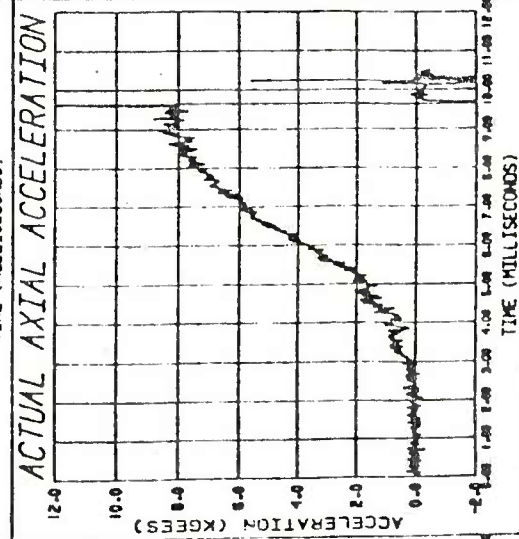
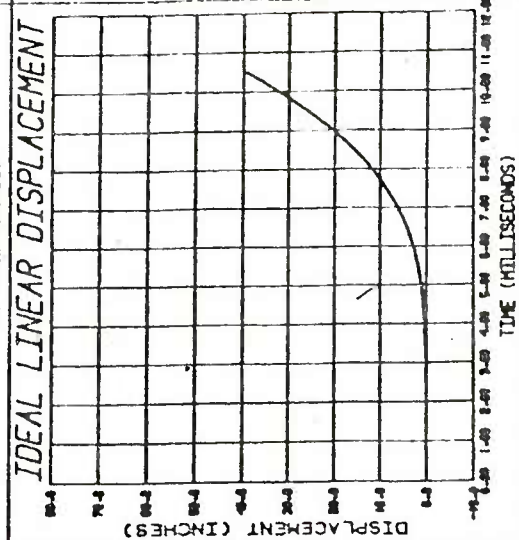
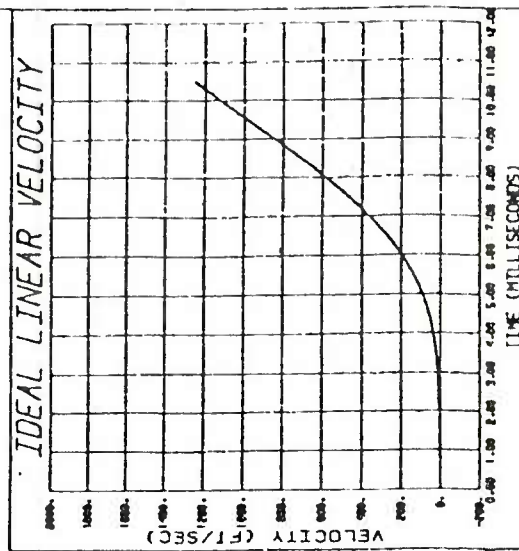
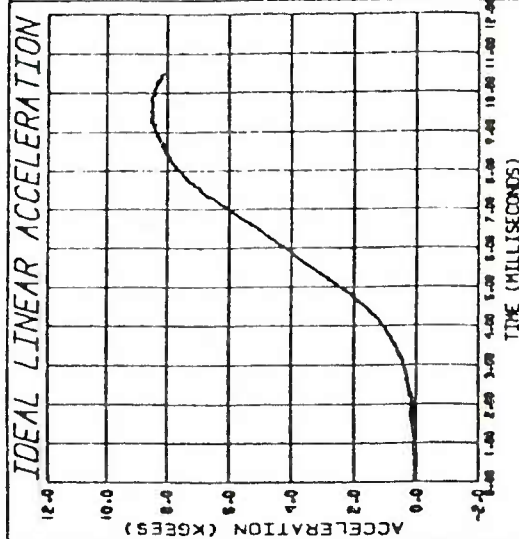
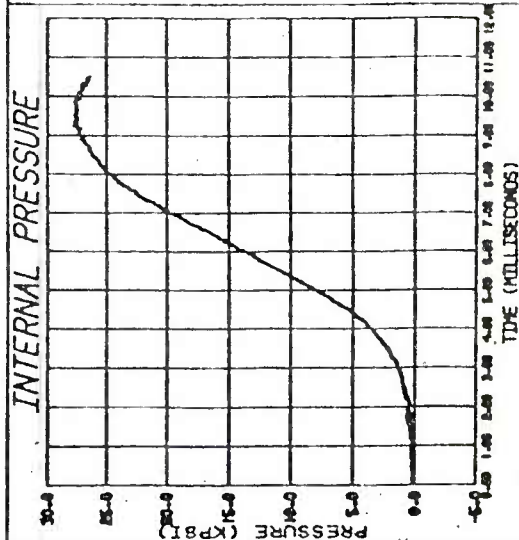
Figure 35. (cont)

APPENDIX

INTERIOR BALLISTIC DATA
COLLECTED DURING THE DEGRADATION TEST

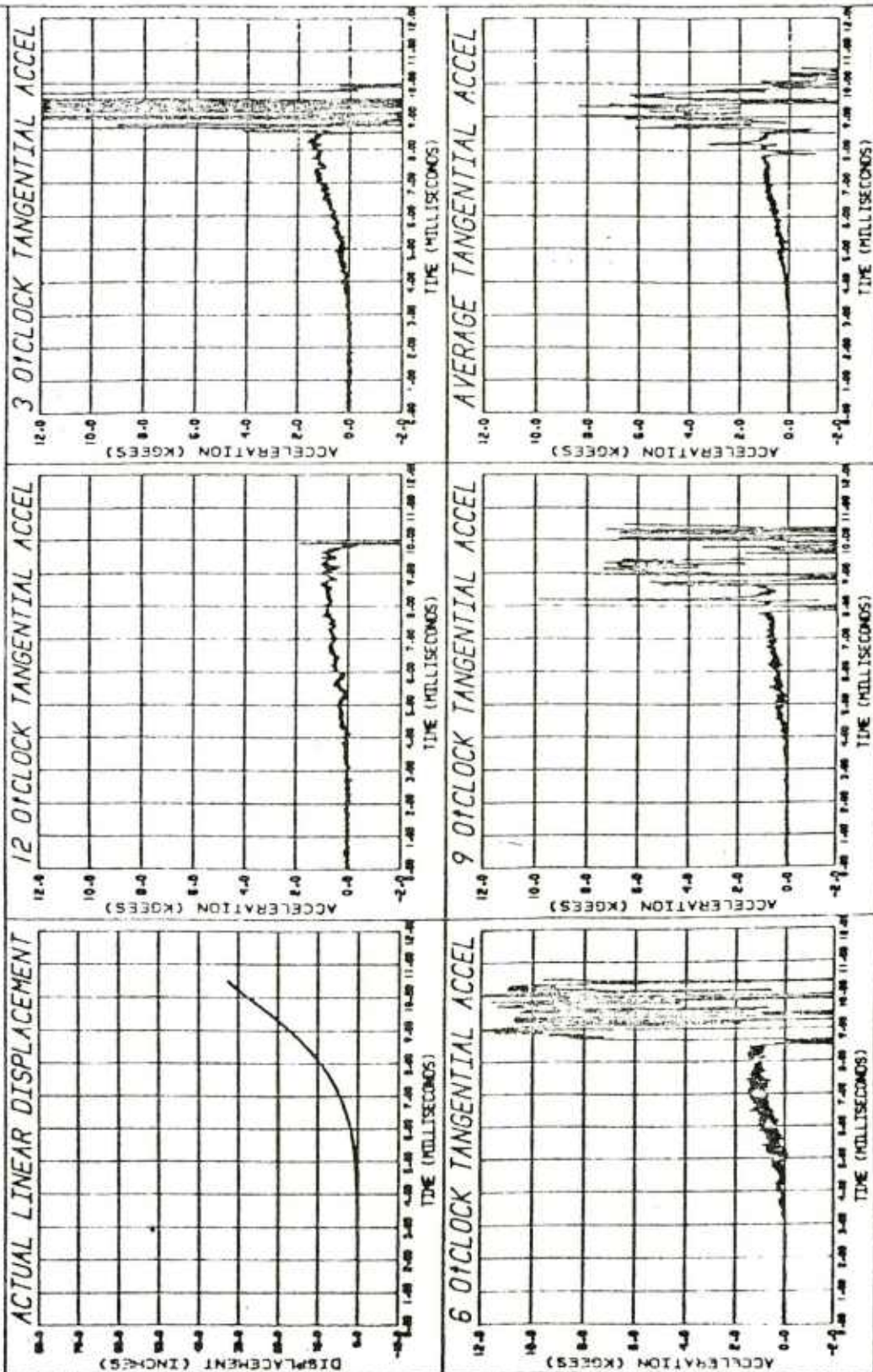
PROCESSED DATA

ROUND NO. 1

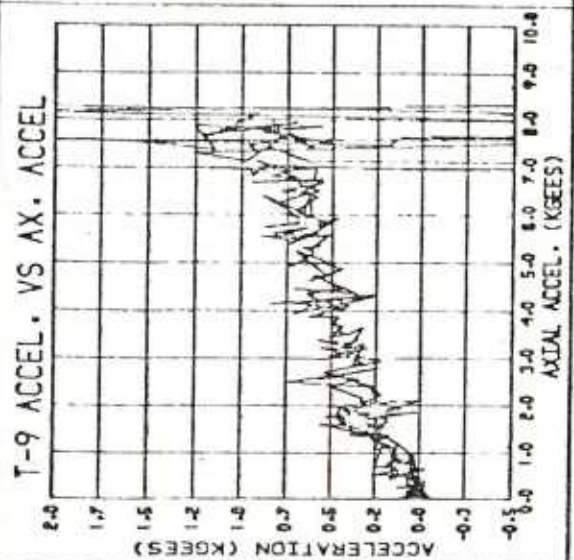
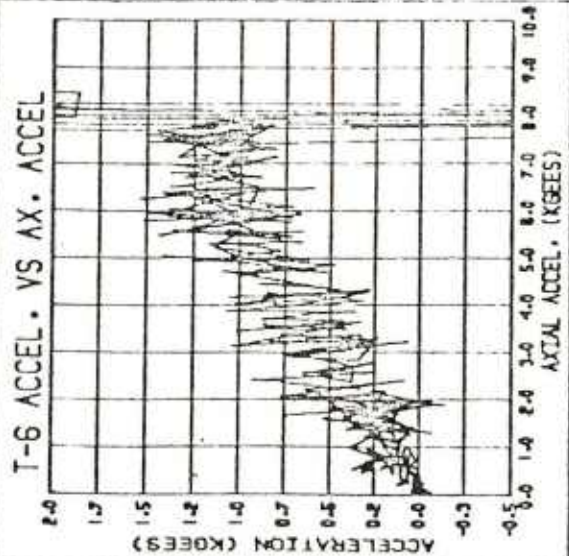
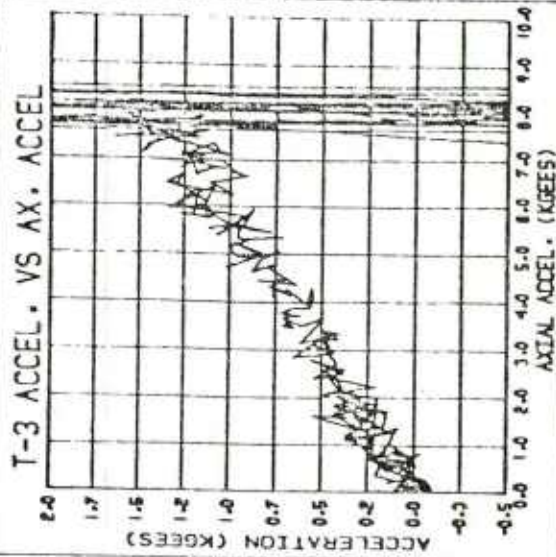
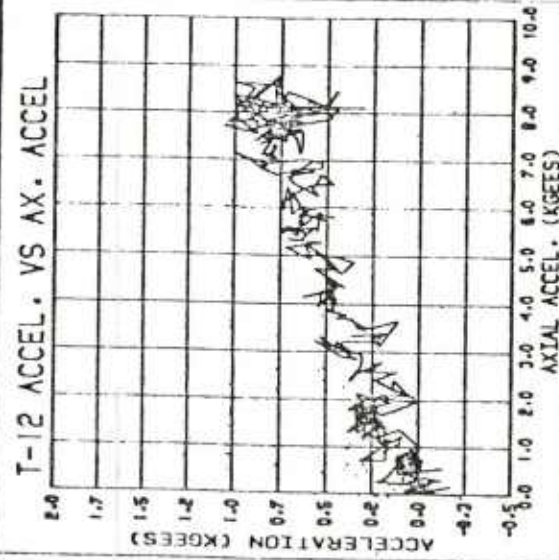
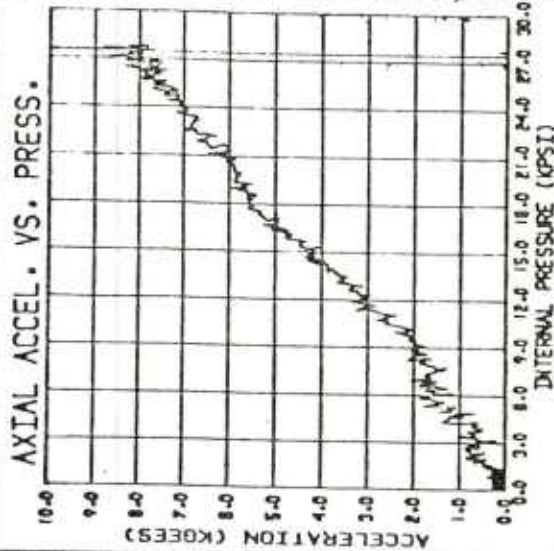


PROCESSED DATA

ROUND NO. 1



FB-4ARM STUDY ROUND NO. 1

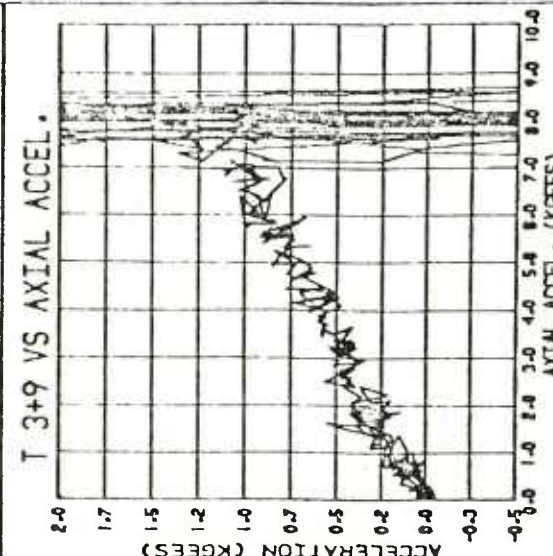
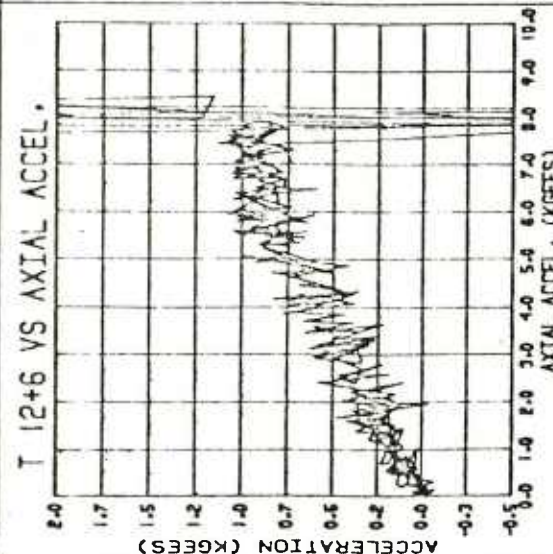
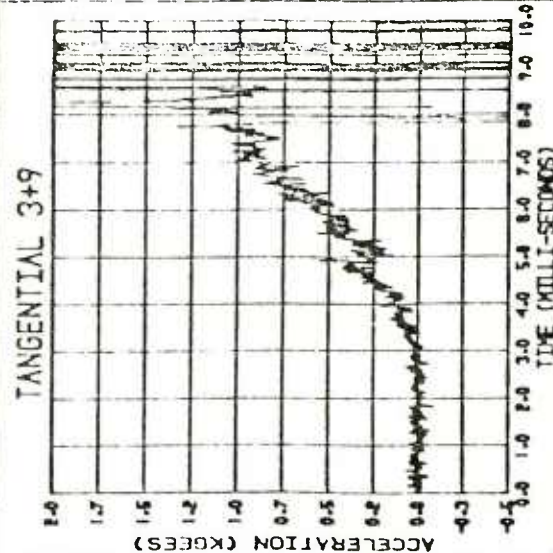
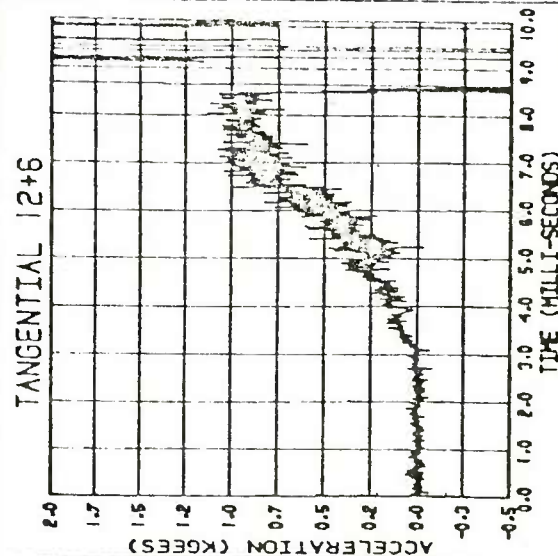
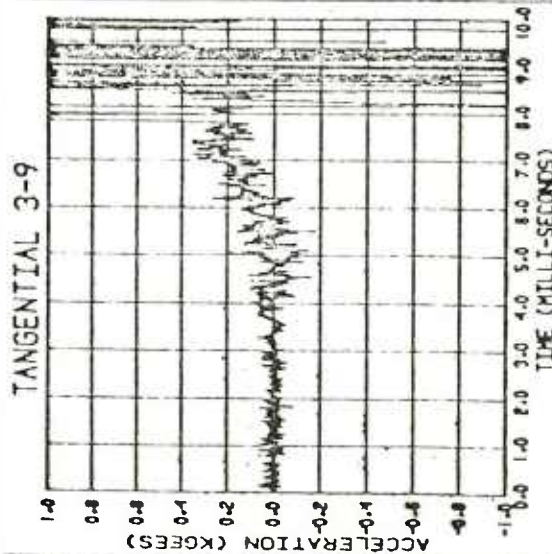
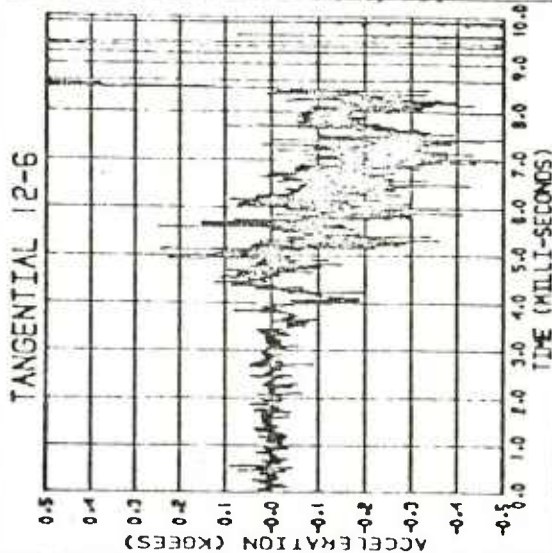


HYDRA VERSION 2.0.12

- 1 -

06/23/83 10:29:49

FB-4ARM STUDY ROUND NO. 1



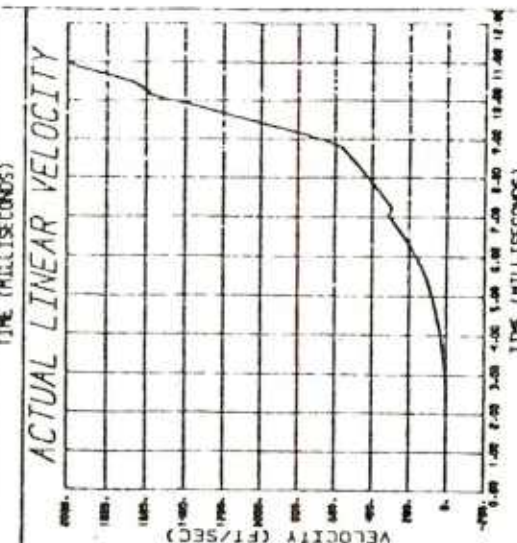
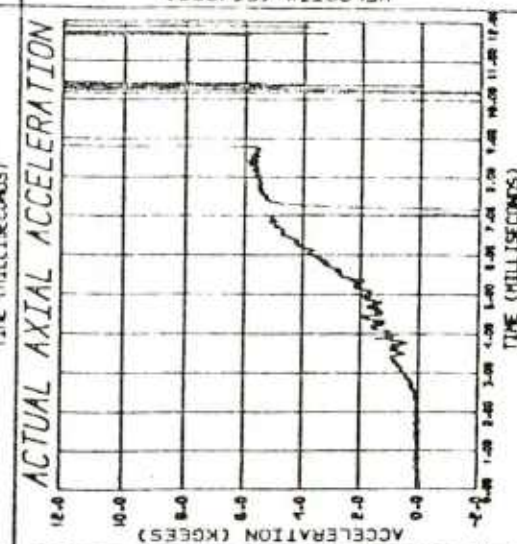
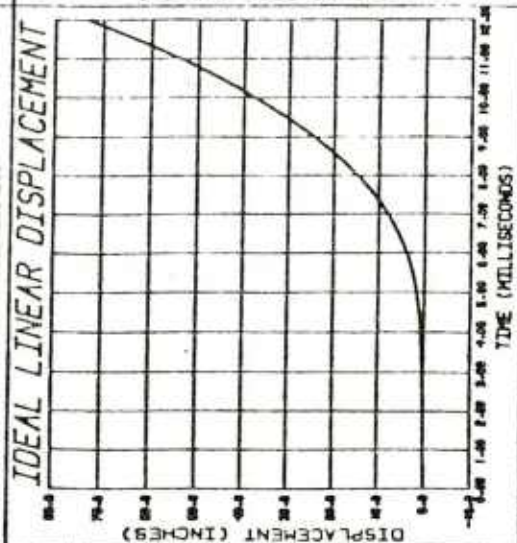
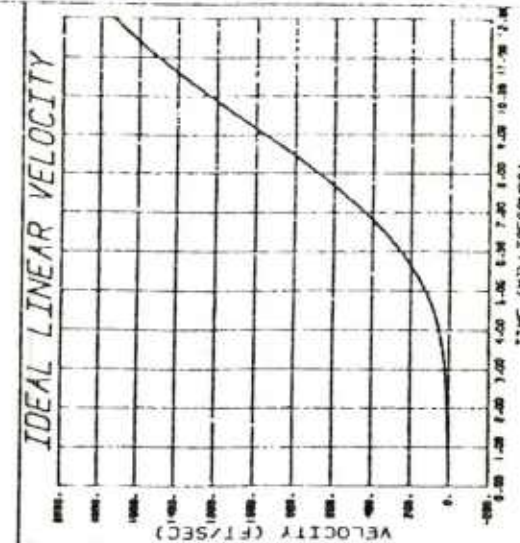
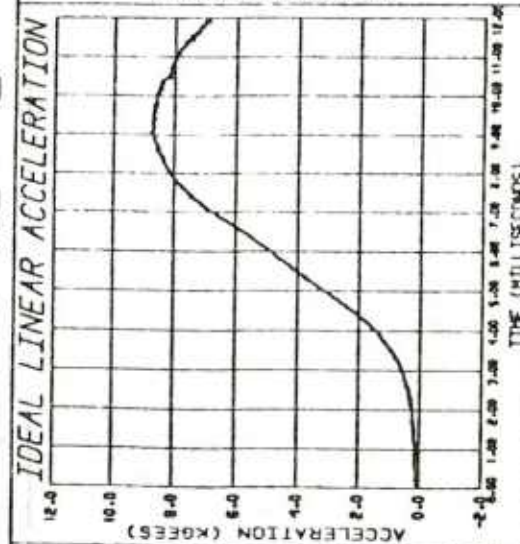
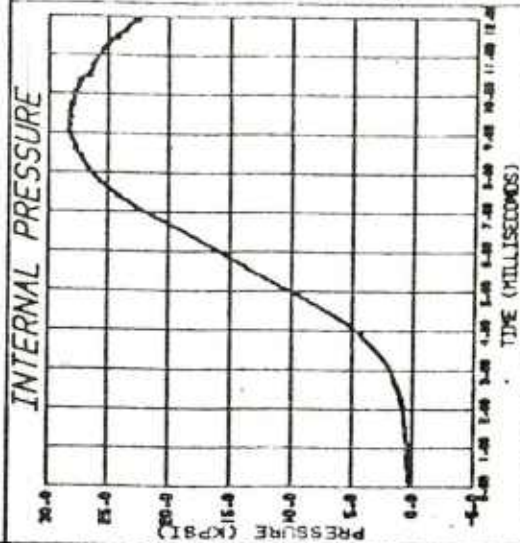
HYDRA VERSION 2.0.12

- 2 -

06/23/83 10:56:23

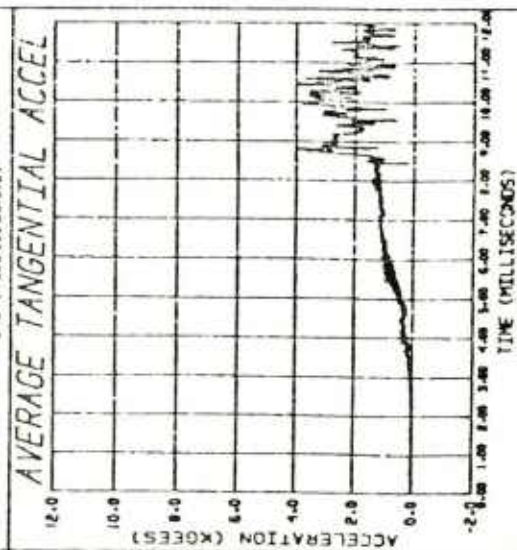
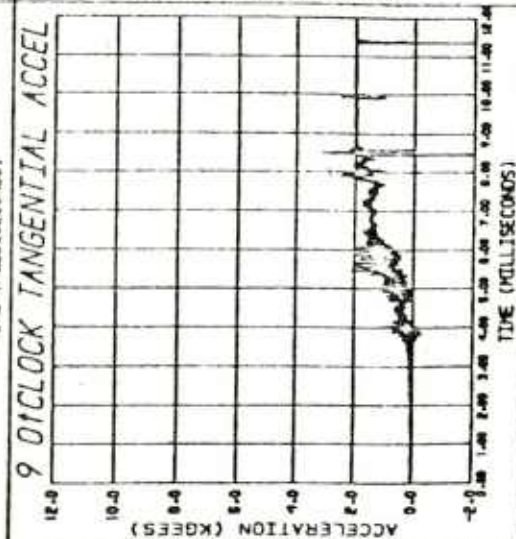
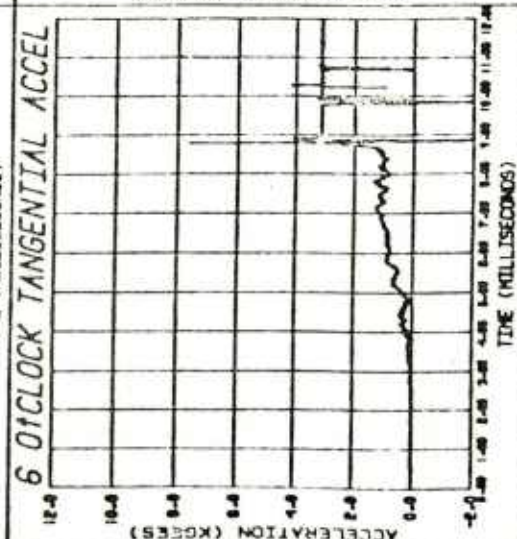
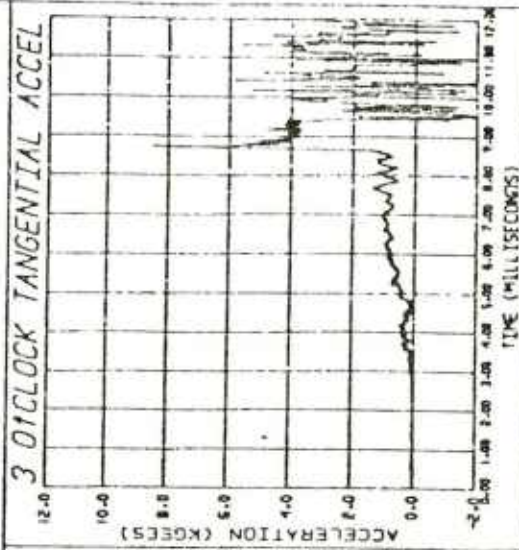
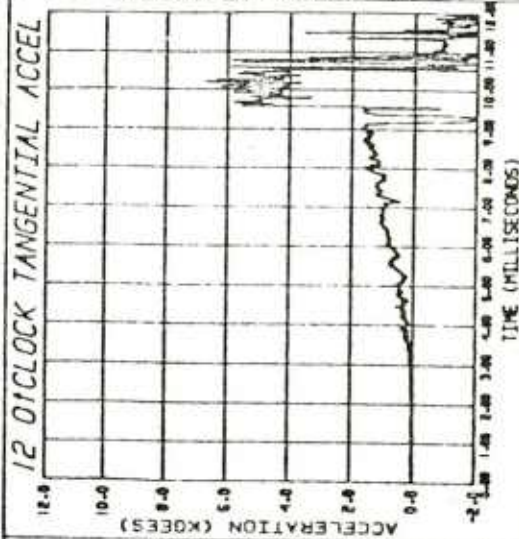
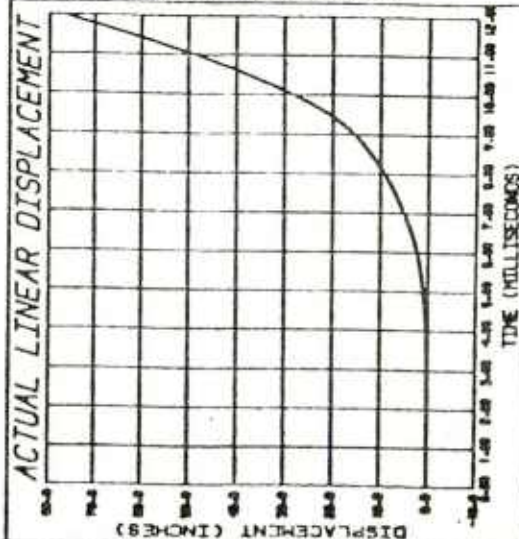
PROCESSED DATA

ROUND NO. 6

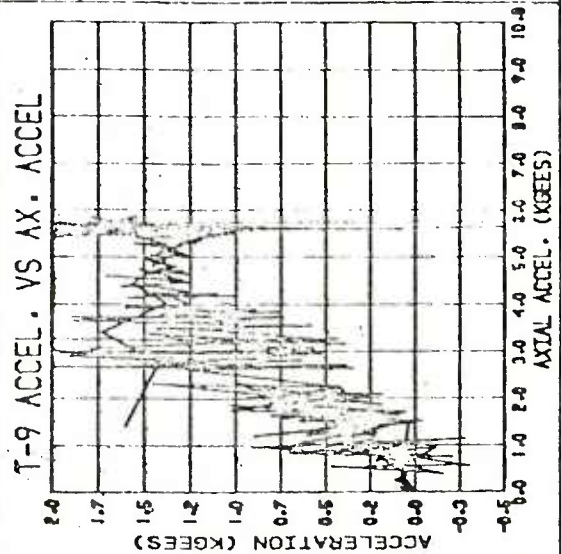
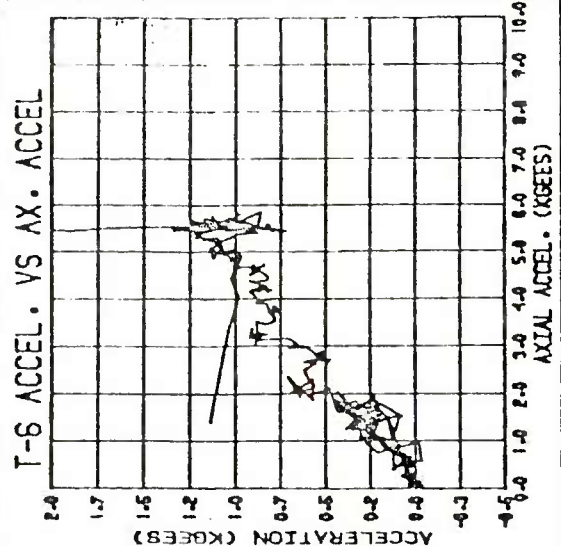
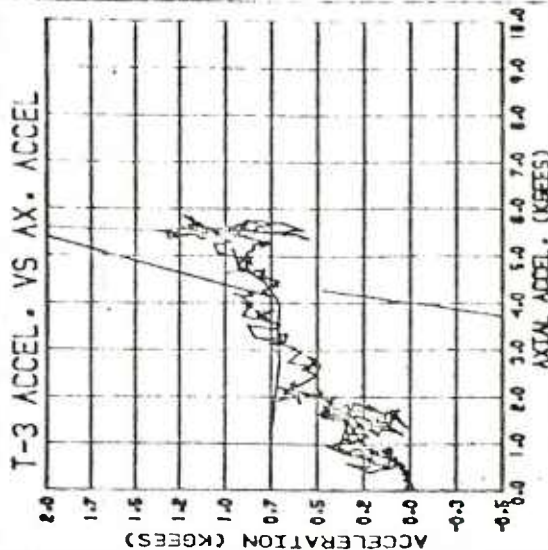
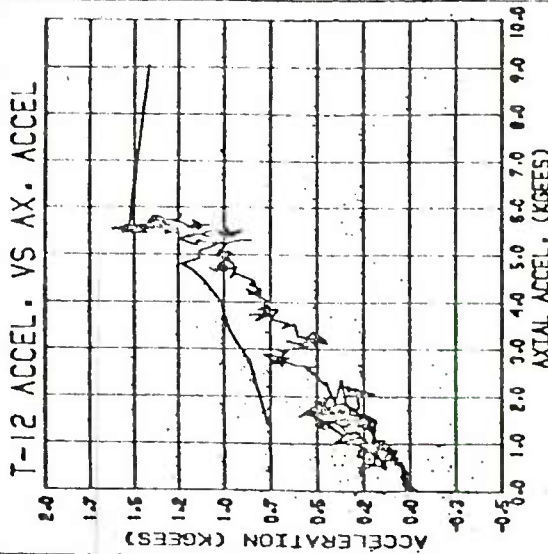
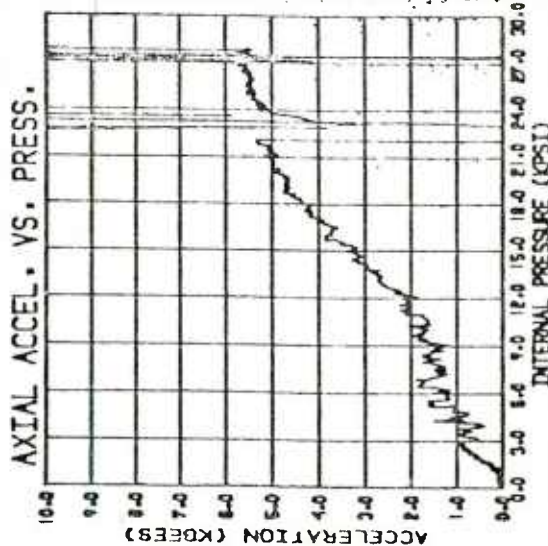


PROCESSED DATA

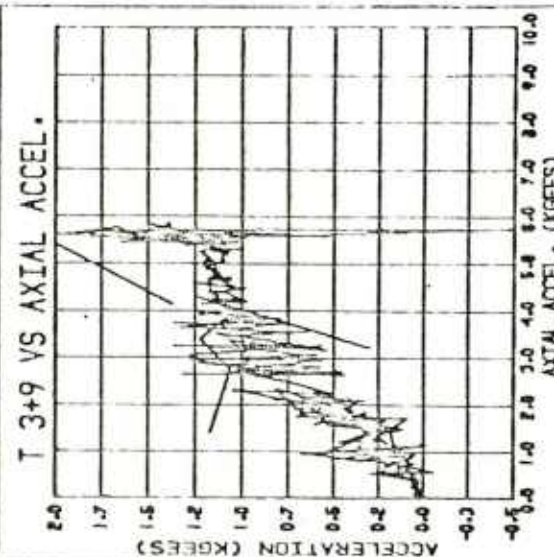
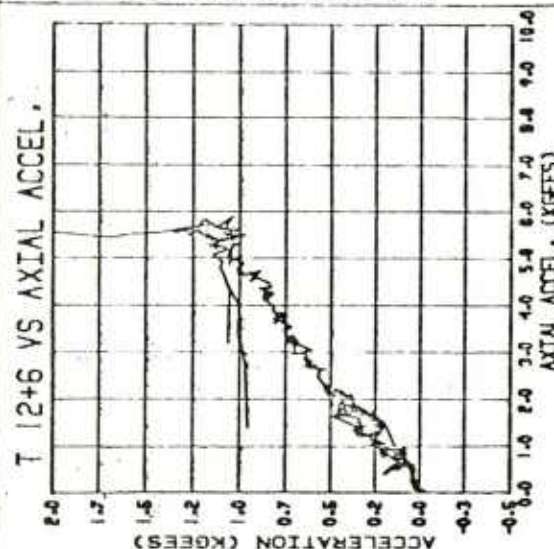
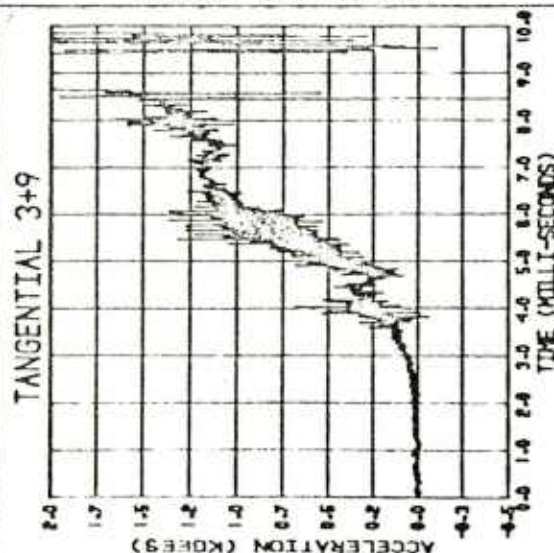
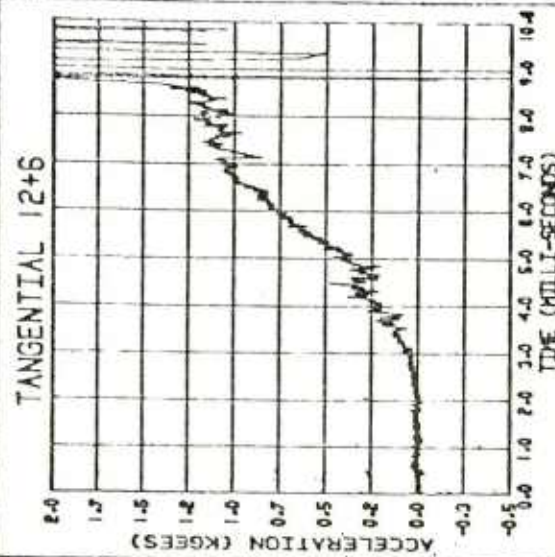
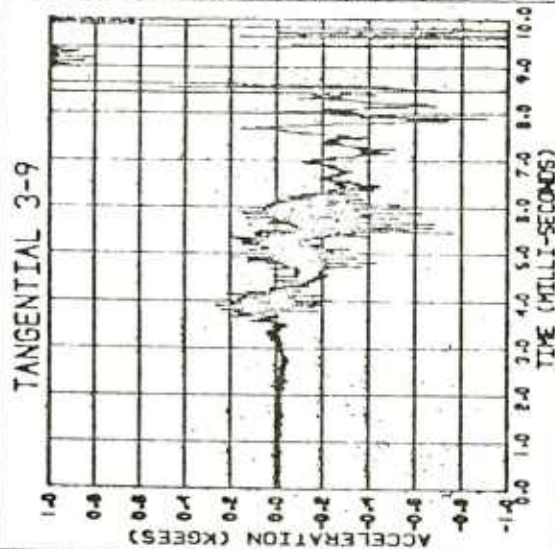
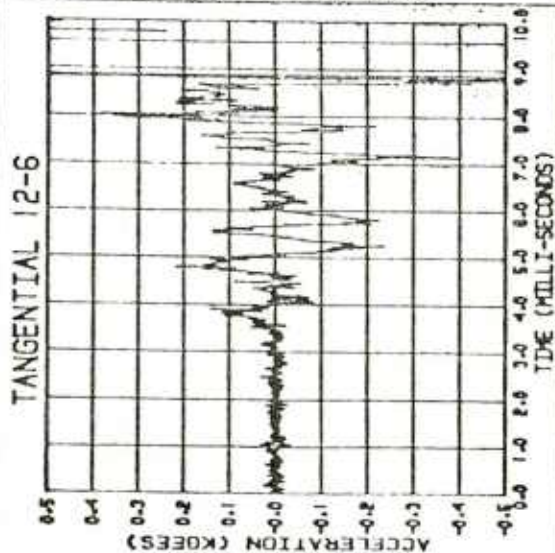
ROUND NO. 6



FB-4ARM STUDY ROUND NO. 6



FB-4ARM STUDY ROUND NO. 6



HYDRA VERSION 2-0.12

- 12 -

06/24/83 10:53:43

DISTRIBUTION LIST

Commander
Armament Research and Development Center
U.S. Army Armament, Munitions and
Chemical Command
ATTN: SMCAR-TSS (5)
SMCAR-LC
SMCAR-LCB
SMCAR-LCE
SMCAR-LCM
SMCAR-LCN
SMCAR-LCS
SMCAR-LCU
SMCAR-LCW (10)
Dover, NJ 07801-5001

Commander
U.S. Army Armament, Munitions and
Chemical Command
ATTN: AMSMC-GCL(D)
Dover, NJ 07801-5001

Administrator
Defense Technical Information Center
ATTN: Accessions Division (12)
Cameron Station
Alexandria, VA 22314

Director
U.S. Army Materiel Systems Analysis
Activity
ATTN: DRXSY-MP
Aberdeen Proving Ground, MD 21005-5066

Commander
Chemical Research and Development Center
U.S. Army Armament, Munitions and
Chemical Command
ATTN: SMCCR-SPS-I
Aberdeen Proving Ground, MD 21010-5423

Commander
Chemical Research and Development Center
U.S. Army Armament, Munitions and
Chemical Command
ATTN: SMCCR-RSP-A
Aberdeen Proving Ground, MD 21010-5423

Director
Ballistic Research Laboratory
ATTN: AMXBR-OD-ST
Aberdeen Proving Ground, MD 21005-5066

Chief
Benet Weapons Laboratory, LCWSL
Armament Research and Development Center
U.S. Army Armament, Munitions and
Chemical Command
ATTN: SMCAR-LCB-TL
Watervliet, NY 12189-5000

Commander
U.S. Army Armament, Munitions and
Chemical Command
ATTN: AMSMC-LEP-L
Rock Island, IL 61299-6000

Director
U.S. Army TRADOC Systems
Analysis Activity
ATTN: ATAA-SL
White Sands Missile Range, NM 88002

Assistant Secretary of the Army
Research and Development
ATTN: Department for Science
and Technology
The Pentagon
Washington, DC 20315

Commander
U.S. Army Materiel Command
ATTN: AMC-SC
5001 Eisenhower Avenue
Alexandria, VA 22304

Commander
U.S. Army Electronics Command
ATTN: Technical Library
Ft. Monmouth, NJ 07703

Commander
U.S. Army Mobility Equipment Research
and Development Command
ATTN: Technical Library
Ft. Belvoir, VA 22060

Commander
U.S. Army Tank-Automotive Research
and Development Command
ATTN: Technical Library, DRSTA-TSL
Warren, MI 48090

Commander
U.S. Military Academy
ATTN: CHMN, Mechanical Engineer Dept.
West Point, NY 10996

Commander
U.S. Army Missile Command
ATTN: Documents Section, Bldg 4484
Redstone Arsenal, AL 35898

Commander
Rock Island Arsenal
ATTN: SMCRI-ENM (Mat Sci Div)
Rock Island, IL 61299

Commander
HQ, U.S. Army Aviation School
ATTN: Office of the Librarian
Ft. Rucker, AL 36362

Commander
U.S. Army Foreign Science and
Technology Center
ATTN: DRXST-SD
220 7th Street, N.E.
Charlottesville, VA 22901

Commander
U.S. Army Materials and Mechanics
Research Center
ATTN: Technical Library, DRXMR-PL (2)
Watertown, MA 02172

Commander
U.S. Army Research Office
ATTN: Chief IPO
P.O. Box 12211
Research Triangle Park, NC 27709

Commander
Harry Diamond Laboratories
ATTN: Technical Library
2800 Powder Mill Road
Adelphia, MD 20783

Commander
Rock Island Arsenal
ATTN: SMCAR-ESM
Rock Island, IL 61299-5000

Director
U.S. Naval Research Laboratory
ATTN: Director, Mech Div
Code 26-27 (DOC Library)
Washington, DC 20375

Mechanical Properties Data Center
Battelle Columbus Laboratory
505 King Avenue
Columbus, OH 43201

Commander
Naval Surface Weapons Center
ATTN: Technical Library
Code X212
Dahlgren, VA 22448